1968

Spatially dependent frequency response of coupled core reactors

Ira Wilson Merritt Jr.
Iowa State University

SPATIALLY DEPENDENT FREQUENCY RESPONSE OF COUPLED CORE REACTORS

by

Ira Wilson Merritt, Jr.

A Dissertation Submitted to the
Graduate Faculty in Partial Fulfillment of
The Requirements for the Degree of
DOCTOR OF PHILOSOPHY

Major Subject: Nuclear Engineering

Approved:

Signature was redacted for privacy.

In Charge of Major Work

Signature was redacted for privacy.

Head of Major Department

Signature was redacted for privacy.

Dean of Graduate College

Iowa State University
Ames, Iowa

1968

TABLE OF CONTENTS

I. INTRODUCTION

The purpose of this thesis is to calculate the spatially dependent frequency response for a realistic model of an actual coupled-core nuclear reactor, to determine what factors are important in affecting this frequency response, and to provide a qualitative explanation of the results. The reactor to be investigated is the Iowa State University UTR-10 reactor. A brief physical description of this reactor is presented in Appendix A and its most important nuclear parameters are presented in Table II.1.

In this study the term coupled-core reactor means that the reactor under consideration will consist of two distinct fissionable assemblies, core one and core two, which are physically coupled in the sense that some neutrons causing fissions in core one originated in core two and vice versa. This relationship is also true between any two adjacent fuel elements in a reactor, but the idea is most useful when the number of assemblies under consideration is relatively small and when each has an appreciable multiplication factor when standing alone.

The reasons for studying oscillation tests are well summarized in a statement by Gyftopoulos (19), who said, "Oscillation tests, or, in general, small perturbation tests are performed to measure transfer functions either to design the reactor regulating system or to investigate stability."

However, before going into the frequency response of coupled reactors a review of the history of the interest in reactor transfer functions will be outlined.

The transfer function of a nuclear reactor was first measured by Harrer, Boyar, and Krucoff (21) at Argonne National Laboratory in 1952 when they applied the rod-oscillator technique to the CP-2 reactor and obtained good agreement with their one-point model at the low frequencies (up to 20 rad/sec) which were investigated.

The point model is an adequate representation for a nuclear reactor as long as the reactor flux shape does not differ significantly from the fundamental mode, or steady state flux shape. However, as reactor size increases this criterion fails at increasingly lower frequencies. Hence there is interest in the spatially dependent reactor response, or alternately, in the ability to locate a detector in a reactor at a position where the point-model response is closely approximated.

Interest in the frequency response of coupled-core reactors was also first reported from Argonne National Laboratory (4, 5) where in 1959 Baldwin (5) attempted to describe the behavior of the Argonaut reactor by writing a separate diffusion equation for each core and including an interaction term with the source in each equation. This interaction term in one core was proportional to the flux in the other core at a previous time, τ, where τ is a delay

time characteristic of the time it takes a disturbance to travel from one core to the other. The biggest problem with this model is that it requires knowledge of the coupling coefficient for each core and the delay time between cores. These are not quantities that are readily available for most reactors.

Although done earlier, Avery's work (4) was considerably more elaborate than that of Baldwin. Avery wrote a point neutron kinetic equation for each neutron population group in a coupled reactor. These groups were based upon an identification of neutrons by the core in which they originated and the core in which they were lost to the chain reaction. This led directly to the definition of partial lifetimes, multiplication factors, and fission sources. These quantities were defined from general definitions of the total quantities as adjoint weighted integral parameters. That is, the parameters which go into the kinetics equations are integral properties obtained by adjoint weighting and integration over the reactor. Hence, this method also provides a means for finding the reactor parameters to be used in the kinetics equations.

When a local perturbation is made in a very large nuclear reactor or when fast local changes are made in smaller reactors the time-dependent reactor flux shape is not well represented by the fundamental mode. For these

cases a space-dependent model becomes very desirable.

Gyftopoulos (19) has shown that the transfer function of a reactor is not spatially dependent when the reactivity is computed in a consistent manner. In this paper what is calculated is not a spatially dependent transfer function but the response of a coupled reactor to an oscillating absorber,

$$G(x,x',j\omega) = \delta\varphi(x,x',j\omega)/\delta\Sigma_a(x',j\omega)$$

where x represents the detector location, x' represents the oscillator location, and ω is the frequency of oscillation.

The first attempt made to describe the spatially dependent response of a reactor to an oscillating absorber was in a classic paper by Weinberg and Schweinler (41) in 1948.

Since that time almost all efforts aimed at describing the spatial dependence of the reactor response have been by means of a modal expansion technique in which the space- and time-dependent flux, $\varphi(x,t)$, is approximated by a series of products of space-dependent expansion modes, $\psi_i(x)$, and time-dependent coefficients, $a_i(t)$. The flux is approximated by

$$\varphi(x,t) \cong \sum_{i=1}^{N} \psi_i(x)a_i(t) \ .$$

There are two steps in this type of analysis: the selection of the space functions and the determination of

the time coefficients. In this discussion several versions will be described corresponding to different methods of chosing the space functions.

The space modes used for synthesizing the flux may be either orthogonal or nonorthogonal and the simplest set of orthogonal modes are solutions of the Helmholtz equation.

$$\nabla^2\varphi + B^2\varphi = 0$$

Use of these solutions was proposed by Foderaro and Garabedian (14, 15) but they have the disadvantage of being very difficult to obtain for complex reactor geometries. Other sets of basis vectors which are also eigenfunctions are the lambda and omega modes (25, 26). The lambda modes are obtained by solving an eigenvalue equation of the form

$$L\psi_n = \frac{1}{\lambda_n} M\psi_n$$

where the L-operator is the multigroup removal operator and the M-operator is the multigroup production operator. The omega modes are obtained by solving an expression of the form

$$[L-M]\psi_n = \omega_n T\psi_n$$

where T is the diagonal matrix whose elements are the reciprocal neutron group speeds. These modes have been used to solve problems but are not very convenient since they do not have the property of finality. According to

Kaplan (26), a set of modes has the property of finality if the time coefficients of the modes are independent of the number of terms used to approximate the flux. That is, if a set of modes has the property of finality the time coefficients of each mode can be determined separately. This is advantageous because it is easier to solve a single equation than a set of simultaneous equations. Kaplan shows how to construct such modes and his natural modes satisfy an equation of the form

$$L_o \psi_n = \omega_n \psi_n$$

where the L_o-operator is the steady-state operator which results when the multigroup equations are cast into the form

$$L\varphi = \dot{\varphi}$$

where

$$\varphi = \text{col}[\varphi_F \varphi_S C] \ .$$

The modal analysis techniques previously described use eigenfunctions of the unperturbed problem as the basis functions of the solution. Another possibility, but which uses non-orthogonal modes, is the application of the "synthesis" technique. The idea behind this method is that if a series of asymptotic shapes, $\psi_i(x)$, are chosen from the solution of simpler but related problems, a set of "mixing coefficients", $a_i(t)$, can be obtained so that an approximate

solution to the problem at hand can be constructed.

The type of space modes used in this paper is another set of nonorthogonal modes called Green's Function modes, which were first introduced by Dougherty and Shen (13). To obtain these modes the reactor is divided into regions and the fission cross section is everywhere set equal to zero. A distributed source is then introduced into each of the regions--a fission source is used in multiplying regions and a pseudosource is introduced into nonmultiplying regions (see Appendix C)--and the resulting flux shape is taken as the mode which originates in that region of the reactor. An eigenvalue problem does not have to be solved to obtain these modes and they can be tailored to suit a problem about which one may have a priori knowledge. That is, the spatial distribution of the modes is determined using engineering judgment. The advantage of being able to distribute the modes at will is that they can be located in higher density in regions where the flux is expected to vary most rapidly and this should result in a better solution than would be otherwise possible. In particular it has been shown (9) that the solution to problems involving localized step changes in reactivity converges much faster for Green's Function modes than for Helmholtz modes.

Most of the work using modal analysis has centered around time-domain investigations rather than around studies

in the frequency domain and the limited published work related to reactor frequency responses deals largely with experimental (20) and analytic (11, 16) results for the heavy-water moderated NORA reactor. Other work includes Loewe's (31) investigation of the differences between the frequency responses obtained by using the Telegrapher's equation and the diffusion equation for both bare and reflected light-water and heavy-water moderated slab reactors. Loewe found the differences in responses predicted by the Telegrapher's equation and the diffusion equation were negligible below 10^4 rad/sec but he presented limited results dealing with detailed space dependence of the reactor frequency responses.

The only published work which includes spatially dependent frequency responses for coupled-core reactors is that by Carter and Danofsky (10), who studied a tightly coupled unreflected reactor. The main objective of their investigation was to study the convergence of Green's Function modes and to investigate the use of coupling modes in nonmultiplying regions. As a result, although they published some frequency-response curves they made little comment about them.

In light of the little published work dealing with spatial effects in coupled nuclear reactors and in view of the increased consideration being given to coupled fast-thermal power reactors and the clustering of nuclear rocket

engines, this seems to be an appropriate area for further study. It is hoped that an effort to determine what reactor parameters have an important effect on the spatially dependent frequency response of the UTR-10 reactor might also be useful to others in other areas of work.

II. METHOD OF ANALYSIS USING GREEN'S FUNCTION MODES

A. Determination of Criticality

The method used in applying Green's Function modes to the frequency analysis of a nuclear reactor begins much the same way as other modal techniques. First a reactor model and its associated nuclear parameters are chosen and the steady-state flux and adjoint distributions are obtained. The prototype reactor model used in this study is shown in Figure II.1 and represents a one-dimensional idealization of the Iowa State University UTR-10 reactor.

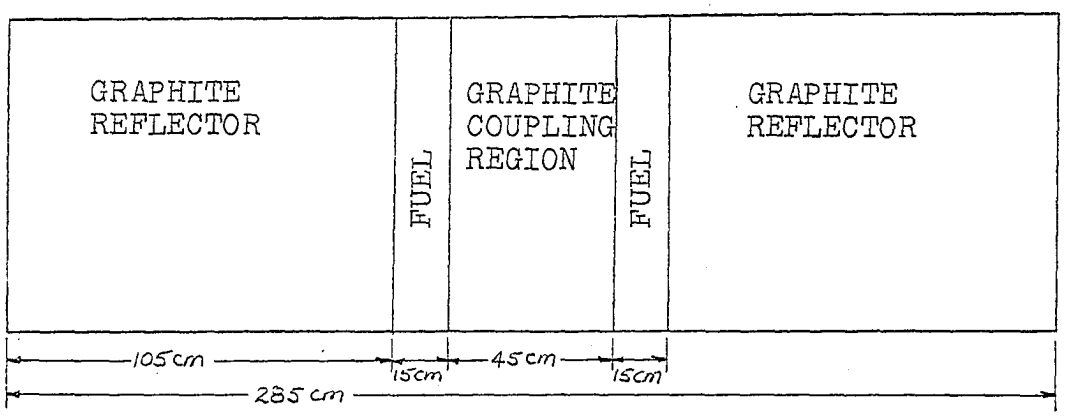

Figure II.1. Dimensions of UTR-10 reactor.

Table II.1 contains the two-energy-group nuclear data (2, 35, 39) which were used to represent the prototype reactor. In this diffusion approximation fast fission and absorption in the fast group were considered to be negligible. The exact form of the representation used is given by Equations C.16, C.17, and C.18.[1] For a first approximation

[1] See Appendix C.

it was assumed that the U-235 content was the same in each core tank and unless otherwise stated this will also be the case in all other examples. It will be seen later that none of the conclusions are changed for small flux tilts which might result from unequal loading.

The first estimate of the transverse buckling, which was used to describe the leakage of neutrons through the two sides and top and bottom of the reactor, was obtained by making a horizontal and vertical flux map through a core tank, extrapolating the fluxes to zero and obtaining the buckling in each direction by assuming the flux obeyed an equation of the form

$$\varphi(z) = A \sin B_z z \cdots$$

The total transverse buckling, B_T^2, is the sum of the two components

$$B_T^2 = B_y^2 + B_z^2 = 0.00216 \text{ cm}^{-2} .$$

Table II.1. Reactor parameters

Reactor Parameter	Region				
	north reflector	north core	coupling region	south core	south reflector
D_F cm	1.14	1.30	1.14	1.30	1.14
D_s cm	0.843	0.121	0.843	0.121	0.843
Σ_a cm^{-1}	0.000284	0.0716	0.000284	0.0716	0.000284
Σ_r cm^{-1}	0.00296	0.0210	0.00296	0.0210	0.00296
Σ_f cm^{-1}	0.000	0.0499	0.000	0.0499	0.000

At criticality the solution of the diffusion equation and its adjoint must satisfy conditions requiring (1) that the fluxes and adjoints go to zero at the extrapolated boundaries of the reactor,

$$\bar{\Phi}(0) = \bar{\Phi}(285) = \underline{0} \qquad \bar{\Phi}^{+}(0) = \bar{\Phi}^{+}(285) = \underline{0} \qquad \text{(II.1)}$$

(2) that the fluxes and their currents be continuous at all internal material interfaces,

$$\bar{\Phi}(x=x_j^-) = \bar{\Phi}(x=x_j^+) \qquad \bar{\Phi}^{+}(x=x_j^-) = \bar{\Phi}^{+}(x=x_j^+) \qquad \text{(II.2)}$$

$$\mathscr{D}_j \frac{\partial}{\partial x} \bar{\Phi}(x=x_j^-) = \mathscr{D}_{j+1} \frac{\partial}{\partial x} \bar{\Phi}(x=x_j^+) \qquad \text{(II.3)}$$

$$\mathscr{D}_j \frac{\partial \bar{\Phi}^{+}}{\partial x} (x=x_j^-) = \mathscr{D}_{j+1} \frac{\partial \bar{\Phi}^{+}}{\partial x} (x=x_j^+)$$

where

$$\mathscr{D}_j = \begin{bmatrix} D_{F_j} & 0 \\ 0 & D_{S_j} \end{bmatrix} , \quad \bar{\Phi} = \begin{bmatrix} \varphi_F \\ \varphi_S \end{bmatrix} , \quad \bar{\Phi}^{+} = \begin{bmatrix} \varphi_F^{+} \\ \varphi_S^{+} \end{bmatrix}$$

and the x_j correspond to the reactor material interfaces and (3) that the fluxes $\bar{\Phi}(x)$ and $\bar{\Phi}^{+}(x)$ be finite and non-negative.

When the homogeneous boundary conditions, II.1, and the continuity conditions, II.2 and II.3, are applied to the two-group diffusion equations a 2n x 2n set of homogeneous equations results

$$Q\underline{c} = \underline{0} \qquad \text{(II.4)}$$

where n is two times the number of internal material interfaces plus two. The reactor is adjusted to criticality by

changing a parameter, usually the thermal absorption cross section, so that the determinant of the coefficient matrix, Q, is zero.

Since the set of parameters which makes the reactor critical is now specified, the solution of the two-group diffusion equations may be evaluated in each region of the reactor after solving for the matrix of coefficients, $\underline{c}$, in II.4. From this solution vector the fast- and thermal-group fluxes can be calculated.

A similar procedure is followed for the adjoint system. Typical shapes for the neutron flux and adjoint distributions are shown in Figures II.2 and II.3 for the prototype reactor of this study.

A parametric analysis was made on this prototype model and it was found that both the transverse buckling and coupling-region size had pronounced effects on the flux and adjoint distributions. As the transverse buckling was increased, the leakage from the reactor increased and the most pronounced effect was to reduce the peaking of the thermal flux in the reflector regions. Similarly, when the transverse buckling was decreased the thermal flux peaked more in the reflectors because fewer fast and thermal neutrons were lost to leakage. Changing the size of the coupling region caused the thermal flux to increase slightly as the cores were moved closer together and caused the fast flux to decrease less in the coupling region.

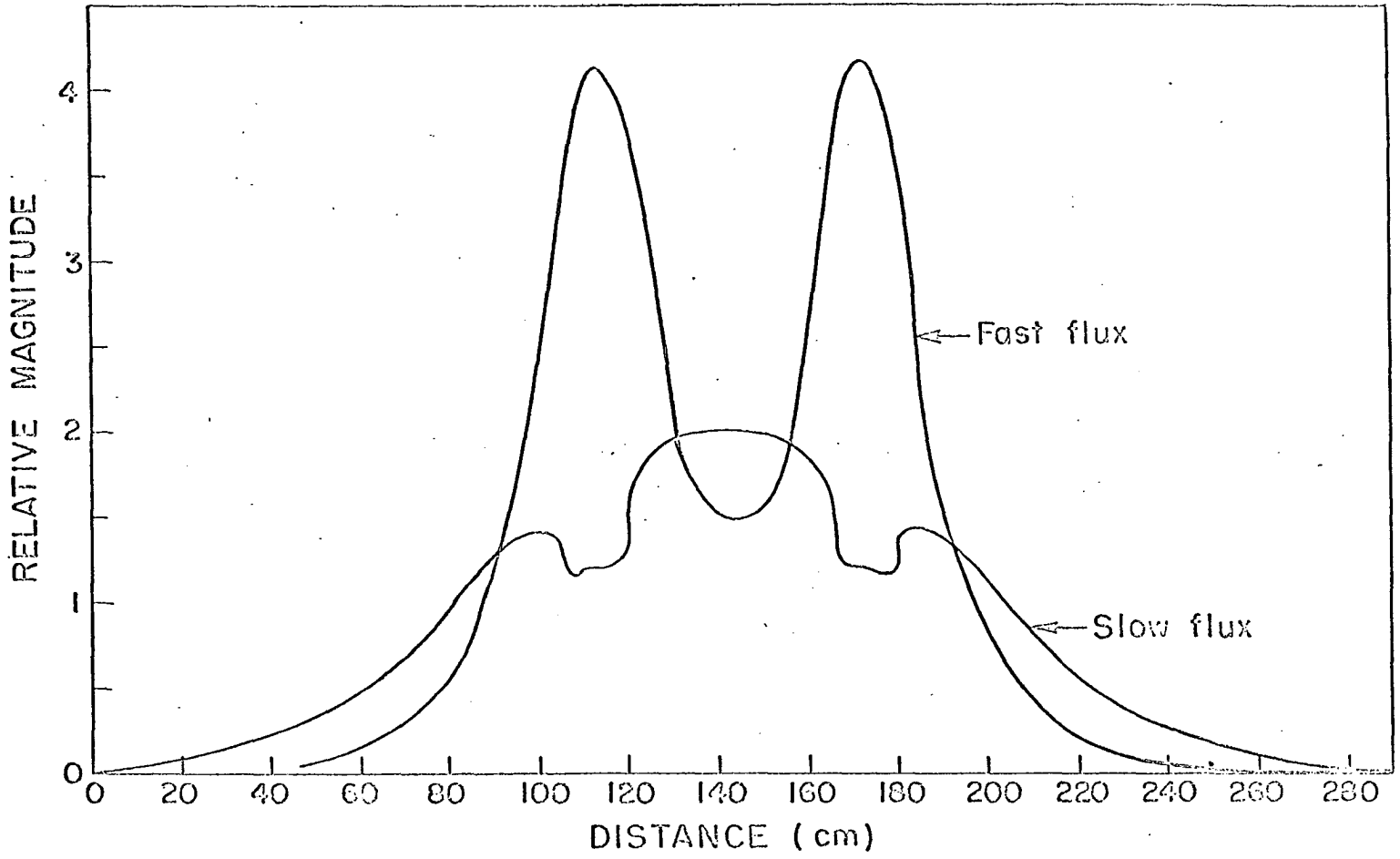

Figure II.2. UTR-10 prototype reactor fluxes.

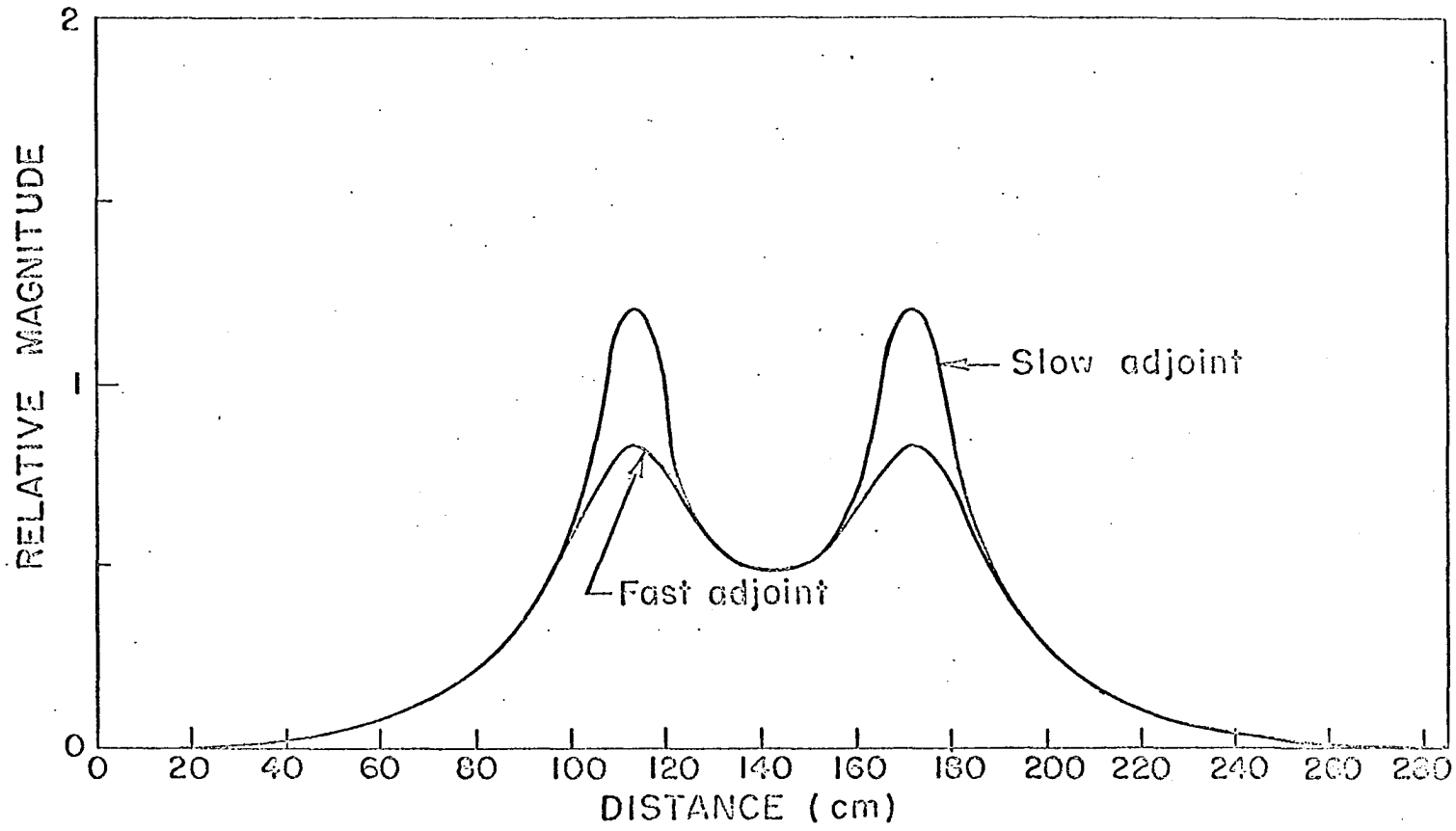

Figure II.3. UTR-10 prototype reactor adjoint distributions.

The adjoint function, Figure II.3, is frequently called the importance function and may be thought of as a relative measure of the worth, or importance, of a neutron in sustaining a chain reaction (24). As the cores were moved together the slow adjoint distribution changed little while the fast adjoint distribution became much flatter in and between the cores. The fact that the fast adjoint was almost constant in and between the cores suggests that a fast neutron at any point in these regions has about the same worth for sustaining the chain reaction.

When a flux tilt was desired, it was produced by selectively changing the thermal absorption cross section in one core and adjusting the cross section in the other core until the reactor was critical. This caused the reactivities of the two cores to be different and resulted in the flux tilt. For small tilts, 1.4:1 or less, the characteristics of the flux shapes were not changed but only shifted in magnitude relative to one another, as is illustrated in Figure V.13.

B. Evaluation of Space Modes

The basic assumption of modal analysis is that the flux can be represented by a sum of products of space-dependent modes and time-dependent coefficients

$$\varphi(x,t) \cong \sum_{i=1}^{N} \psi_i(x) a_i(t).$$

These space modes are obtained by solving Equations C.28 and C.29 from Appendix C. If N, the number of modes used in the approximation,is chosen to be five so that one mode is present to represent each region of the prototype reactor, the set of modes for the fluxes and adjoints illustrated in Figures II.4, II.5, II.6 and II.7 is obtained. To minimize confusion only the modes representing the first three regions of the reactor are illustrated except in Figure II.4 where all five are shown. For the symmetric case being considered, the modes representing regions 1 and 2 are mirror images of those representing regions 5 and 4 respectively.

The Green's Function modes in themselves contain a considerable amount of information about the reactor. Figure II.4 is a graph of the fast-flux modes where the wide modes representing the fuel regions, regions 2 and 4, illustrate the effect of the large diffusion length of fast neutrons. This allows them to be present in significant numbers relatively far from where they originated. The modes representing regions 1, 3, and 5 are negative and much smaller than the positive source modes of regions 2 and 4. These reflector modes have been plotted to a different scale so that their shapes can be more easily seen and they are negative because of the negative fast-neutron sources in these regions. That is, fast neutrons are removed from the fast group in the reflectors by

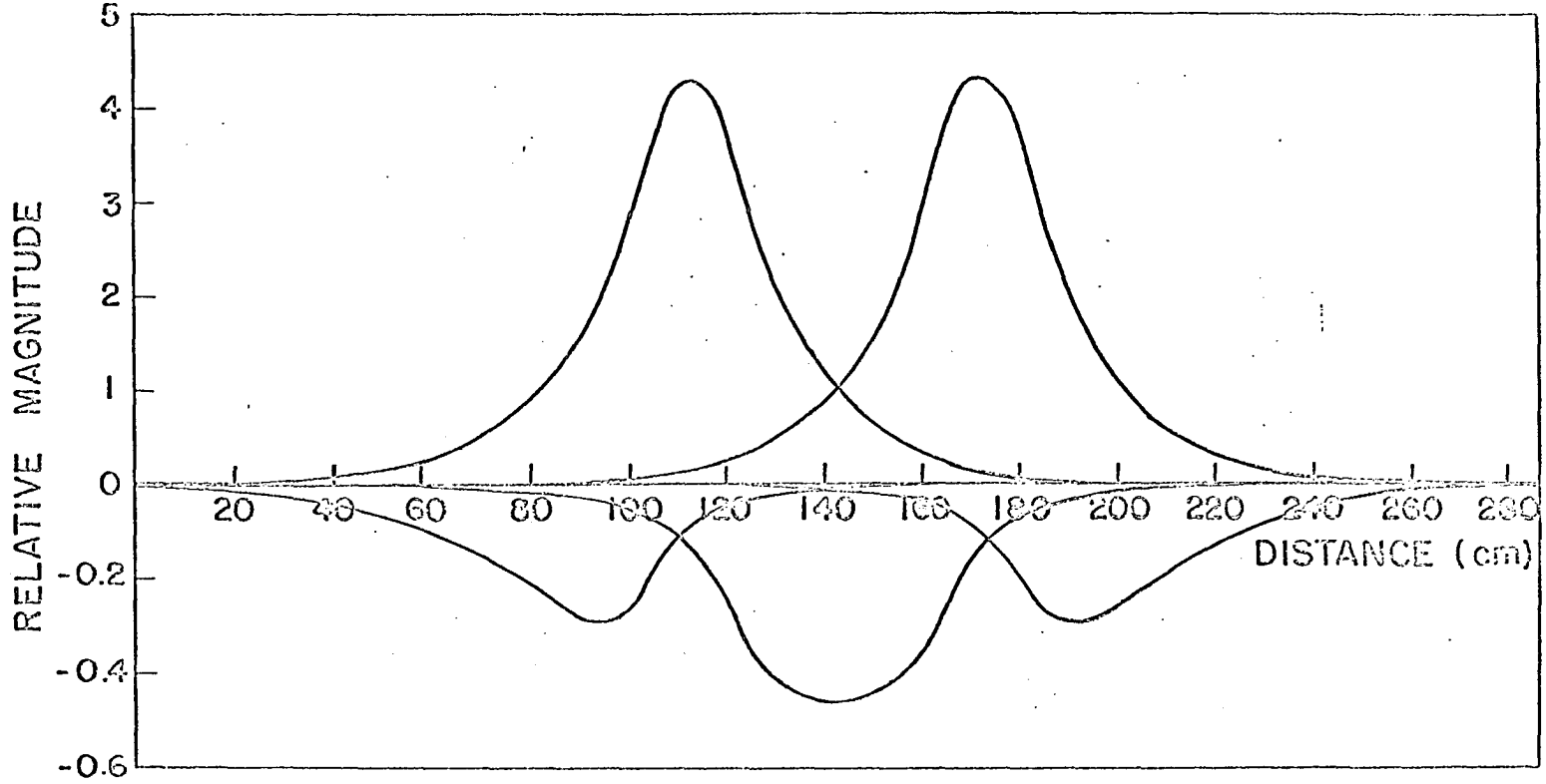

Figure II.4. Fast flux modes.

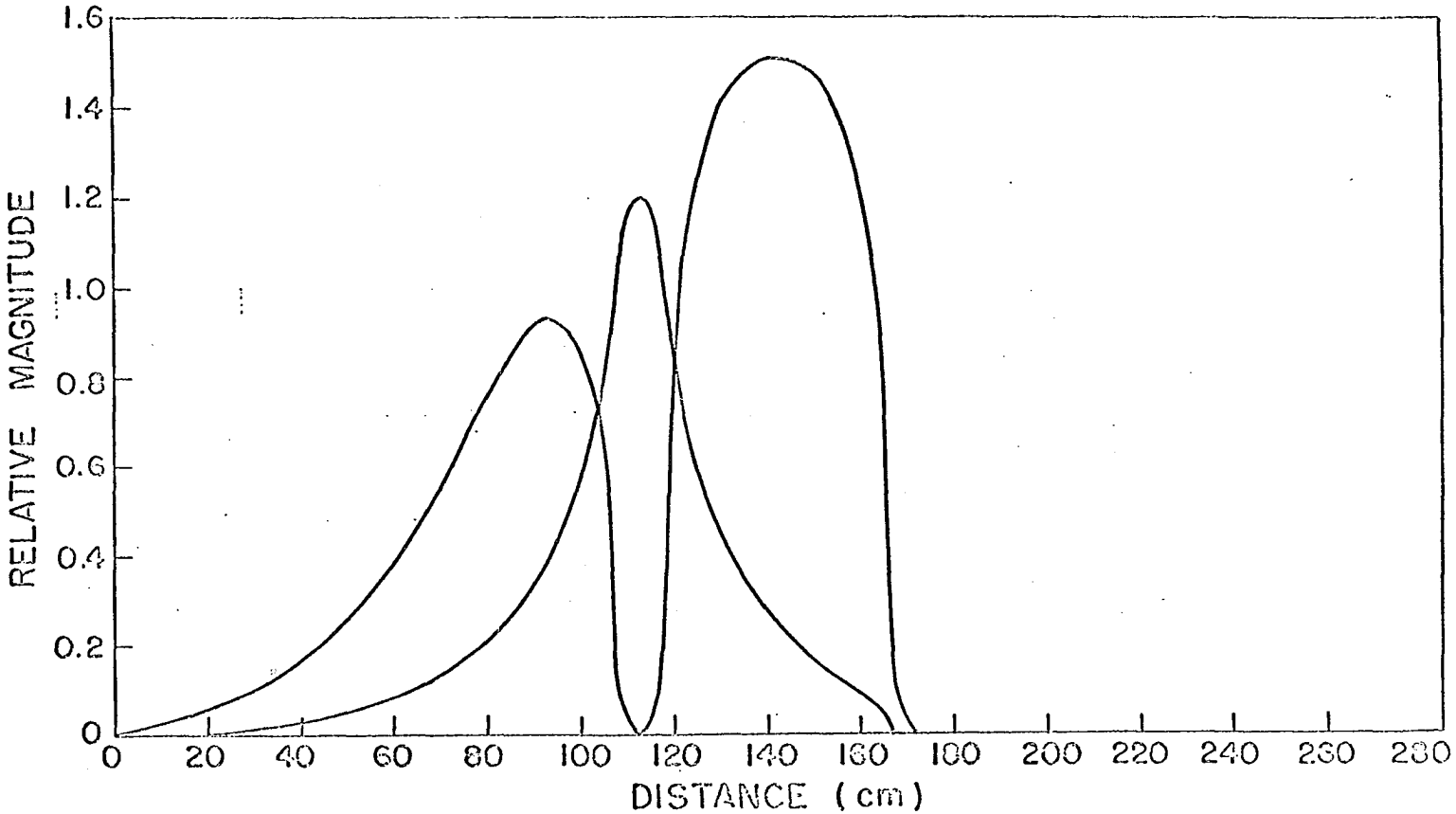

Figure II.5. Slow flux modes.

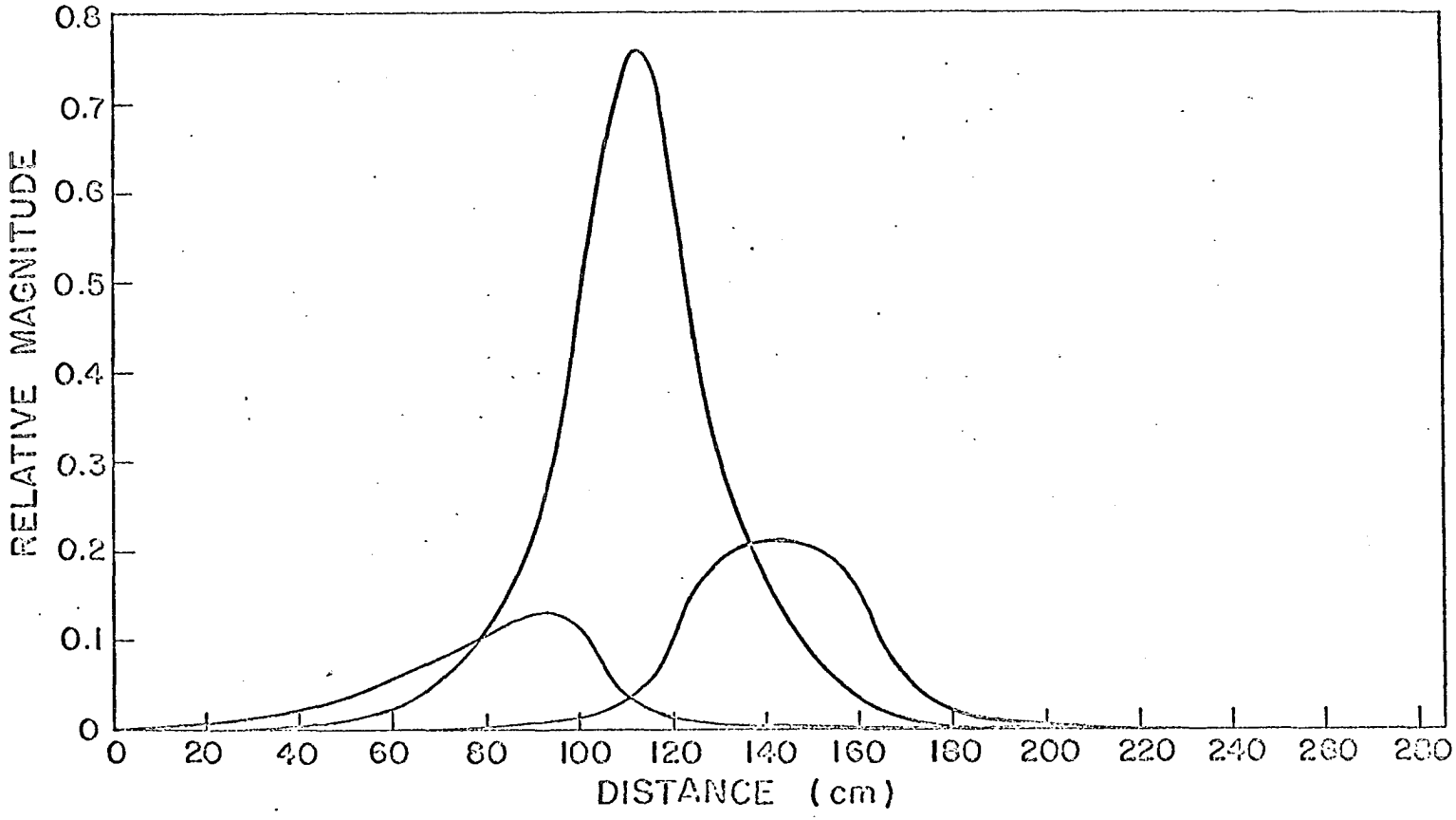

Figure II.6. Fast adjoint modes.

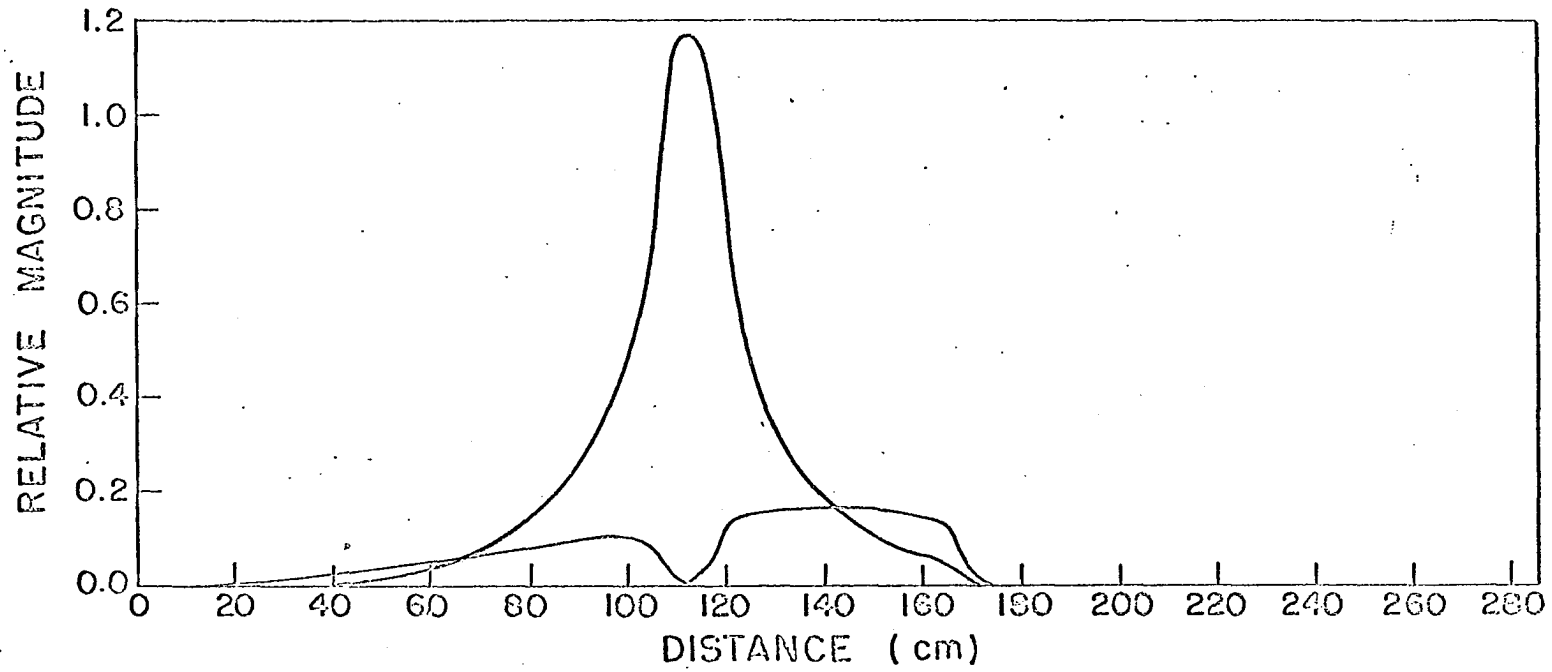

Figure II.7. Slow adjoint modes.

leakage and by slowing down to the thermal group.

Figure II.5 represents the thermal-group modes and illustrates the effect of the difference in the diffusion coefficient and cross section between the multiplying and nonmultiplying regions. An effect of the large absorption cross section in the fuel is that the reflector modes are essentially completely attenuated in passing through the fuel regions. This implies that the reflector regions are decoupled from each other as far as direct exchange of thermal neutrons is concerned. Consequently a thermal source placed in one reflector would be completely attenuated in passing through a fuel region. However, this applies only to the original source neutrons and not to any progeny produced by fission within the core. The thermal-group modes for the reflector regions are positive and caused by the thermal neutron source due to the slowing down of fast neutrons in these regions.

From Figure II.6 it can be seen that the fast-adjoint modes are similar to the fast-flux modes except that the adjoint modes for the fuel regions are more strongly peaked. This reflects the fact that loss by fast leakage is only slightly less than loss by fast removal in the moderator. In the fuel, removal by slowing down dominates and production of thermal neutrons in the fuel is very important in sustaining the chain reaction. The most obvious difference between the fast-adjoint modes and the fast modes is that

the fast-adjoint reflector modes are positive. This indicates that a fast neutron in the reflector has a definite worth to the system and reflects the fact that absorption in the direct system results in a source in the adjoint system since the two are duals of each other.

The slow-adjoint modes of Figure II.7 illustrate many phenomena similar to those discussed above so the arguments will not be repeated.

C. Synthesis of the Frequency Response

The technique used to obtain the frequency-dependent coefficients of the space modes is the simidirect method of the calculus of variations. In applying this technique the approximations for the fluxes

$$\varphi(x,t) \cong \sum_{i=1}^{N} \psi_i(x) a_i(t) \tag{II.6}$$

and for the adjoints

$$\varphi^+(x,t) \cong \sum_{i=1}^{N} \psi_i^+(x) a_i^+(t) \tag{II.7}$$

are taken as the trial functions to be substituted into the functional, F, of Equation II.8 and the Euler-Lagrange equations for II.8, which are the equations defining the coefficients of the space modes, are the reduced neutron kinetics equations.

After substituting the trial functions, II.6 and II.7,

into the functional, the procedure is to integrate the functional with respect to space, take the variation of the reduced time-dependent equation with respect to the adjoint variable, set the variation equal to zero, and solve the resulting set of equations for the frequency-dependent coefficients of the direct system.

The functional used by Dougherty and Shen is a modification, to allow a natural-current boundary condition, of a functional first proposed by Selengut (37). The modified functional is

$$F[\varphi^+,\varphi] = \int_0^\tau \int_{x_o}^{x_n} dtdx\{\bar{\Phi}^{+^T} v^{-1} \frac{\partial \bar{\Phi}}{\partial t} + \frac{\partial \bar{\Phi}^{+^T}}{\partial x} \mathcal{D} \frac{\partial \Phi}{\partial x} - \Phi^{+^T} H \Phi\} . \tag{II.8}$$

where

$$\Phi^{+^T} = [\varphi_F^+ \varphi_S^+] \quad \text{and} \quad \Phi = \text{col}[\varphi_F \varphi_S]$$

Substitution of the representation of the two-group diffusion equations from Appendix C into Equation II.8 gives

$$F[\varphi_F^+,\varphi_S^+,\varphi_F,\varphi_S] = \int_0^\tau \int_{x_o}^{x_n} dtdx\{[\varphi_F^+\varphi_S^+] \begin{bmatrix} v_F^{-1} & 0 \\ 0 & v_S^{-1} \end{bmatrix} \frac{\partial}{\partial t} \begin{bmatrix} \varphi_F \\ \varphi_S \end{bmatrix}$$

$$+ \frac{\partial}{\partial x} [\varphi_F^+\varphi_S^+] \begin{bmatrix} D_F & 0 \\ 0 & D_F \end{bmatrix} \frac{\partial}{\partial x} \begin{bmatrix} \varphi_F \\ \varphi_S \end{bmatrix} - [\varphi_F^+\varphi_S^+] \begin{bmatrix} -\Sigma_{re} & G \\ \Sigma_r & -\Sigma_{ae} \end{bmatrix} \begin{bmatrix} \varphi_F \\ \varphi_S \end{bmatrix} . \tag{II.9}$$

Multiplying out the matrix form of the functional, F becomes

$$F[\varphi_F^+, \varphi_s^+, \varphi_F, \varphi_s] = \int_0^\tau \int_{x_o}^{x_n} dt dx \Big(\varphi_F^+ v_F^{-1} \frac{\partial \varphi_F}{\partial t} + \varphi_s^+ v_s^{-1} \frac{\partial \varphi_s}{\partial t}$$

$$+ \frac{\partial \varphi_F^+}{\partial x} D_F \frac{\partial \varphi_F}{\partial x} + \frac{\partial \varphi_s^+}{\partial x} D_s \frac{\partial \varphi_s}{\partial x} + \varphi_F^+ \Sigma_{re} \varphi_F - \varphi_F^+ G \varphi_s$$

$$- \varphi_s^+ \Sigma_r \varphi_F + \varphi_s^+ \Sigma_{ae} \varphi_s \Big) \ . \qquad \text{(II.10)}$$

To simplify exposition, the approximation II.6

$$\varphi(x,t) \cong \sum_{i=1}^{N} \psi_i(x) a_i(t)$$

will be rewritten in an equivalent matrix form as

$$\varphi(x,t) \cong \psi(x) a(t) \ , \qquad \text{(II.11)}$$

where

$$\psi(x) = [\psi_1(x), \psi_2(x), \ \ldots, \ \psi_N(x)] \qquad \text{(II.12)}$$

and

$$a^T(t) = [a_1(t), a_2(t), \ \ldots, \ a_N(t)] \ . \qquad \text{(II.13)}$$

Substituting this simplified description of the approximation into the integrand of II.10 yields

$$F = \int_0^\tau \int_{x_o}^{x_n} dt dx \Big(\psi_F^+ a_F^+ v_F^{-1} \frac{\partial a_F}{\partial t} + \psi_s^+ a_s^+ v_s^{-1} \psi_s \frac{\partial a_s}{\partial t}$$

$$+ \frac{\partial \psi_F^+}{\partial x} a_F^+ D_F \frac{\partial \psi_F}{\partial x} a_F + \frac{\partial \psi_s^+}{\partial x} a_s^+ D_s \frac{\partial \psi_s}{\partial x} a_s + \psi_F^+ a_F^+ \Sigma_{re} \psi_F a_F - \psi_F^+ a_F^+ G \psi_s a_s$$

$$- \psi_s^+ a_s^+ \Sigma_r \psi_F a_F + \psi_s^+ a_s^+ \Sigma_{ae} \psi_s a_s \Big) \qquad \text{(II.14)}$$

and integrating out the space dependence leaves the reduced functional

$$F = \int_0^T dt \left(\left\langle \psi_F^+ a_F^+ v_F^{-1} \psi_F \frac{\partial a_F}{\partial t} \right\rangle + \left\langle \psi_s^+ a_s^+ v_s^{-1} \psi_s \frac{\partial a_s}{\partial t} \right\rangle \right.$$

$$+ \left\langle \frac{\partial \psi_F^+}{\partial x} a_F^+ D_F \frac{\partial \psi_F}{\partial x} a_F \right\rangle + \left\langle \frac{\partial \psi_s^+}{\partial x} a_s^+ D_s \frac{\partial \psi_s}{\partial x} a_s \right\rangle + \left\langle \psi_F^+ a_F^+ \Sigma_{re} \psi_F a_F \right\rangle$$

$$\left. - \left\langle \psi_F^+ a_F^+ G \psi_s a_s \right\rangle - \left\langle \psi_s^+ a_s^+ \Sigma_r \psi_F a_F \right\rangle + \left\langle \psi_s^+ a_s^+ \Sigma_{ae} \psi_s a_s \right\rangle \right) \qquad \text{(II.15)}$$

which is a function of only one independent variable, time. Where

$$\left\langle f(x) \right\rangle = \int_{\text{reactor}} f(x)dx \qquad \text{(II.16)}$$

The variational method now allows the evaluation of the coefficients of the direct modes by taking the variation of the functional with respect to the adjoint time-dependent coefficients and setting these variations equal to zero. This yields equations of the form

$$\frac{\delta F}{\delta a_{F_i}^+} = \left\langle \varphi_{F_i}^+ v_F^{-1} \psi_F \frac{\partial a_F}{\partial t} + \frac{\partial \psi_{F_i}^+}{\partial x} D_F \frac{\partial \psi_F}{\partial x} a_F \right.$$

$$\left. + \psi_{F_i}^+ \Sigma_{re} \psi_F a_F - \psi_{F_i}^+ G \psi_s a_s \right\rangle = 0 \qquad \text{(II.17)}$$

and

$$\frac{\delta F}{\partial a_{s_i}^+} = \left\langle \psi_{s_i}^+ v_s^{-1} \psi_s \frac{\partial a_s}{\partial t} + \frac{\partial \psi_{s_i}^+}{\partial x} D_s \frac{\partial \psi_s}{\partial x} a_s \right.$$

$$\left. - \psi_{s_i}^+ \Sigma_r \psi_F a_F + \psi_{s_i}^+ \Sigma_{ae} \psi_s a_s \right\rangle = 0 \, . \qquad \text{(II.18)}$$

Now let $A = \text{col}[a_F a_s]$ and represent $\frac{\partial A}{\partial t}$ as $\dot{A}$. Then the set

of equations represented by Equations II.17 and II.18 may be written as

$$\Lambda \dot{A} = KA \tag{II.19}$$

or in expanded form

$$\begin{bmatrix} \left\langle \psi_{F_i}^{+} v_F^{-1} \psi_{F_j} \right\rangle_{ij} & 0 \\ 0 & \left\langle \psi_{s_i}^{+} v_s^{-1} \psi_{s_j} \right\rangle_{ij} \end{bmatrix} \begin{bmatrix} \dot{a}_F \\ \dot{a}_s \end{bmatrix} =$$

$$\begin{bmatrix} -\left\langle \frac{\partial \psi_{F_i}^{+}}{\partial x} D_F \frac{\partial \psi_{F_j}}{\partial x} + \psi_{F_i}^{+} \Sigma_{re} \psi_{F_j} \right\rangle_{ij} & \left\langle \psi_{F_i}^{+} G \psi_{s_j} \right\rangle_{ij} \\ \left\langle \psi_{s_i}^{+} \Sigma_r \psi_{F_j} \right\rangle_{ij} & -\left\langle \frac{\partial \psi_{s_i}^{+}}{\partial x} D_s \frac{\partial \psi_{s_j}}{\partial x} + \psi_{s_i}^{+} \Sigma_{ae} \psi_{s_j} \right\rangle_{ij} \end{bmatrix} \begin{bmatrix} a_F \\ a_s \end{bmatrix}.$$

To simplify the writing of the K matrix let

$$\Lambda_F = \left\langle \psi_{F_i}^{+} v_F^{-1} \psi_{F_j} \right\rangle_{ij}$$

$$\Lambda_s = \left\langle \psi_{s_i}^{+} v_s^{-1} \psi_{s_j} \right\rangle_{ij}$$

$$\xi = \left\langle \frac{\partial \psi_{F_i}^{+}}{\partial x} D_F \frac{\partial \psi_{F_j}}{\partial x} + \psi_{F_i}^{+} \Sigma_{re} \psi_{F_j} \right\rangle_{ij}$$

$$\mu = \left\langle \psi_{F_i}^{+} G \psi_{s_j} \right\rangle_{ij}$$

$$\varsigma = \left\langle \psi_{si}^{+} \Sigma_r \psi_{F_j} \right\rangle_{ij}$$

$$\eta = \left\langle \frac{\partial \psi_{s_i}^{+}}{\partial x} D_s \frac{\partial \psi_{s_j}}{\partial x} + \psi_{s_i}^{+} \Sigma_{ae} \psi_{s_j} \right\rangle_{ij}$$

so that II.19 becomes

$$\begin{bmatrix} \Lambda_F & 0 \\ 0 & \Lambda_s \end{bmatrix} \begin{bmatrix} \dot{a}_F \\ \dot{a}_s \end{bmatrix} = \begin{bmatrix} -\xi & \mu \\ \zeta & -\eta \end{bmatrix} \begin{bmatrix} a_F \\ a_s \end{bmatrix} . \qquad \text{(II.20)}$$

The time dependence of the slow absorption cross section is assumed to be of the form

$$\Sigma_a(t) = \Sigma_a(0) + \Delta\Sigma_a e^{j\omega t} \qquad \text{(II.21)}$$

where $\Sigma_a(0)$ is the value of the cross section at which the reactor is just critical and $\Delta\Sigma_a e^{j\omega t}$ represents a sinusoidal oscillation of magnitude $\Delta\Sigma_a$ and frequency ω. The matrices μ and η may be expanded into components as follows

$$\mu = \mu_p + \mu_d = \left\langle \psi^+_{F_i} \nu\Sigma_f(1-\beta)\psi_{s_j} \right\rangle_{ij} + \left\langle \psi^+_{F_i} S_D \psi_{s_j} \right\rangle_{ij}$$

$$\eta = \eta_o + \Delta\eta(t) = \left\langle \frac{\partial \psi^+_{s_i}}{\partial x} D_s \frac{\partial \psi_{s_j}}{\partial x} + \psi^+_{s_i} \Sigma^o_a e \psi_{s_j} \right\rangle_{ij}$$

$$+ \left\langle \psi^+_{s_i} \Delta\Sigma_a e^{j\omega t} \psi_{s_j} \right\rangle_{ij}$$

and the operator S_D can be rewritten to allow a convenient evaluation of the delayed-neutron contribution to a sinusoidal driving function. From Appendix C

$$S_D\varphi_s(x,t) = \nu\Sigma_f \sum_{i=1}^{M} \lambda_i \beta_i \int_{-\infty}^{t} \varphi_s(x,\tau) e^{-\lambda_i(t-\tau)} d\tau$$

and in a general modal representation of the problem $\varphi_s(x,\tau)$ becomes $\sum_{j=1}^{N} \psi_{s_j}(x) a_{s_j}(\tau)$. Since small sinusoidal

perturbations are made, the reactor response will be approximately linear and the output will be of the same form as the input. This allows the expansion of the vector, $A(t)$, in terms of an initial steady-state component, $A(0)$, and a perturbed component, $\Delta A(t) = \hat{A}e^{j\omega t}$, where $\hat{A}$ is a frequency-dependent complex number. For a particular mode then

$$a_{s_j}(t) = a_{s_j}(0) + \Delta a_{s_j}(t) \tag{II.22}$$

and the precursor concentration from a single modal component of the flux is

$$S_D\psi_{s_j}(x)a_{s_j}(t) = \psi_{s_j}(x)\nu\Sigma_f \sum_{i=1}^{M} \lambda_i\beta_i \int_{-\infty}^{t} [a_{s_j}(0) + \Delta a_{s_j}(t)]e^{-\lambda_i(t-\tau)}d\tau \tag{II.23}$$

where $\Delta a_{s_j}(t)$ represents the time-dependent portion of $a_j(t)$. Since $a_{s_j}(0) = 1$, the integral in II.23 can be rewritten as

$$\int_{-\infty}^{t} e^{-\lambda_i(t-\tau)}d\tau + \int_{-\infty}^{t} \Delta a_{s_j}(t)e^{-\lambda_i(t-\tau)}d\tau \tag{II.24}$$

and the first integral in II.24 can be evaluated directly

$$e^{-\lambda_i t}\int_{-\infty}^{t} e^{\lambda_i\tau}d\tau = e^{-\lambda_i t}\left(\frac{e^{\lambda_i t}}{\lambda_i} - \frac{e^{-\infty}}{\lambda_i}\right) = \frac{1}{\lambda_i} \quad . \tag{II.25}$$

The second integral in II.24 can be evaluated after observing that for the sinusoidal driving function

$$\Delta a_{s_j}(\tau) = \hat{a}_{s_j}e^{j\omega t} \quad , \tag{II.26}$$

where $\hat{a}_{s_j}$ is a complex variable which is a function of frequency. Substitution of II.26 into the second integral of II.24 yields

$$\int_{-\infty}^{t} \hat{a}_j e^{j\omega t} e^{-\lambda_i (t-\tau)} d\tau = \hat{a}_j e^{-\lambda_i t} \int_{-\infty}^{t} e^{\tau(\lambda_i + j\omega)} d\tau$$

$$= \hat{a}_j e^{-\lambda_i t} \left[\frac{e^{\tau(\lambda_i + j\omega)}}{\lambda_i + j\omega}\right]_{-\infty}^{t} = \hat{a}_j \frac{(\lambda_i - j\omega)}{\lambda_i^2 + \omega^2} e^{j\omega t}. \quad \text{(II.27)}$$

Therefore the delayed-neutron contribution, $S_D \psi_{s_j}(x) a_{s_j}(t)$, becomes

$$S_D \psi_{s_j}(x) a_{s_j}(t) = \psi_{s_j}(x) \nu\Sigma_f \sum_{i=1}^{M} \lambda_i \beta_i \left[\frac{1}{\lambda_i} + \frac{\hat{a}_j (\lambda_i + j\omega)}{\lambda_i^2 + \omega^2} e^{j\omega t}\right], \quad \text{(II.28)}$$

or for one group of delayed neutrons

$$S_D \psi_{s_j}(x) a_{s_j}(t) = \psi_{s_j}(x) \nu\Sigma_f \beta + \left(\frac{\nu\Sigma_f \lambda^2 \beta}{\lambda^2 + \omega^2} + j \frac{\omega \nu\Sigma_f \lambda \beta}{\lambda^2 + \omega^2}\right) e^{j\omega t}. \quad \text{(II.29)}$$

The delayed-neutron contribution consists of a steady-state part plus a real and an imaginary oscillating component. These last two contributions are frequency dependent and their contributions become negligible when the frequency, ω, is large compared to the delayed-neutron decay constant, λ. This is consistent with the usual assumptions and observations.

It is convenient to rewrite the K matrix as being due to a sum of different contributions, that is

$$\begin{bmatrix} -\xi & \mu_p+\mu_d \\ \zeta & -(\eta_o+\Delta\eta(t)) \end{bmatrix} = \begin{bmatrix} -\xi & \mu_p \\ \zeta & -\eta_o \end{bmatrix} + \begin{bmatrix} 0 & \mu_d \\ 0 & 0 \end{bmatrix} + \begin{bmatrix} 0 & 0 \\ 0 & -\Delta\eta(t) \end{bmatrix}$$

or

$$K = K_p + K_d + \delta K$$

where K_p represents the contribution due to prompt neutrons

K_d represents the contribution due to delayed neutrons

δK represents the contribution due to the oscillating absorber.

The form of Equation II.19 now becomes

$$\Lambda\dot{A} = [K_p + K_d + \delta K]A \ . \qquad \text{(II.30)}$$

Substituting the form of the solution into II.30 gives

$$j\omega\Lambda\hat{A}e^{j\omega t} = [K_p + K_d + \delta K][A(0) + \hat{A}e^{j\omega t}] \ . \qquad \text{(II.31)}$$

Multiplying II.31 out, neglecting products of second order terms and recognizing that

$$K_pA_o + K_dA_o = [K_p + K_d]A_o = K_oA_o = \underline{0}$$

Equation II.31 reduces to

$$j\omega\Lambda\hat{A}e^{j\omega t} = K_p\hat{A}e^{j\omega t} + K_d\hat{A}e^{j\omega t} + \delta KA_o \ . \qquad \text{(II.32)}$$

From the definition of δK

$$\delta K = \begin{bmatrix} 0 & 0 \\ 0 & -\left\langle \psi^+_{s_j} \Delta\Sigma_a e^{j\omega t} \psi_{s_j} \right\rangle_{ij} \end{bmatrix} = e^{j\omega t}\ \varkappa \qquad \text{(II.33)}$$

so that substituting II.33 into II.32, the linearized equation becomes

$$[j\omega\Lambda - (K_p+K_d)]\hat{A} = \varkappa A_o. \qquad \text{(II.34)}$$

which in expanded form is

$$\begin{bmatrix} \xi+j\omega\Lambda_F & -(\mu_p+\mu_d) \\ -\zeta & \eta_o+j\omega\Lambda_s \end{bmatrix} \begin{bmatrix} a_F \\ a_s \end{bmatrix} = \begin{bmatrix} 0 \\ -\delta\eta(t) \end{bmatrix}. \qquad \text{(II.35)}$$

This equation can be solved directly for the complex oscillatory component of the flux from which the frequency response can be synthesized.

D. Block Diagram of Method of Solution Using Green's Function Modes

In order to clarify the procedure described in the previous three sections, the steps performed in this analysis are summarized below in block diagram form.

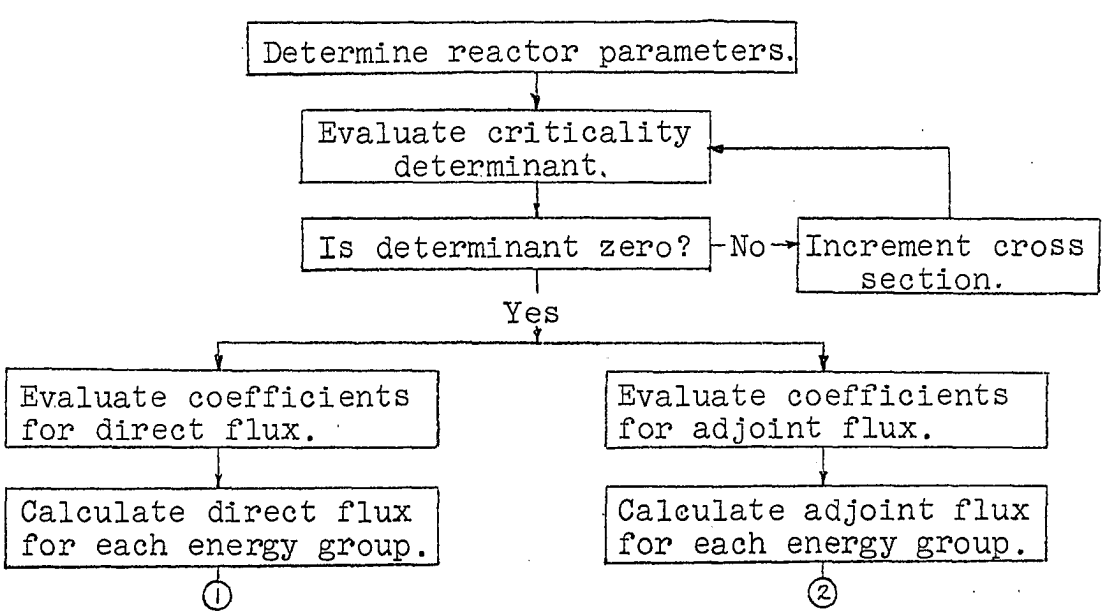

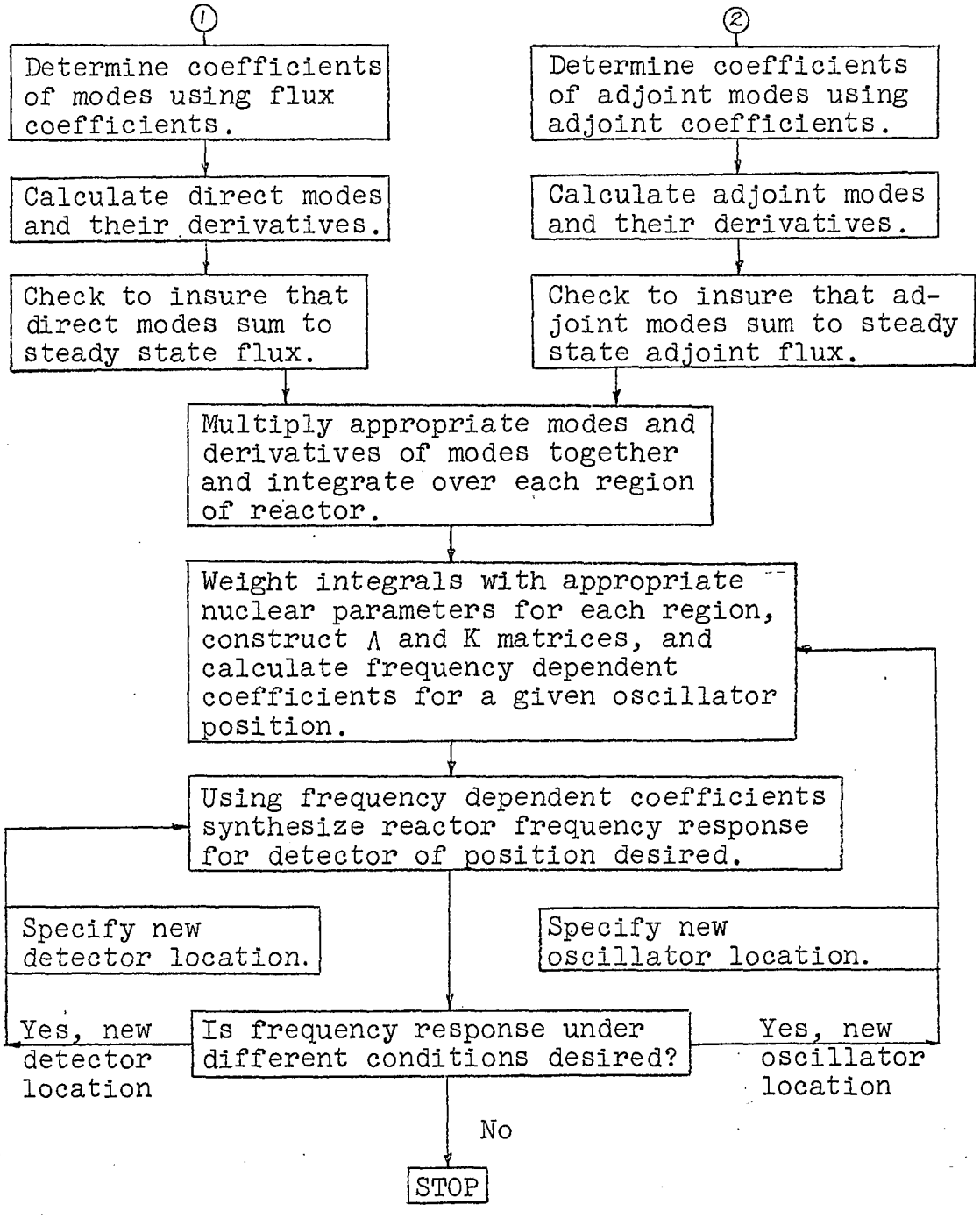

If a new reactor geometry or new material properties are required the calculation must begin at the beginning again with evaluation of a new criticality determinant for the system.

III. COMPARISON OF RESULTS FROM VARIOUS MODELS

A. The One-Point Model

The one-point model is the simplest description possible for a nuclear reactor and is presented as a reference to which the behavior of other descriptions can be compared. This comparison will be only heuristic and not in the hope that other models will duplicate the results of the one-point model.

The transfer functions considered in this study represent reactors in a state of power equilibrium. That is, the reactors are delayed critical. Some analyses have been performed for reactors in a state of period equilibrium and their transfer functions have been found to differ considerably from those of reactors at the steady state (8, 34, 38), but this will not be of concern here.

The well known one-point neutron kinetics equations including delayed neutrons are

$$\frac{dn(t)}{dt} = \frac{[(k_{eff} - \beta)-1]}{\ell} n(t) + \sum_{i=1}^{M} \lambda_i c_i(t) \qquad \text{(III.1)}$$

$$\frac{dc_i(t)}{dt} = \frac{k_{eff}\,\beta}{\ell} n(t) - \lambda_i c_i(t) \; . \qquad \text{(III.2)}$$

Applying the usual approximations of

$$k_{eff}(t) = k_{eff}(0) + \delta k e^{j\omega t} \qquad \text{(III.3)}$$

and M=1, the reactor transfer function can be shown to be

$$G_R(s) = \frac{\delta n(s)}{n_o \delta k(s)} = \frac{1}{\ell} \frac{(s+\lambda)}{s(s+\lambda+\beta/\ell)} \cong \frac{1}{\ell} \frac{(s+\lambda)}{s(s+\beta/\ell)} \qquad \text{(III.4)}$$

and the straight-line approximation of the Bode plot for this transfer function follows

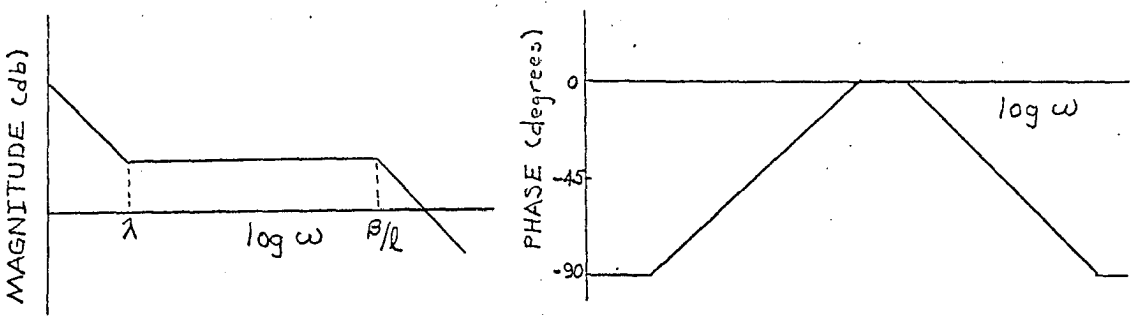

B. Avery's Two-Point Model

1. Oscillation of a core

The equations for the transfer function of a two-point reactor are derived using Avery's notation (4) in Appendix B. These equations were solved using the parameters of the UTR-10 prototype and the transfer functions and partial responses for a reactivity oscillation in core one are shown in Figures III.1, III.2 and III.3.

The response of core one, where it is the driving core, is shown in Figure III.1. This response is quite similar to that of the one-point model with breaks in the magnitude occurring at λ and β/ℓ rad/sec and with the slope of the magnitude curve being about 20 db/dec in the vicinity of the break and almost 20 db/sec at its asymptotic slope.

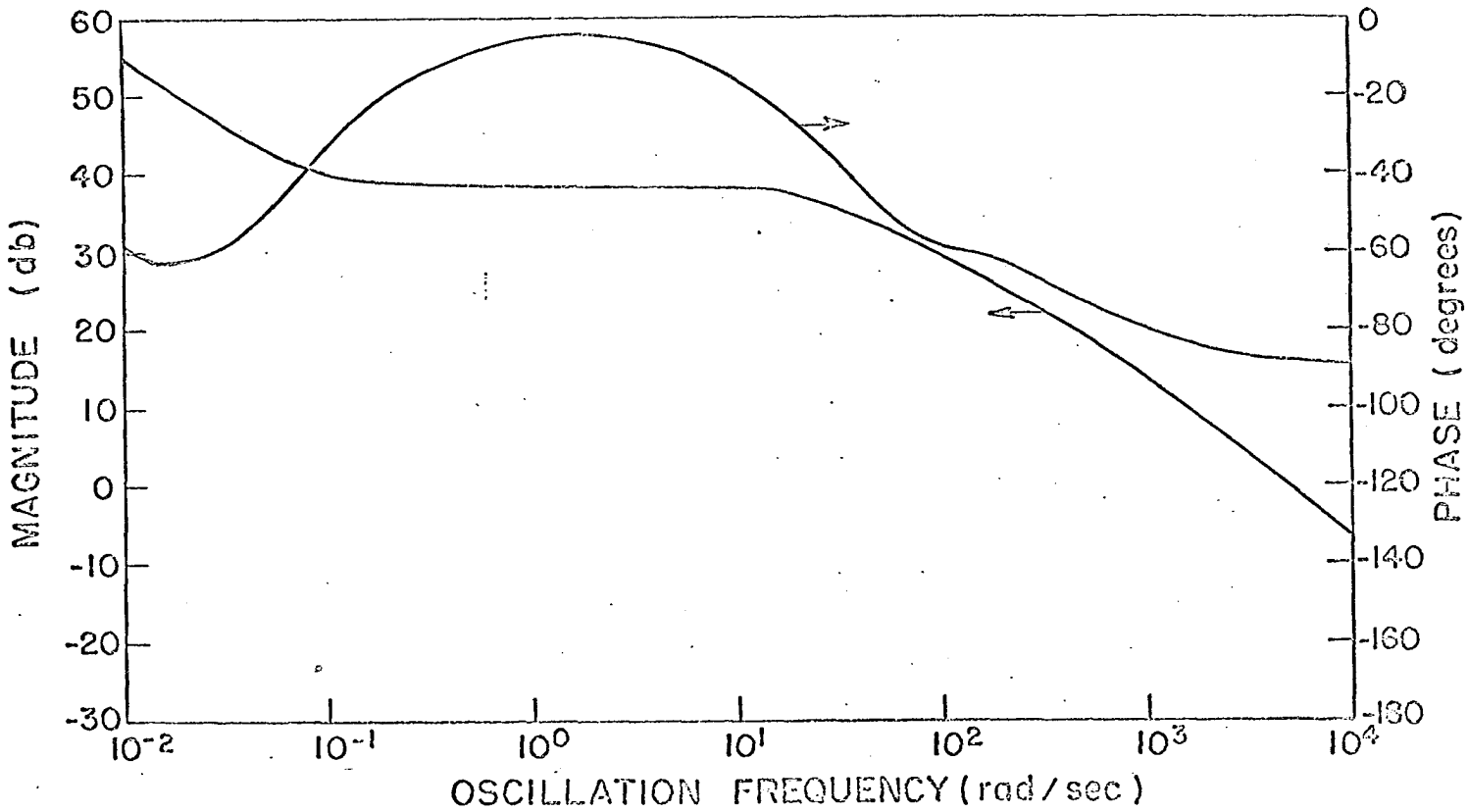

Figure III.1. Response of S_1 to oscillation of core one.

The phase behavior is also much like that of the one-point model except for the small bump in the several hundred radian region and except for the very-low frequency behavior. The decrease in the phase lag at very-low frequencies is characteristic of the phase behavior of subcritical reactors (28) and has also been observed when the two-point model is used to describe coupled fast-thermal systems (33).

The total source in core one, S_1, is due to the sum of component sources due to neutrons in core one which originated in core one, S_{11}, and due to neutrons in core one which originated in core two, S_{12}.

$$S_1 = S_{11} + S_{12}$$

Since the S_{11} type neutrons are the predominant type in core one the response of these neutrons is essentially identical to the overall response of the core, hence their response will not be plotted separately. However, when the response of S_{12} type neutrons is calculated, Figure III.2, an apparently previously unobserved behavior is evident. Instead of falling off at 20 db/dec after the β/ℓ break, the magnitude continues to roll-off to about 60 db/dec before quickly recovering. This recovery of the magnitude produces a sink at about 800-900 rad/sec.

A sink will be said to occur in the magnitude of the reactor response if the slope of the magnitude changes

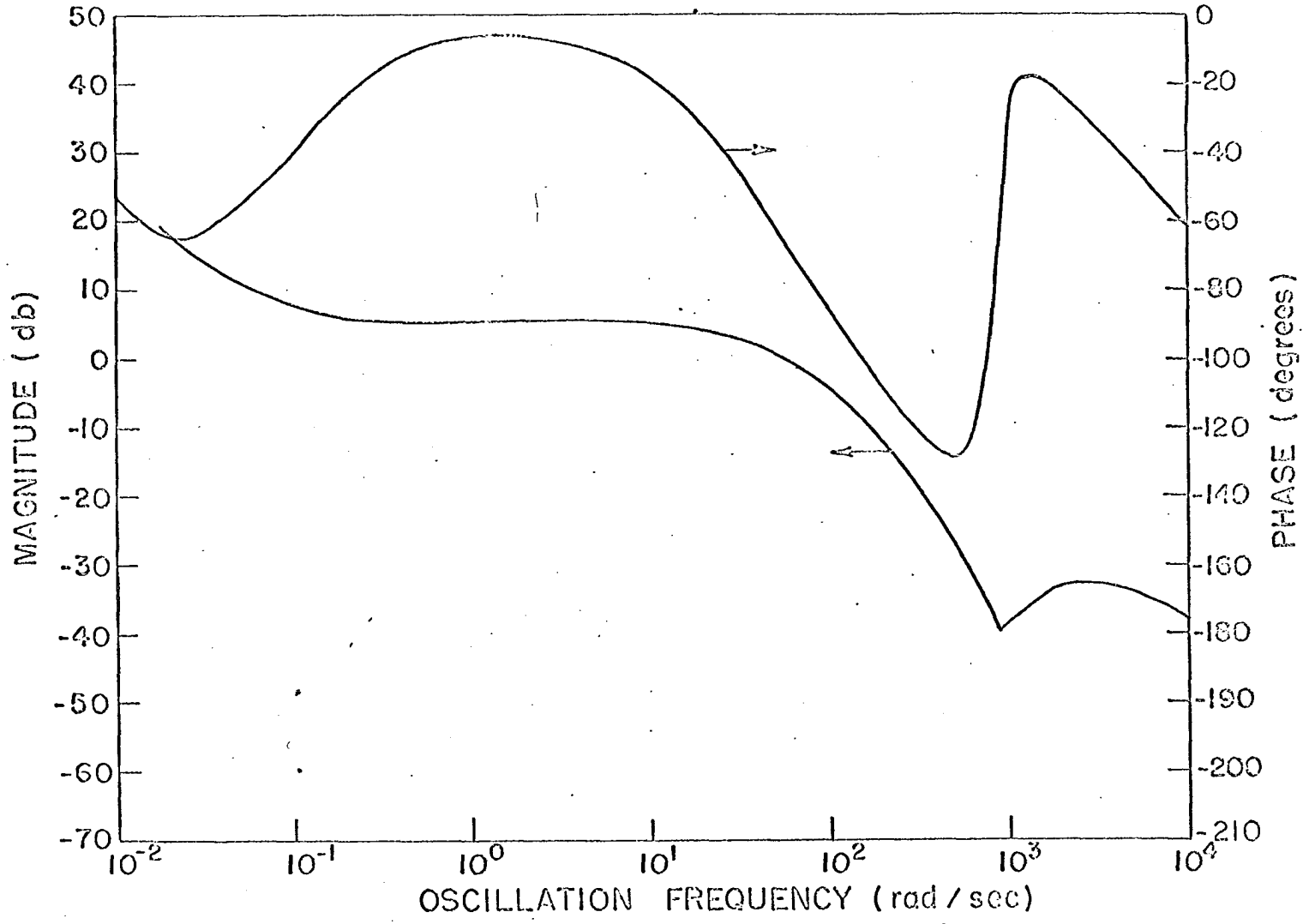

Figure III.2. Response of S_{12} to oscillation of core one.

sign from negative to positive at any point and the sink frequency is the frequency at which the sink occurs.

The phase behavior of the S_{12} population is much like that of the S_1 or S_{11} populations until the sink frequency is approached. Near the sink the phase lag undergoes a rapid decrease from about -130° to about -18° before it begins to increase again. Once past the sink the magnitude approaches an asymptotic slope of 20 db/dec and the phase becomes asymptotic to -90°.

A response similar to that of the S_{12} population is also found in the space-dependent model. The mechanism for the cause of both appears to be similar and a mechanism to explain the space-dependent results is proposed in Chapter IV. In the two-point model the sink occurs in neutron population group 12 but it is in the equivalent of the 21 group that the sink occurs in the two-group space-dependent model. Since the shapes of these responses are similar, a similar mechanism could cause them both and a time delay in the system seems capable of qualitatively describing both results. In the two-point model a sinusoidal oscillation in the neutron density is thought to propagate from core one to core two and return to core one 180° out of phase with the neutron density oscillation being generated in that core by the reactivity oscillation. This results in a partial cancellation of the neutron-density oscillation and causes a sink in the magnitude of the

reactor response.

Figure III.3 represents the response of core two to a sinusoidal oscillation of core one. The high-frequency response of the driven core, core two, is a result of the input signal--the output from core one--being filtered again. This produces a 40 db/dec slope in the magnitude beyond the β/ℓ break and an asymptotic phase lag of -180° instead of just -90°.

The response of the S_{22} population group is almost identical to that of the S_{11} response except that at high frequencies the phase lag continues to increase and does not approach an asymptote and the magnitude asymptotically approaches 40 db/dec. As would be expected the S_{21} response exhibits the same general behavior as the S_2 group.

2. Oscillation of the coupling

When the coupling between the two point cores is oscillated, the situation is much simpler than before and is analogous to placing a reactivity oscillator in the coupling region between the cores of a coupled-core reactor. In this case the response of each of the S_1 and S_2, S_{11} and S_{22}, and S_{12} and S_{21} population pairs is identical. Cores one and two are driven by an oscillating source and they respond with the usual source transfer function as seen in Figure III.4.

The response of the S_{11} and S_{22} population groups looks much like that shown in Figure III.4 up to 100 rad/sec, but

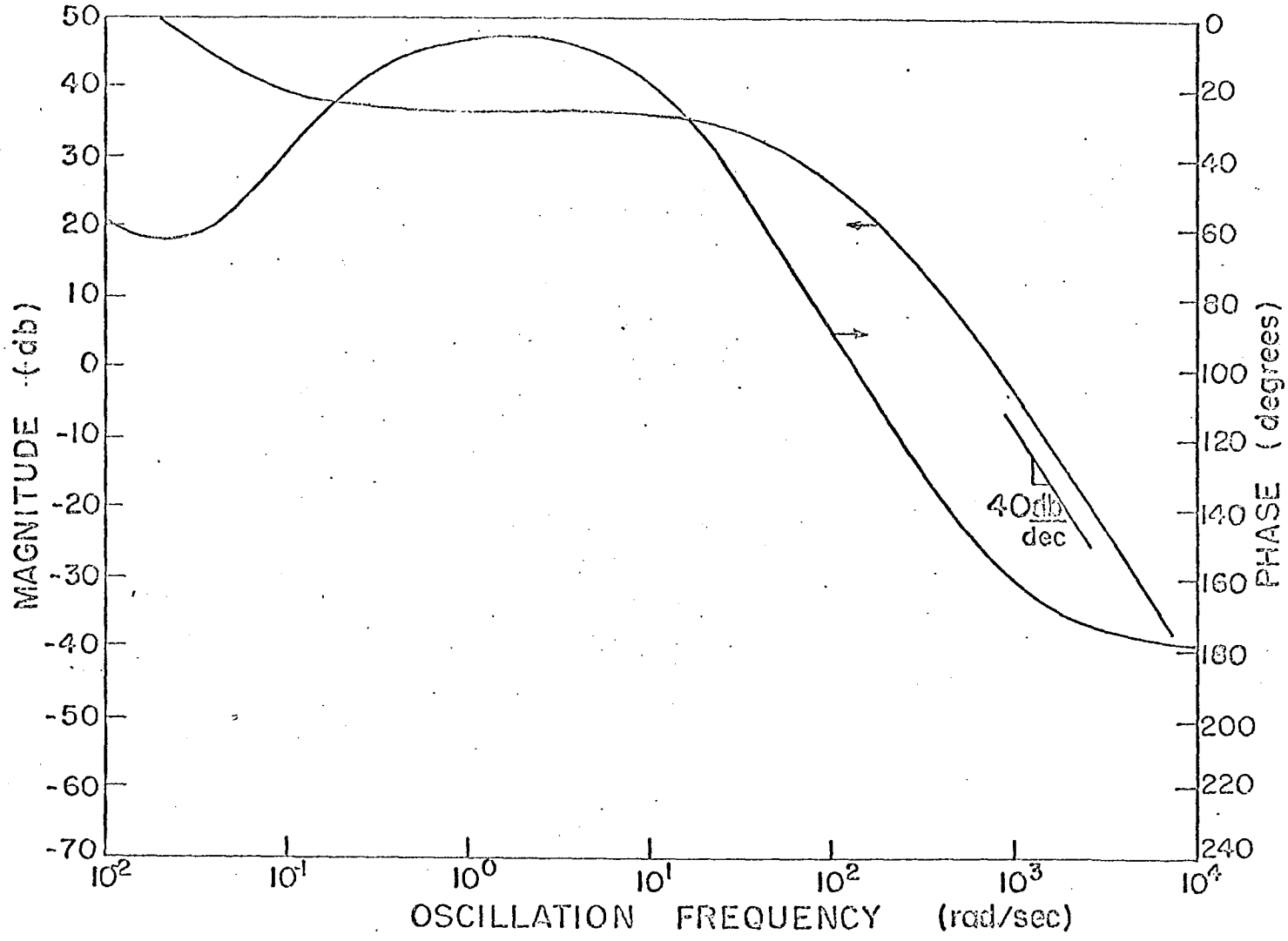

Figure III.3. Response of S_2 to oscillation of core one.

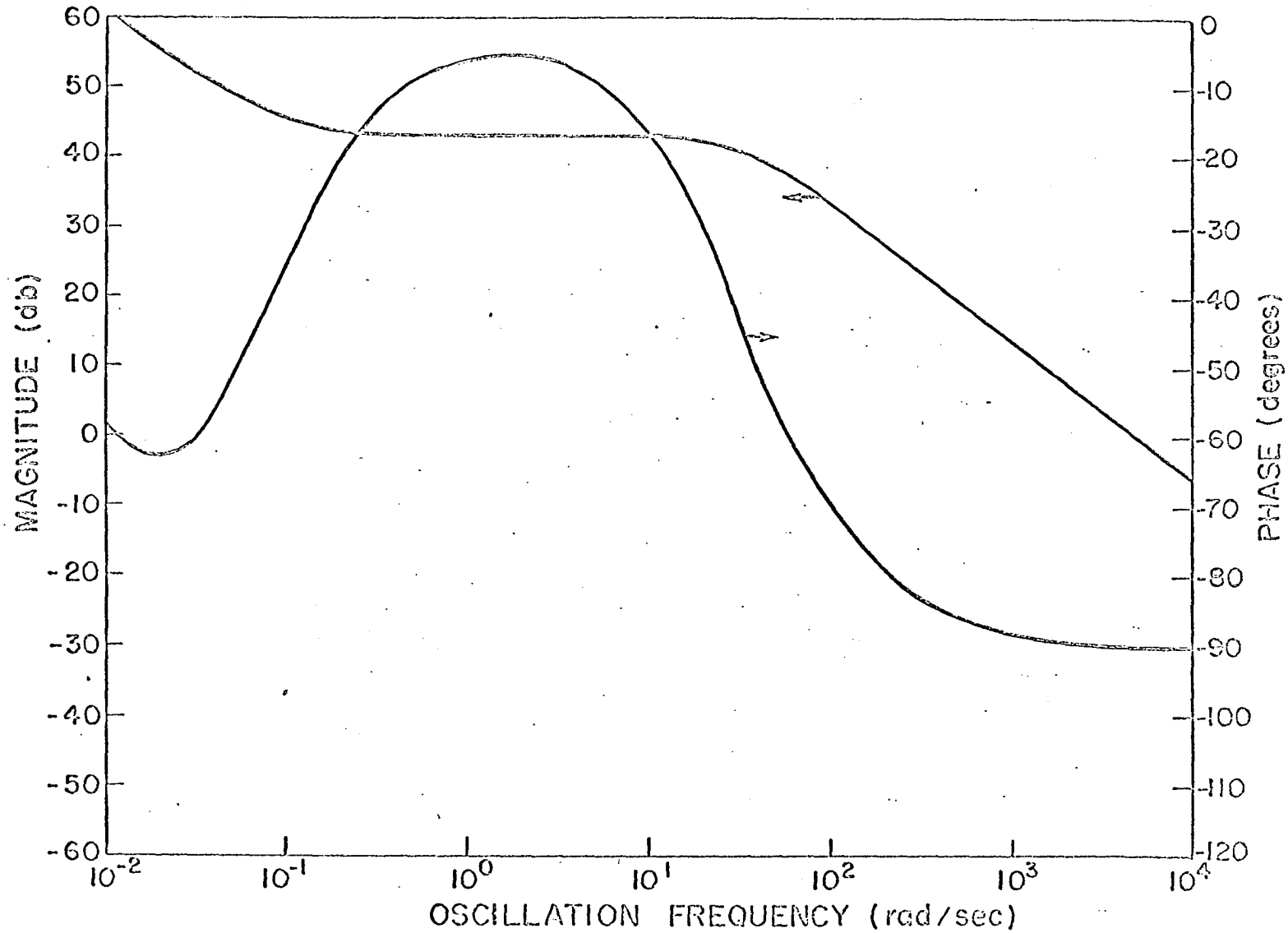

Figure III.4. Response of S_1 or S_2 to oscillation of coupling.

above this frequency the phase shift becomes larger and the magnitude attenuation is greater.

The S_{12}, or S_{21}, population response shows a broad leveling in the magnitude from 200-2000 rad/sec and a gradual phase reversal in this region. This behavior is again believed due to the interaction of exchange neutrons between cores.

These component responses are not described in detail since the results are presented only to provide background information and serve as a basis for comparison.

C. Green's Function Modal Analysis

In this section the convergence of the Green's Function modes will be investigated and some space dependent results will be presented. Green's Function modes are nonorthogonal and this makes the theoretical treatment of their convergence more difficult than the treatment of convergence for orthogonal sets of modes. However, convergence to an exact solution in the limit as the number of modes increases without bound is not necessarily of direct importance in engineering applications since physical requirements permit the use of only a finite (and small) number of modes. For this reason the most common method for determining convergence is to observe whether the solution changes appreciably when an extra mode is added to the approximation. If no

significant change is observable, the approximation is said to have converged.

Since one of the primary objectives of this study is to investigate spatially dependent effects, all of the spatially dependent magnitude responses in this study are normalized to 0 db at the lowest frequency plotted on each figure. This is done in order to make the effects caused by changing the oscillator and detector locations more apparent.

1. Two modes

When only two Green's Function modes are used to describe a coupled-core reactor it is reasonable to choose each of the modes to originate in a fuel region. If this is done it is not possible to obtain an adequate description of the system in either the time or the frequency domain. Figure III.5 represents a typical result when a plane oscillator and detector are located in the center of one core. No significant spatial dependence is predicted by the two-mode representation as the detector is moved about the reactor.

2. Five modes

It has been found that in order to describe a coupled nuclear system using Green's Function modes it is essential that a mode(s) representing the coupling region be present. These modes were first mathematically described by Carter (9,10) who also suggested that they were necessary for an adequate description of the time behavior of a coupled

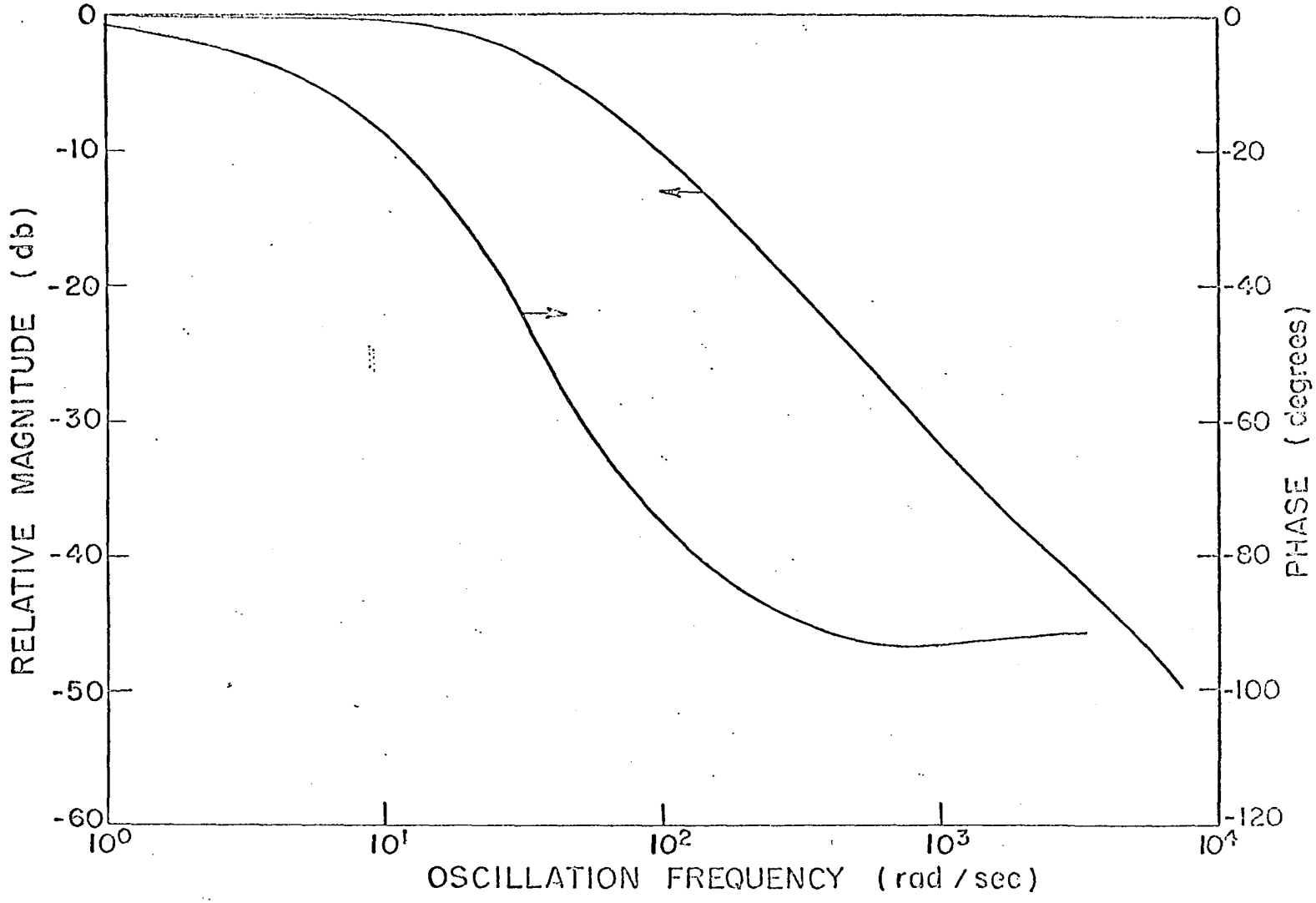

Figure III.5. Typical two-mode frequency response.

reactor. This was subsequently confirmed by McFadden[1] by comparison with an exact solution. This investigation used two, five, and seven mode representations to confirm that such modes are also required in order to obtain an adequate description of the system in the frequency domain.

A review of some of these results follows after a brief description of the model.

The dimensions of the one-dimensional model used to represent the UTR-10 reactor are shown in Figure II.1 and the oscillator and detector positions investigated in this study are illustrated in Figure III.6.

Detector locations are designated by the letters A through E in Figure III.6 and they are positioned in all the models used in this study so that the detectors A and E are 20 cm from the nearest fuel region interface and B, C, and D are located in the center of the left core tank, coupling region, and right core tank respectively.

The oscillator locations were taken to be: (1) 12 cm from the left fuel region, (2) in the center of the left fuel region, and (3) in the center of the coupling region. These locations correspond to possible access points in the Iowa State University UTR-10 reactor.

---

[1]McFadden, James, Ames, Iowa. Results of computer calculations. Private communication. 1968.

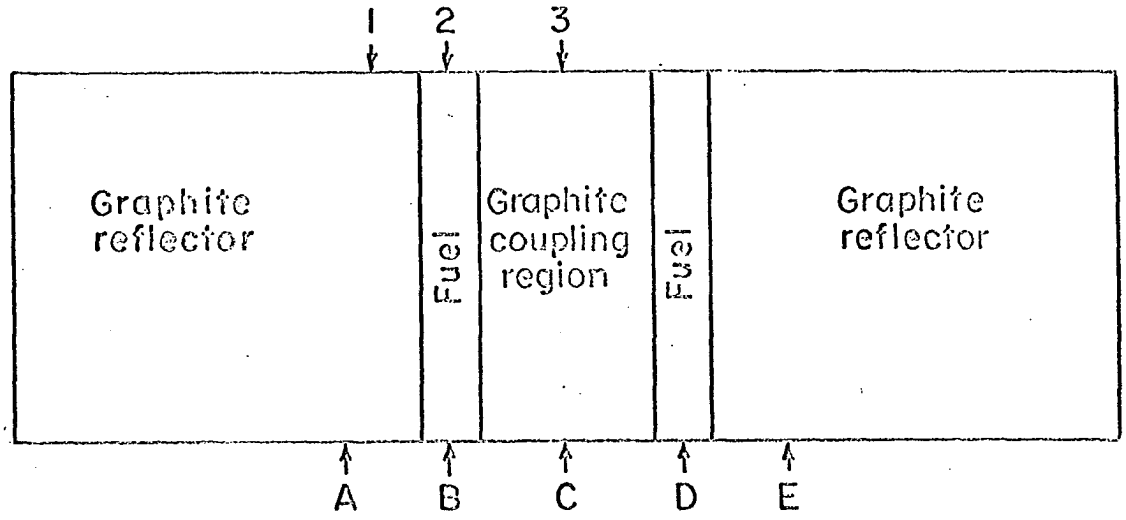

Figure III.6. Schematic diagram of UTR-10 reactor.

For a five-mode analysis each distinct material region of the reactor was represented by a mode. The derivations of the equations for these modes and the manipulation of the two-group neutron-diffusion equations into a form convenient for this analysis are shown in Appendix C. The equations which must be solved to determine the frequency-dependent coefficients for the synthesis of the frequency response are derived in Section II.D. The frequency response is synthesized by evaluating an equation of the form

$$\varphi(x, j\omega) \cong \sum_{i=1}^{N} \psi_i(x) a_i(j\omega)$$

where N is the number of modes in the expansion and x fixes the detector location. The oscillator location and type, i.e., energy dependence and size, were specified before the frequency-dependent coefficients were obtained.

Throughout the rest of this chapter a localized plane oscillator, with absorber in only the thermal group, will be assumed to be located in the center of the left core tank and the detector will be moved to positions A, B, C, D, and E.

Typical results for a five-mode analysis of the UTR-10 prototype reactor are illustrated in Figures III.7 and III.8. Fundamental differences, and some similarities, are apparent between these responses and the spatially dependent response of a conventional reactor.

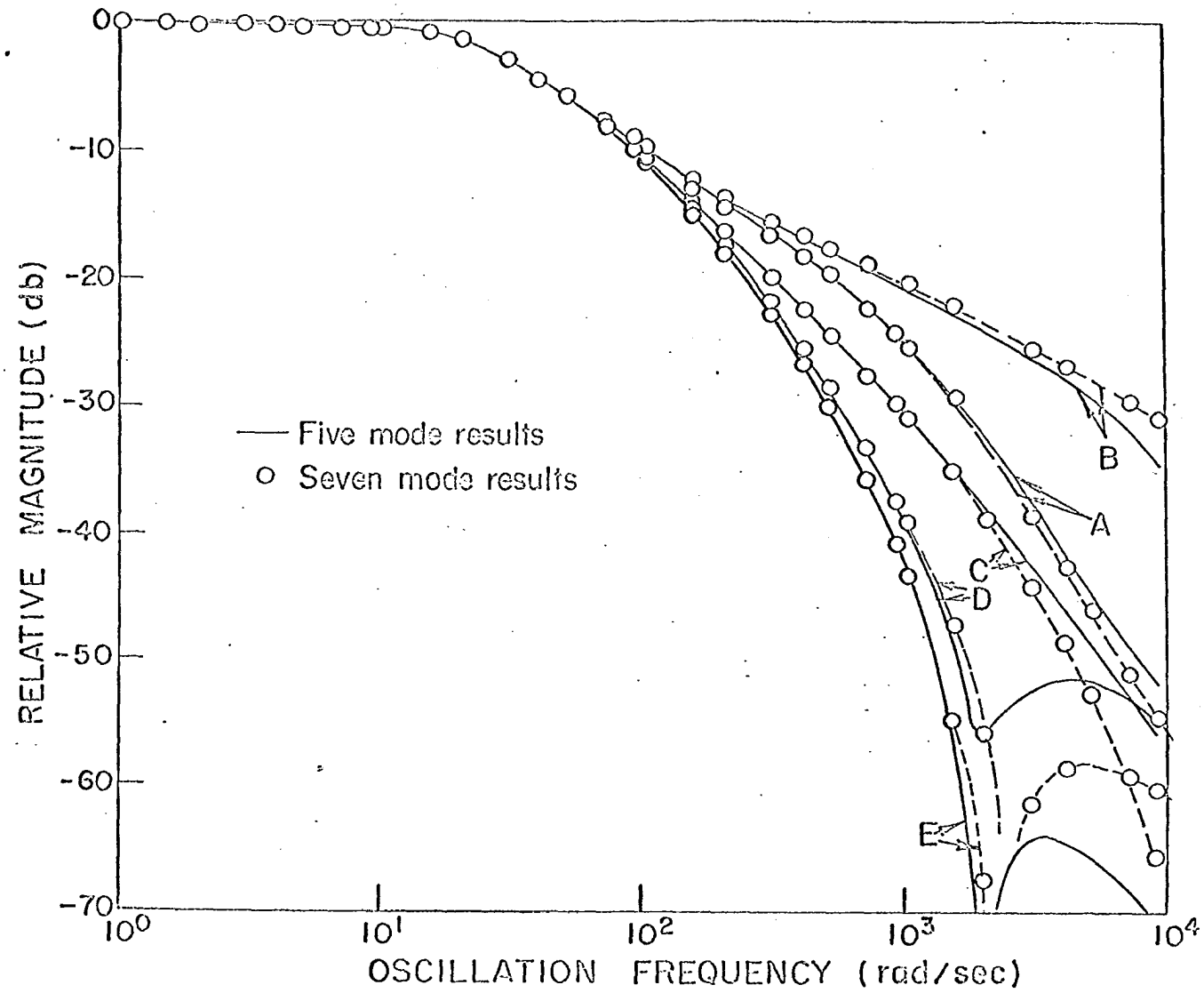

Figure III.7. Magnitude response of UTR-10 prototype reactor with oscillator at position 2.

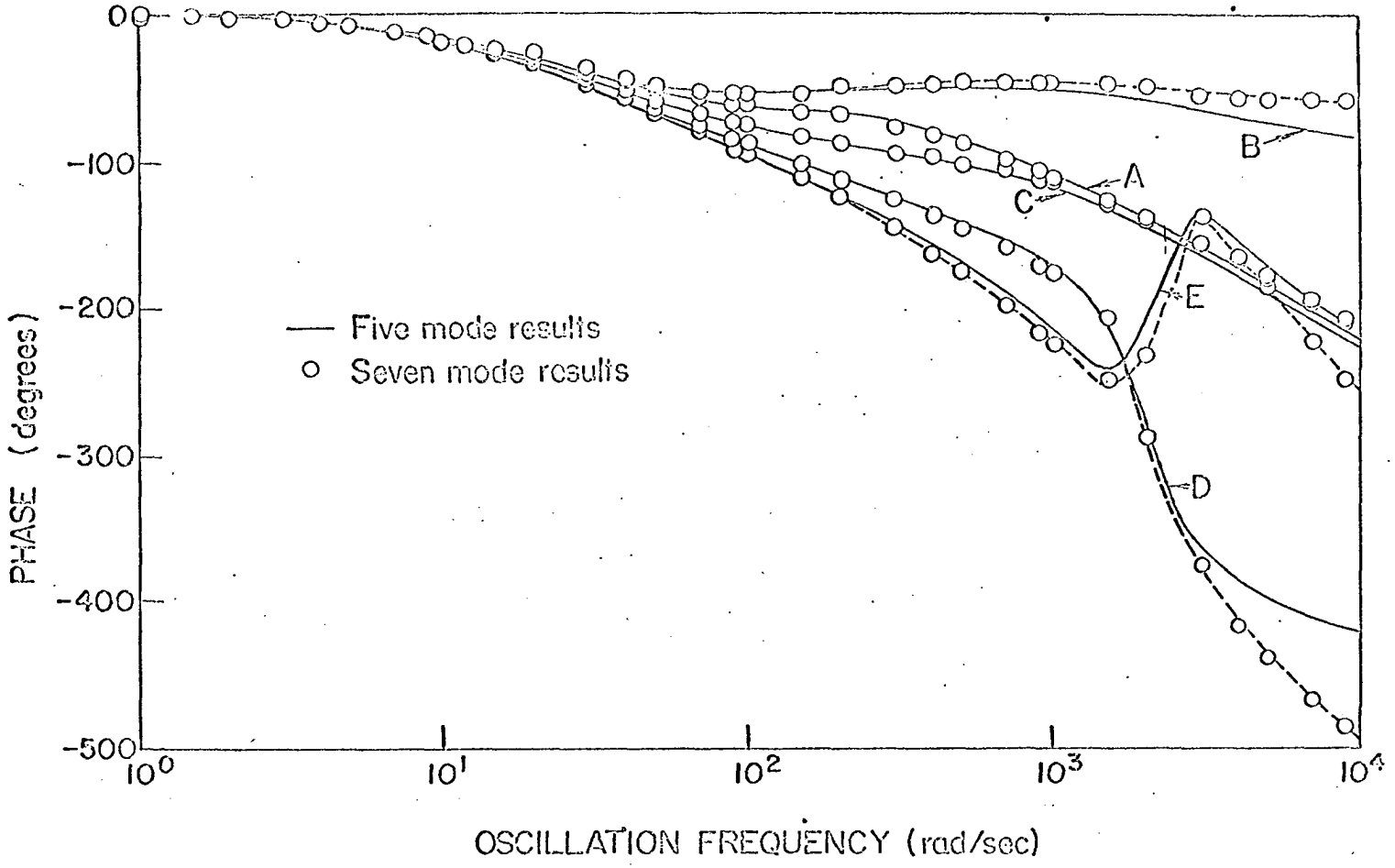

Figure III.8. Phase response of UTR-10 prototype reactor with oscillator at position 2.

One of the similarities between these results for a coupled reactor and experimental results for a conventional heavy-water reactor (9) is the slight resonance in the magnitude and phase which is present when the oscillator and detector are located at the same point. Except when the detector is located in the driven core or beyond, the other detector positions also yield results qualitatively in agreement with results obtained experimentally by Hansson and Foulke (20) for the NORA reactor.

One of the significant differences between the results obtained here and those previously reported is that both "conventional" behavior and a sink have been observed in a consistent set of results on a single reactor type. In addition a mechanism is proposed to explain the presence of the sink. The occurrence of the sink is not without precedent in nuclear systems. Kylstra and Uhrig (30) experimentally observed multiple sinks in both light-water and heavy-water slab subcritical assemblies and Hendrickson (22) observed a similar phenomenon in cross-spectral-density measurements on the Iowa State University UTR-10 reactor, under slightly different circumstances. Thus there is good reason to believe that the sink actually exists and can be directly measured in a physical system.

3. Seven modes

A sample problem using seven modes was run as a check on the convergence of the five-mode solution. The two extra modes were added in the left fuel region, so that it was represented by three modes in the seven-mode analysis. The additional modes were added to the driving region because it is the region in which a reactivity change is being made and hence the flux is changing most rapidly there. Similarly, if a time-domain analysis were being made with a reactivity change in the left core tank one would be inclined to add more modes near where the change was being made since that is where the flux would experience the greatest change.

As can be seen from Figures III.7 and III.8, the agreement between the five- and seven-mode calculations is very good up to 1500 rad/sec. While results are not included on these figures for frequencies less than 1 rad/sec the agreement for low frequencies was excellent. Thus it can be said with reasonable certainty that the five-mode results should be accurate up to 1500 rad/sec and above that they should show trends well enough to draw general conclusions. That is, above 1500 rad/sec the differences between the five- and seven-mode results are in quality and not in kind.

IV. POSSIBLE MECHANISM FOR CAUSE OF SINK

A distinctive feature of the frequency responses obtained in this study is a sink, or sudden decrease in the magnitude of the frequency response followed by a rapid recovery, at frequencies between 2000 and 3000 radians per second.

It is believed that this phenomenon is caused by a superposition of two waves of the same frequency and approximately the same amplitude but which are 180° out of phase. This phase difference could be caused by a simple time delay in the system. If so, the frequency of the first sink can be determined to be $\omega = \pi/\tau$ since

$$\omega = 2\pi f$$

$$f = 1/T$$

$$\tau = T/2$$

where

$\omega \sim$ frequency, rad/sec

$T \sim$ period of the wave, sec

$\tau \sim$ magnitude of the delay, sec.

For the two group model used in this study it is proposed that when the oscillator is in one core tank the fast-neutron-group oscillation propagates essentially instantly across the coupling region and is thermalized in the other core tank. The thermal-group oscillation propagates much more slowly through the fuel regions and across the

coupling region and arrives at the driven core after the fast oscillation. Then, at some frequency the transit time of the thermal group is such that the thermal oscillation arrives at the driven core 180° out of phase with the thermalized fast wave. The result is partial cancellation of the neutron oscillation in the driven core and a decrease in the magnitude of the frequency response at that frequency.

The neutron wave velocities in the various reactor regions can be calculated (32, 42) and for a 45 cm internal reflector the transit time from the center of one core to the center of the other for an oscillation of 2000 rad/sec is 1.55 msec. This transit time implies that a sink should occur at 2020 rad/sec which is in good agreement with the observed frequency of about 2000 rad/sec.

A change in the thermal-group speed should cause the sink frequency to change and this effect is observed. For a thermal-group speed of 3000 meters per second the calculated total transit time is 1.226 msec. and this leads to a sink frequency of 2560 rad/sec which agrees favorably with the observed sink at about 2700 rad/sec.

Systems with sinks similar to those found here are relatively common in boiling heat-transfer systems (1, 6). For example the power-boiling boundary transfer function, $z(s)$, is described by

$$z(s) = \frac{1-e^{sT}}{sT}$$

where T is a time constant associated with the time required for water to pass from the inlet of a boiling core to the outlet. When this transfer function is integrated over a range of T to represent an averaging due to the distribution of transit times caused by the velocity distribution in the flow channel, successive sinks are observed with the same general magnitude and phase behavior as seen in the UTR-10 reactor with oscillator at position 2 and detector at position E.

A detailed analysis of this phenomenon would be interesting and could be of practical value, but unfortunately is beyond the scope of this work.

V. PARAMETRIC ANALYSIS USING GREEN'S MODES

The earliest investigations of coupled-core reactors (4, 12) revealed that these reactors are particularly susceptible to flux tilting and that the sensitivity to tilting depends largely upon how tightly the two cores are coupled. Therefore the effect of flux tilting on the frequency response was chosen as one of the parameters to be investigated. Also investigated in this analysis were the effects of (1) a localized versus a volume oscillator, (2) the neutron group speed, (3) neutron energy group, (4) coupling region size and (5) oscillator location. These were chosen as parameters which might be important based upon experience with simpler nuclear reactors and conjecture.

The results of these analyses will be discussed in approximately the inverse order of their effect on the reactor response.

A. Effect of Flux Tilt

When an oscillator is placed in a reactor it contributes a steady-state poisoning effect due to the materials of its construction in addition to the dynamic reactivity effect it produces when its rotor is in motion. The result of this steady-state poisoning is to depress the flux in the vicinity of the oscillator or, in the case of a coupled

reactor, to tilt the flux. The flux was tilted in the UTR-10 prototype reactor by increasing the cross section the desired amount in the core which contained the oscillator and iterating to the required critical cross section in the other core.

It was found that for small flux tilts--at least up to 1.3:1--the effect of flux tilt on the frequency response was negligible except at high frequencies and when far from the oscillator, where the differences were almost negligible. Differences between frequency responses are considered negligible if the magnitudes and phases differ by less than 5%.

B. Localized vs. Volume Oscillator

The differences in responses due to a localized oscillator and a volume oscillator were investigated for the case in which the localized oscillator was represented by a plane absorber at the center of the left core and the volume oscillator was represented by an absorber uniformly distributed throughout the core. No significant differences were observed between the responses to these two oscillators up to 1500 rad/sec. However, it was observed that the response in the vicinity of the sink appeared to be smoothed more when the entire core was oscillated and the sink was also moved to a higher frequency.

C. Neutron Group Speed

It was found that differences in the magnitude of the frequency responses for fast-group speeds of 4.36×10^6 m/sec (15) for the prototype model and 3.0×10^4 m/sec (31) for the comparison model were negligible. However, the smaller fast-group speed resulted in the larger phase shift both as the detector was moved away from the oscillator and as the frequency increased. This increase in phase shift for the smaller fast-group speed was probably due to the fact that the oscillating component of the thermal group at any point is made up of components due to the fast group that is being thermalized at that point and due to the diffusion of the thermal-group oscillation from the oscillator to that point. The manner in which these components add together can cause the phase lag to change.

A thermal-group speed of 3000 m/sec for the comparison model, relative to 2200 m/sec in the prototype model, resulted in considerably less attenuation of the neutron oscillation. This difference increased with both distance from the oscillator and frequency and was caused by the fact that the attenuation length of a neutron wave increases as the velocity of neutrons in the wave increases (32). The phase shift for the larger thermal-group speed was everywhere less than that for the prototype model except at the oscillator where they were about the same. This is

because it takes the slower wave longer to get from place to place and the longer it takes the more phase shift results. For a similar reason the sink is shifted to a higher frequency for the larger thermal-group velocity.

D. Dependence on Neutron Energy Group

For the model being used here a comparison of frequency responses is possible between only two energy groups, the fast group and the thermal group.

When the oscillator is located at position 2 and the detector is located at position B the response of the fast group follows that of the thermal group very closely. However the magnitude attenuation and phase lag of the fast group are much smaller at points A and C than is the case for the thermal group at these points. This is due to the large velocity of the fast group and its associated larger attenuation length. When the detector is located at position D the fast-and thermal-group magnitude responses are virtually identical up to 1500 rad/sec. Above this frequency the effect of the sink becomes dominant and the responses differ somewhat. This phenomenon indicates that the fast response in the driven core is due almost entirely to the oscillation of the slow group in the driven core which has diffused across from the driving core. Similarly the magnitude and the phase shift of the fast group at position E are closer to the response at D than is so for

the thermal group, just as is true in the vicinity of the driving core.

From these results it seems that at the center of the driven core virtually none of the fast-neutron oscillation has come directly from the driving core. This conclusion can be confirmed by examination of Figure II.4 from which it can be seen that the fast mode from one fuel region is essentially completely attenuated before it reaches the center of the opposite core.

It can be seen from Figures V.1 and V.2 that the fast-group response is strongly dependent upon the presence of the driven core. The magnitude and phase responses show very little spatial dependence until the detector is more than half way through the coupling region; then suddenly the presence of the driven core is felt, the magnitude suffers attenuation, and large phase lags are introduced. Eventually as the detector moves through the driven core the response becomes almost space independent again.

In all of the cross-plotted frequency responses which follow, the parametric analysis will show results only for the frequencies ω_1 = 10 rad/sec, ω_2 = 200 rad/sec, ω_3 = 500 rad/sec, ω_4 = 1000 rad/sec and ω_5 = 1500 rad/sec. Hence these values will not be repeated on each figure. These frequencies represent typical behavior in the range of frequencies where convergence of the five-mode approximation is good and covers frequencies from the low-frequency

Figure V.1. Space dependence of fast group magnitude response.

Figure V.2. Space dependence of fast group phase response.

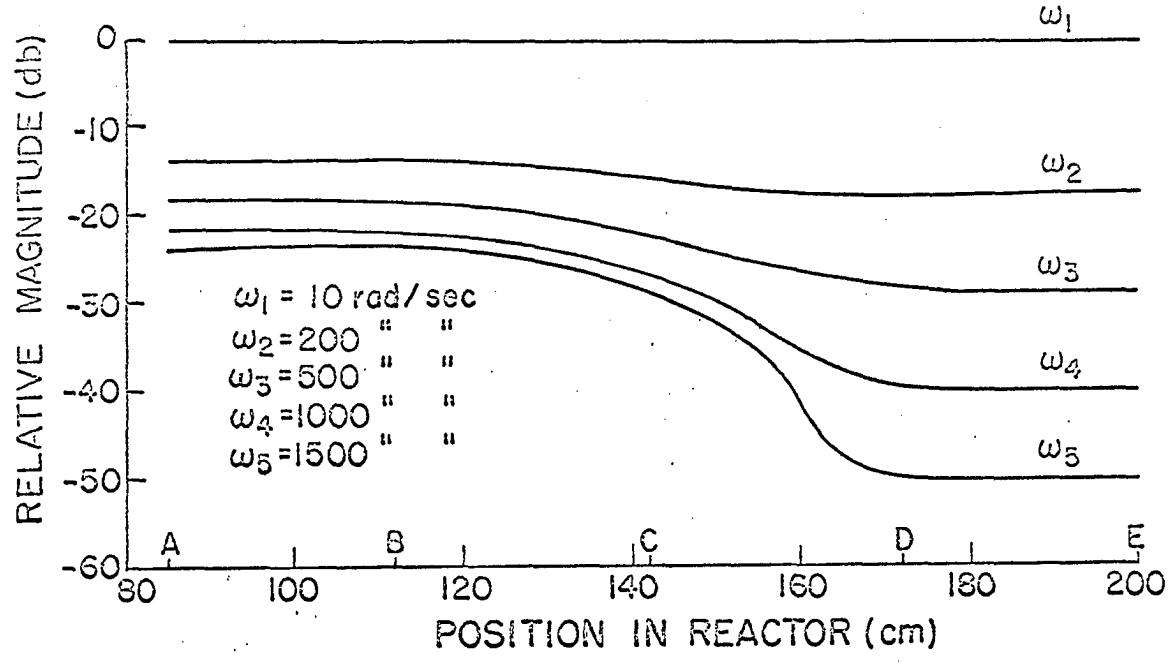
RELATIVE MAGNITUDE (db)
0
-10
-20
-30
-40
-50
-60
ω_1
ω_2
ω_3
ω_4
ω_5
ω_1 = 10 rad/sec
ω_2 = 200 " "
ω_3 = 500 " "
ω_4 = 1000 " "
ω_5 = 1500 " "
A
B
C
D
E
80
100
120
140
160
180
200
POSITION IN REACTOR (cm)

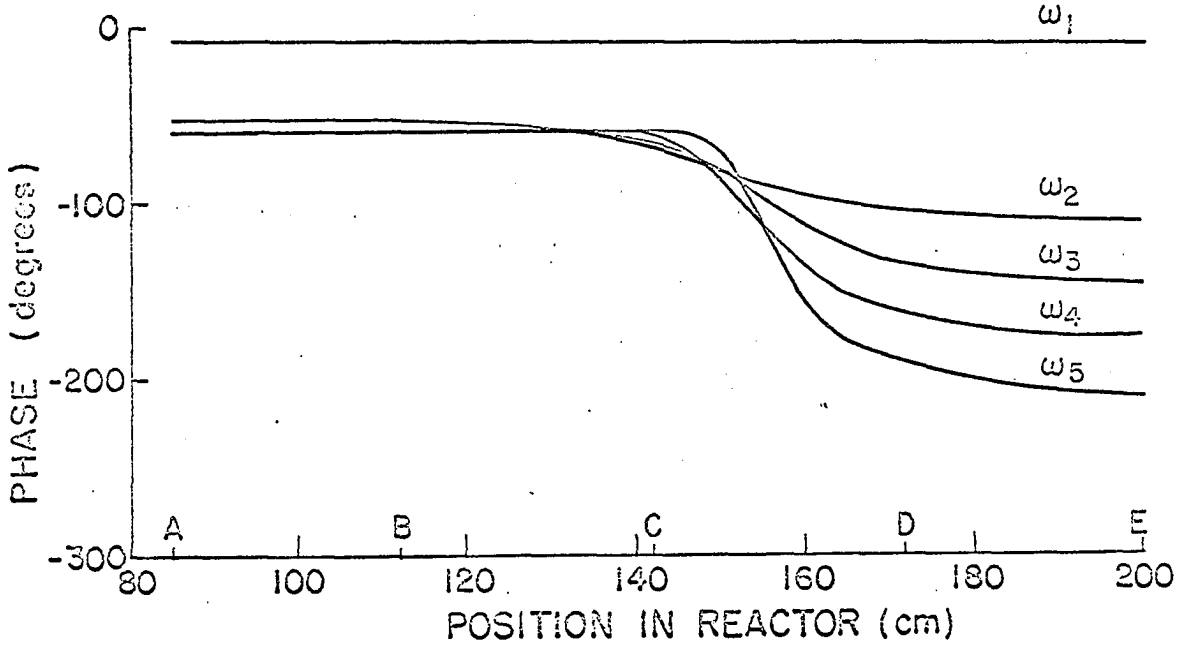
PHASE (degrees)
0
-100
-200
-300
ω_1
ω_2
ω_3
ω_4
ω_5
A
B
C
D
E
80
100
120
140
160
180
200
POSITION IN REACTOR (cm)

region almost up to the sink frequency.

Cross-plotting the reactor responses with frequency as a parameter and location as the independent variable allows the spatial dependence of the effect being investigated to be more easily observed and analyzed.

E. Coupling Region Size

An oversimplification of the general behavior of the reactor frequency response might be stated as follows:

In general, the magnitude decreases and the phase lag increases as the oscillation frequency increases and the detector is moved further from the oscillator, Figures V.3 and V.12. These effects become more pronounced at higher frequencies and detailed behavior is strongly dependent upon oscillator location and core separation distance.

In particular, as coupling distance increases from 20 to 45 cm the magnitude of the reactor response continues to decrease as the detector is moved further from the oscillator and as frequency is increased. However when the separation reaches 50 cm a reinforcement of the magnitude begins to appear at the higher frequencies in the vicinity of the driven core, Figure V.9, and this effect is quite apparent by the time the core separation has reached 60 cm, Figure V.11.

For coupling distances of 20 to 35 cm, little or no

Figure V.3. Space dependence of magnitude, coupling region = 20 cm.

Figure V.4. Space dependence of magnitude, coupling region = 20 cm.

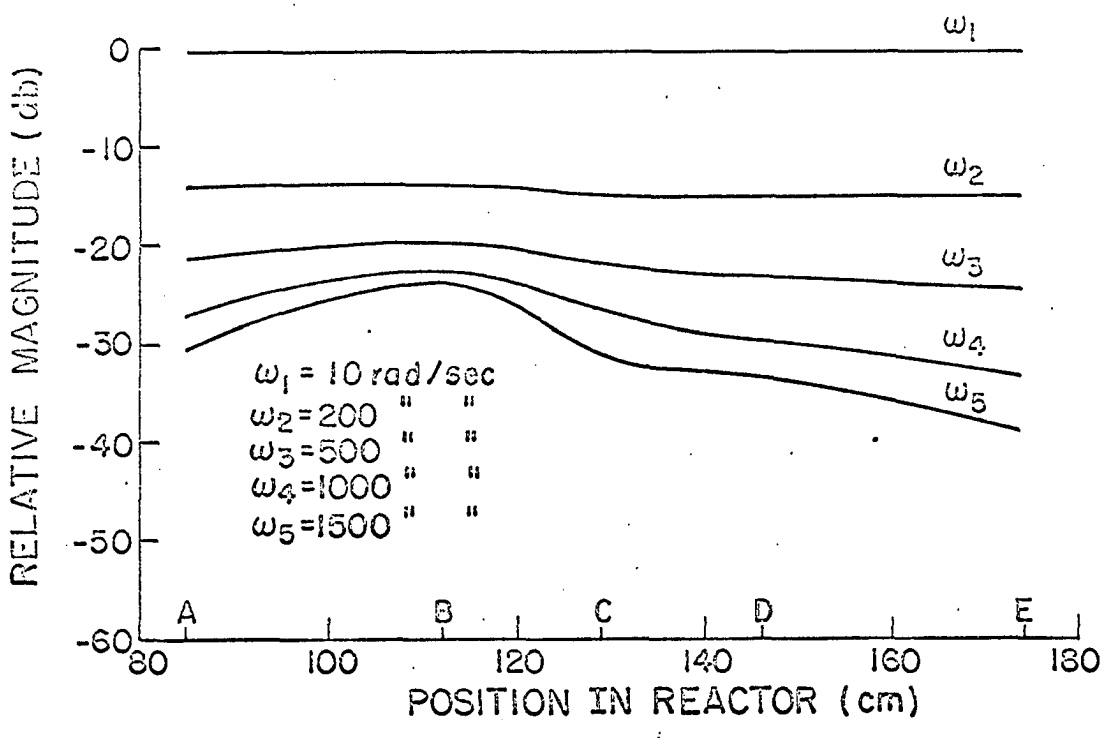
RELATIVE MAGNITUDE (db)
0
-10
-20
-30
-40
-50
-60
ω_1
ω_2
ω_3
ω_4
ω_5
ω_1 = 10 rad/sec
ω_2=200 " "
ω_3=500 " "
ω_4=1000 " "
ω_5=1500 " "
A
B
C
D
E
80
100
120
140
160
180
POSITION IN REACTOR (cm)

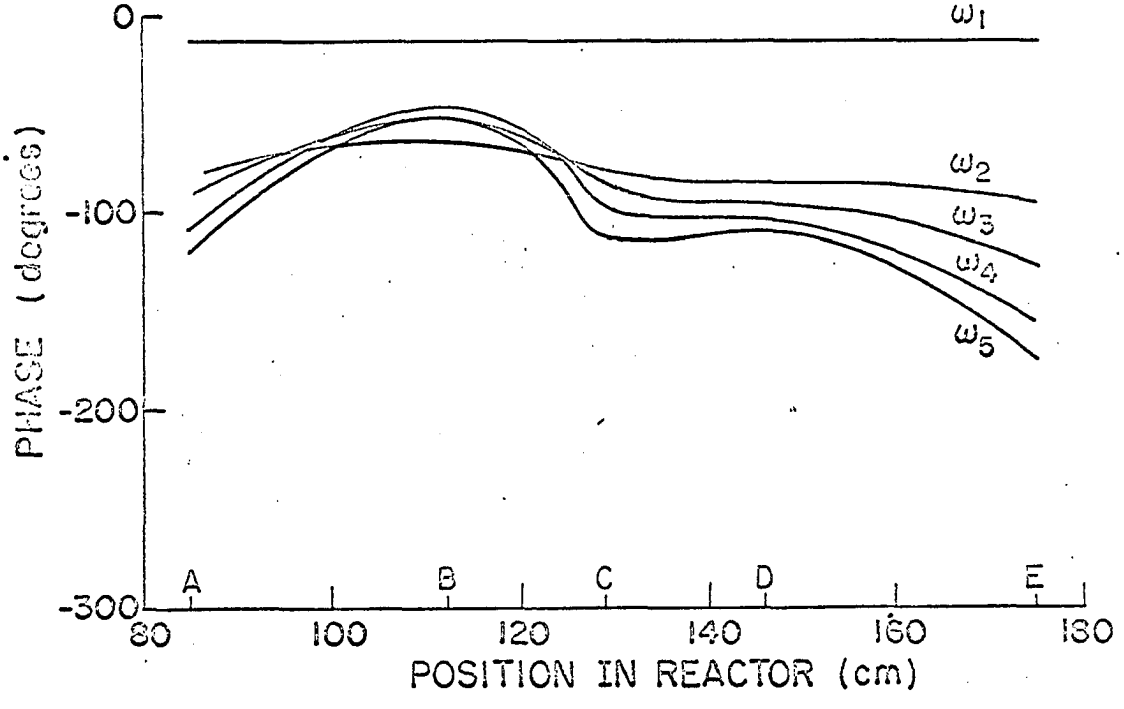
PHASE (degrees)
0
-100
-200
-300
ω_1
ω_2
ω_3
ω_4
ω_5
A
B
C
D
E
80
100
120
140
160
180
POSITION IN REACTOR (cm)

Figure V.5. Space dependence of magnitude, coupling region = 35 cm.

Figure V.6. Space dependence of phase, coupling region = 35 cm.

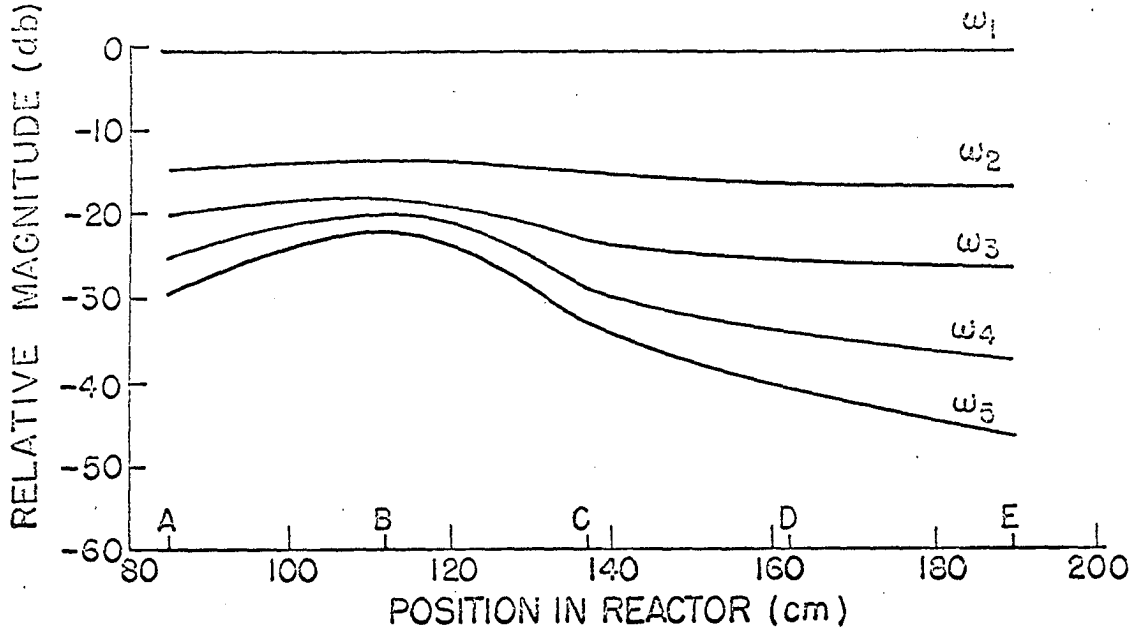
RELATIVE MAGNITUDE (db)
0
-10
-20
-30
-40
-50
-60
ω_1
ω_2
ω_3
ω_4
ω_5
A
B
C
D
E
80
100
120
140
160
180
200
POSITION IN REACTOR (cm)

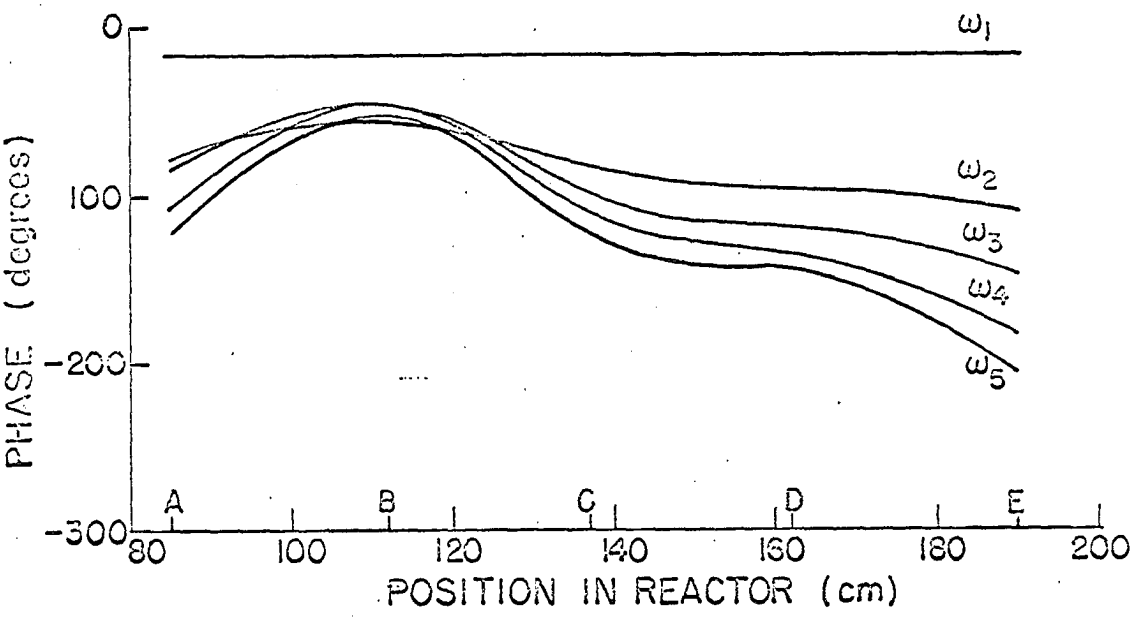
PHASE (degrees)
0
100
-200
-300
ω_1
ω_2
ω_3
ω_4
ω_5
A
B
C
D
E
80
100
120
140
160
180
200
POSITION IN REACTOR (cm)

Figure V.7. Space dependence of magnitude, coupling region = 45 cm.

Figure V.8. Space dependence of phase, coupling region = 45 cm.

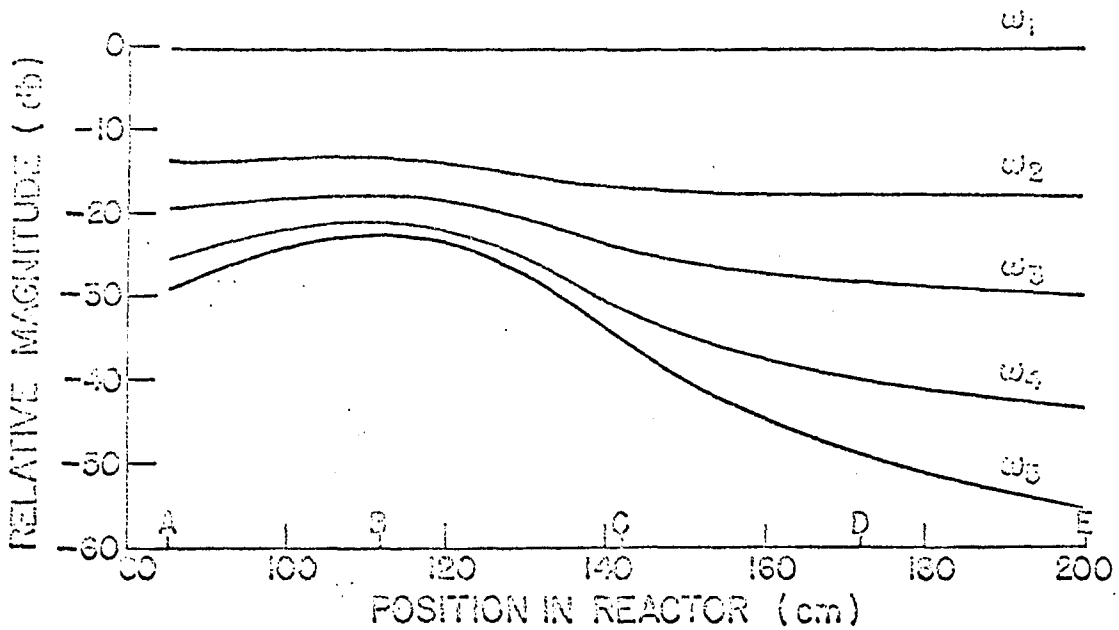
RELATIVE MAGNITUDE (db)
0
-10
-20
-30
-40
-50
-60
ω_1
ω_2
ω_3
ω_4
ω_5
A
B
C
D
E
80
100
120
140
160
180
200
POSITION IN REACTOR (cm)

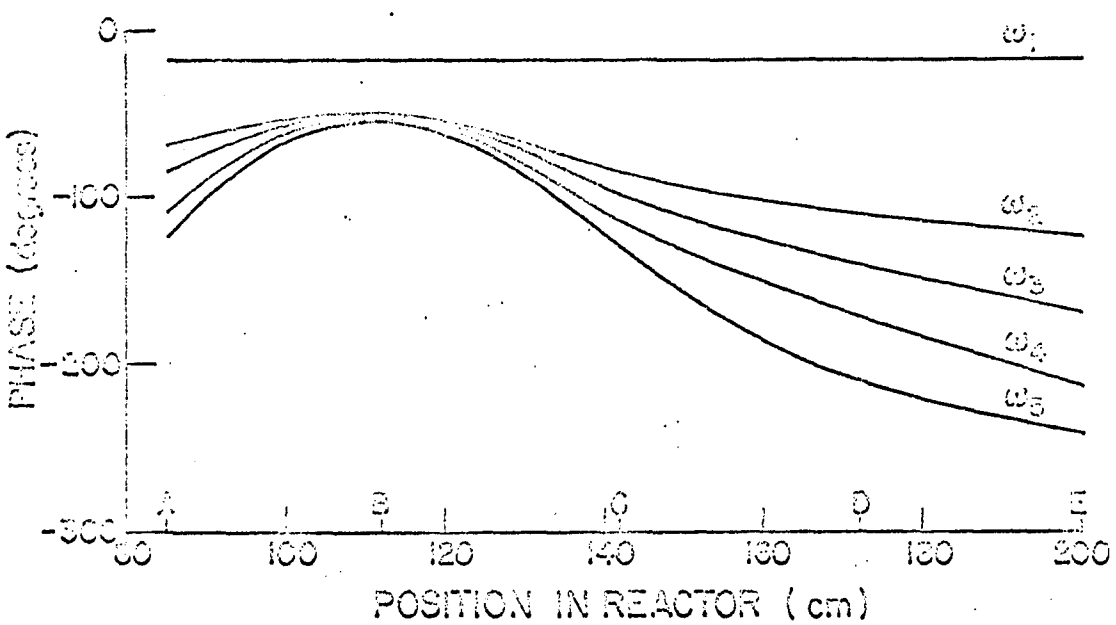
PHASE (degrees)
0
-100
-200
-300
ω_1
ω_2
ω_3
ω_4
ω_5
A
B
C
D
E
80
100
120
140
160
180
200
POSITION IN REACTOR (cm)

Figure V.9. Space dependence of magnitude, coupling region = 50 cm.

Figure V.10. Space dependence of phase, coupling region = 50 cm.

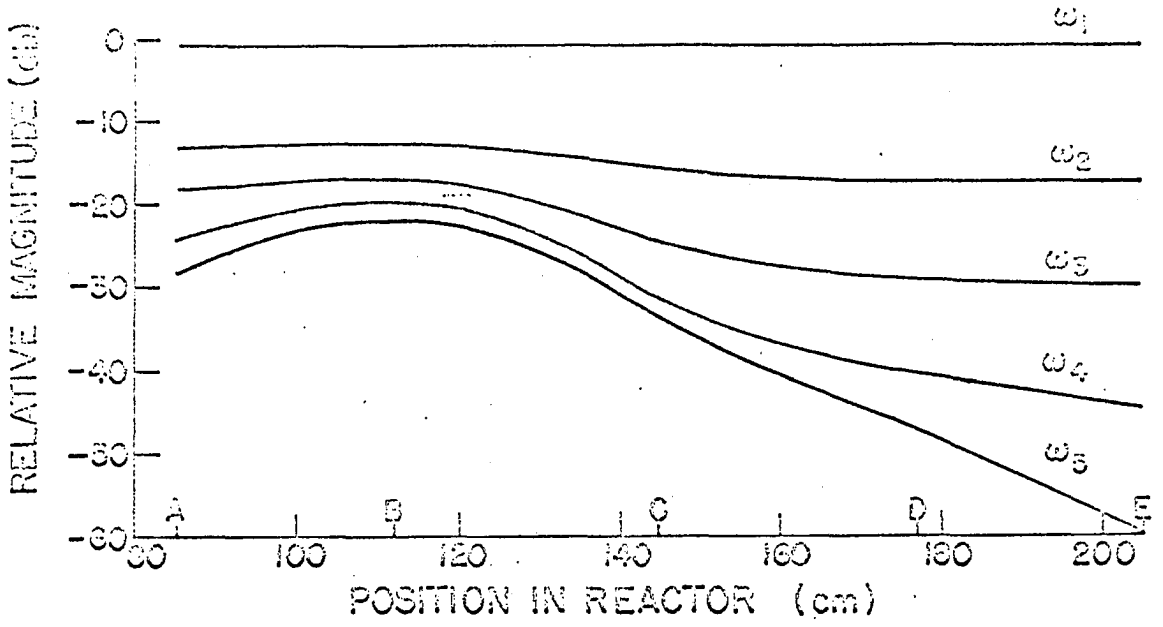
RELATIVE MAGNITUDE (db)
0
-10
-20
-30
-40
-50
-60
ω_1
ω_2
ω_3
ω_4
ω_5
A
B
C
D
E
80
100
120
140
160
180
200
POSITION IN REACTOR (cm)

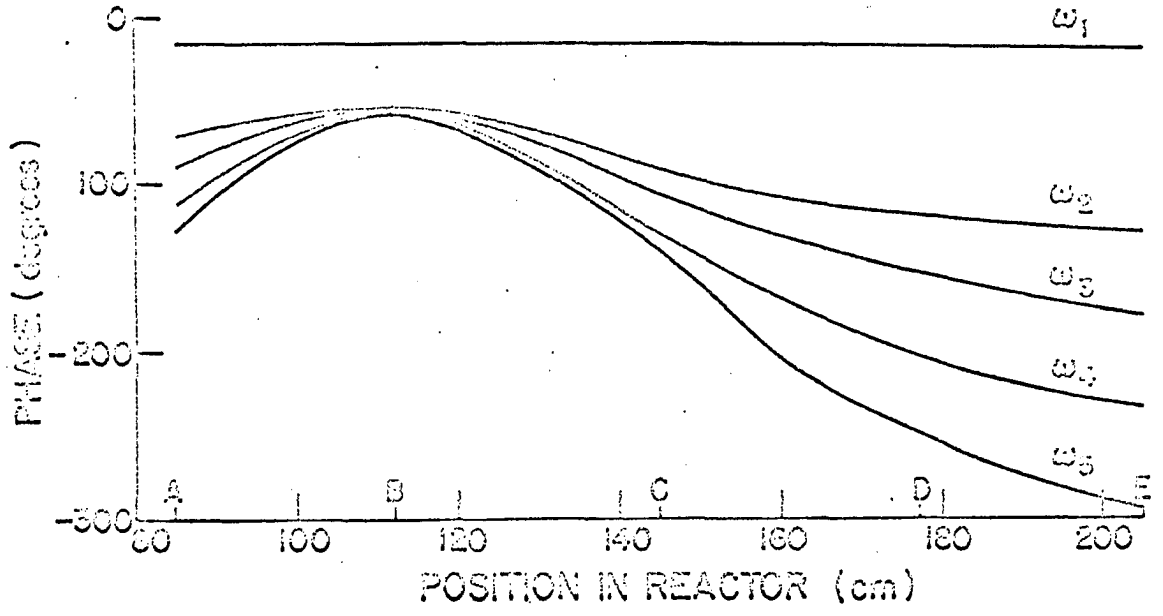
PHASE (degrees)
0
-100
-200
-300
ω_1
ω_2
ω_3
ω_4
ω_5
A
B
C
D
E
80
100
120
140
160
180
200
POSITION IN REACTOR (cm)

Figure V.11. Space dependence of magnitude, coupling region = 60 cm.

Figure V.12. Space dependence of phase, coupling region = 60 cm.

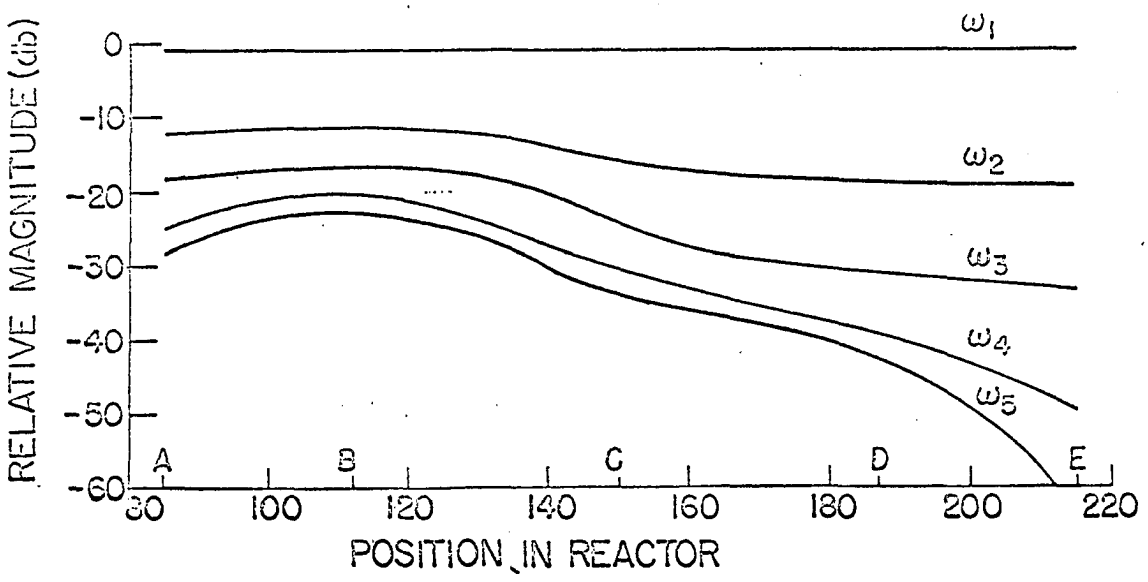
RELATIVE MAGNITUDE (db)
0
-10
-20
-30
-40
-50
-60
ω_1
ω_2
ω_3
ω_4
ω_5
A
B
C
D
E
80
100
120
140
160
180
200
220
POSITION IN REACTOR

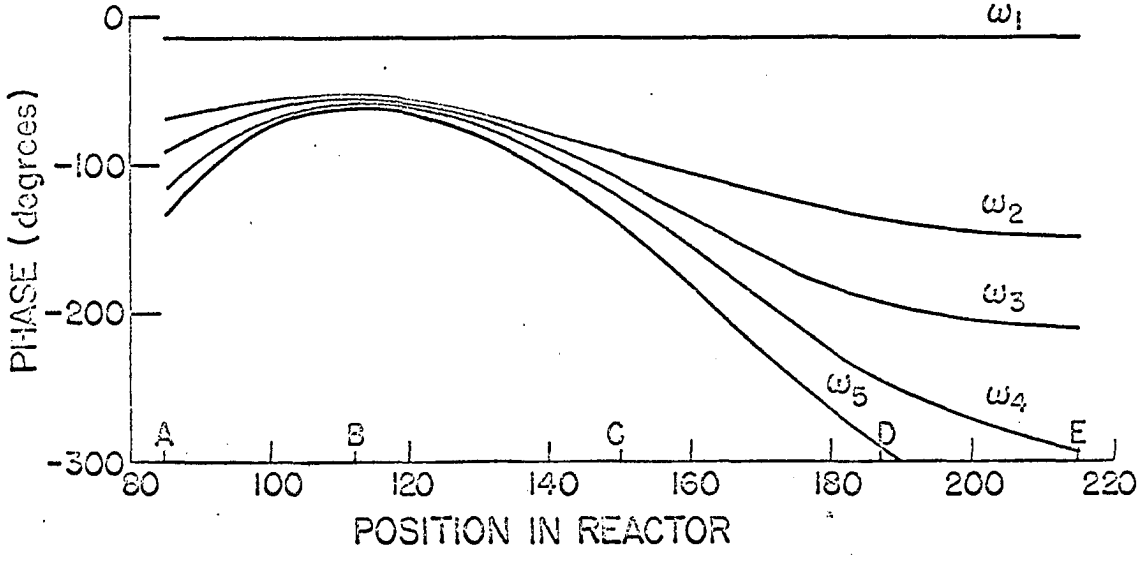
PHASE (degrees)
0
-100
-200
-300
ω_1
ω_2
ω_3
ω_4
ω_5
A
B
C
D
E
80
100
120
140
160
180
200
220
POSITION IN REACTOR

phase shift is contributed at any frequency by the reactor in a region from the center of the coupling region to the outer edge of the driven core. This effect is shown in Figures V.4 and V.6.

In summary it can be said that coupling distance has a considerable effect on the detailed frequency response of a reactor and a change of 10-15 cm in the coupling region size can make a considerable difference in the response.

F. Effect of Oscillator and Detector Location on Response of the I.S.U. UTR-10 Reactor

The fast- and thermal-flux distributions for the Iowa State University UTR-10 reactor (I.S.U. UTR-10) are shown in Figure V.13 for the flux tilt experimentally measured on Dec. 19, 1967, with the cold core loaded, shim-safety rod at 8.0 inches, and regulating rod at 2.5 inches. The transverse buckling is larger in this model than in the prototype reactor used earlier so the thermal flux peaking is reduced, otherwise the flux distributions are much alike.

This section describes the results of the calculation of the spatially-dependent frequency response for an actual coupled nuclear reactor, the I.S.U. UTR-10. The spatial dependence of the frequency response caused by oscillator location will be examined in addition to the dependence on detector position. There are three potential oscillator locations of particular interest in the I.S.U. UTR-10,

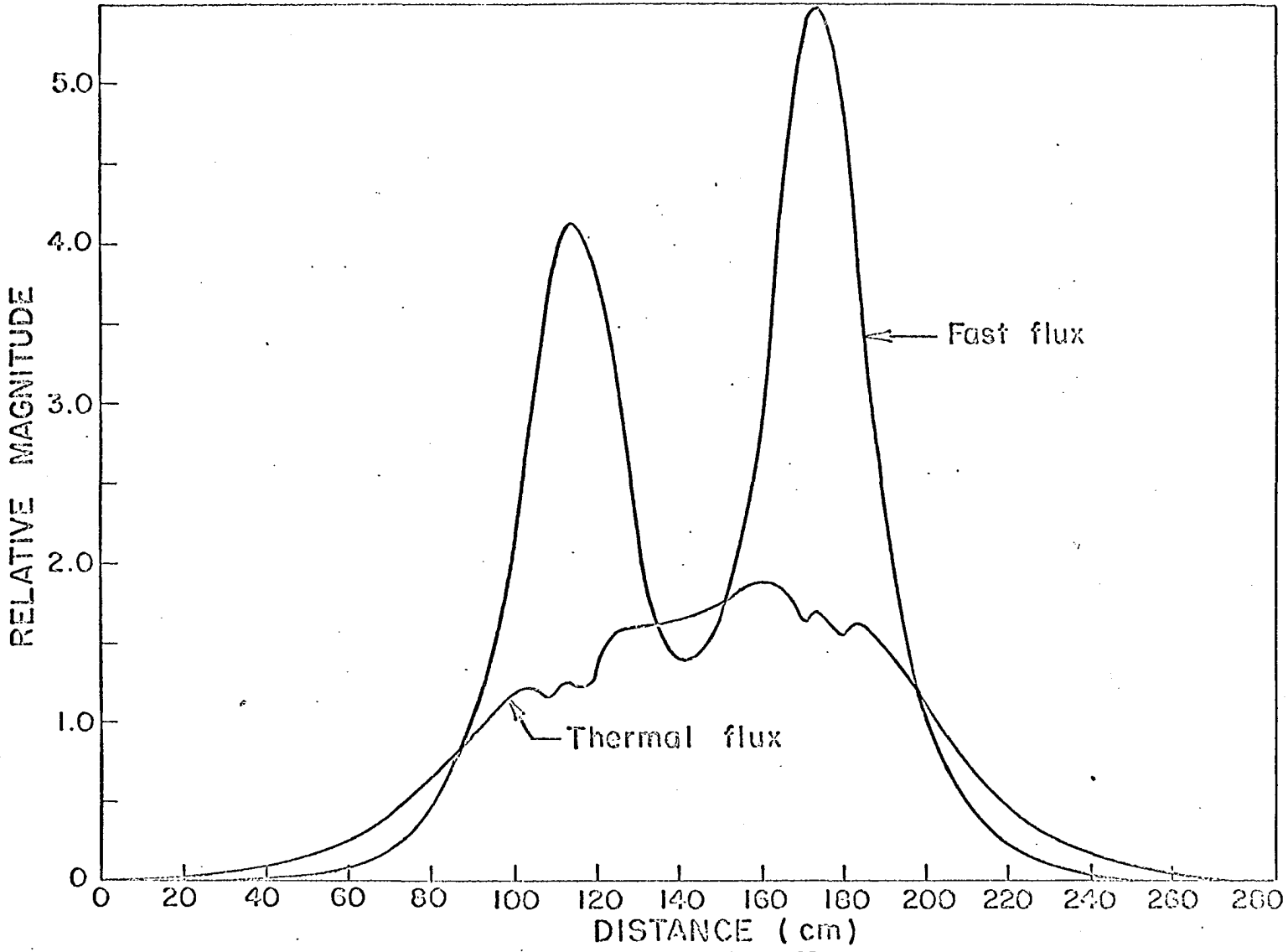

Figure V.13. Iowa State University UTR-10 reactor fluxes.

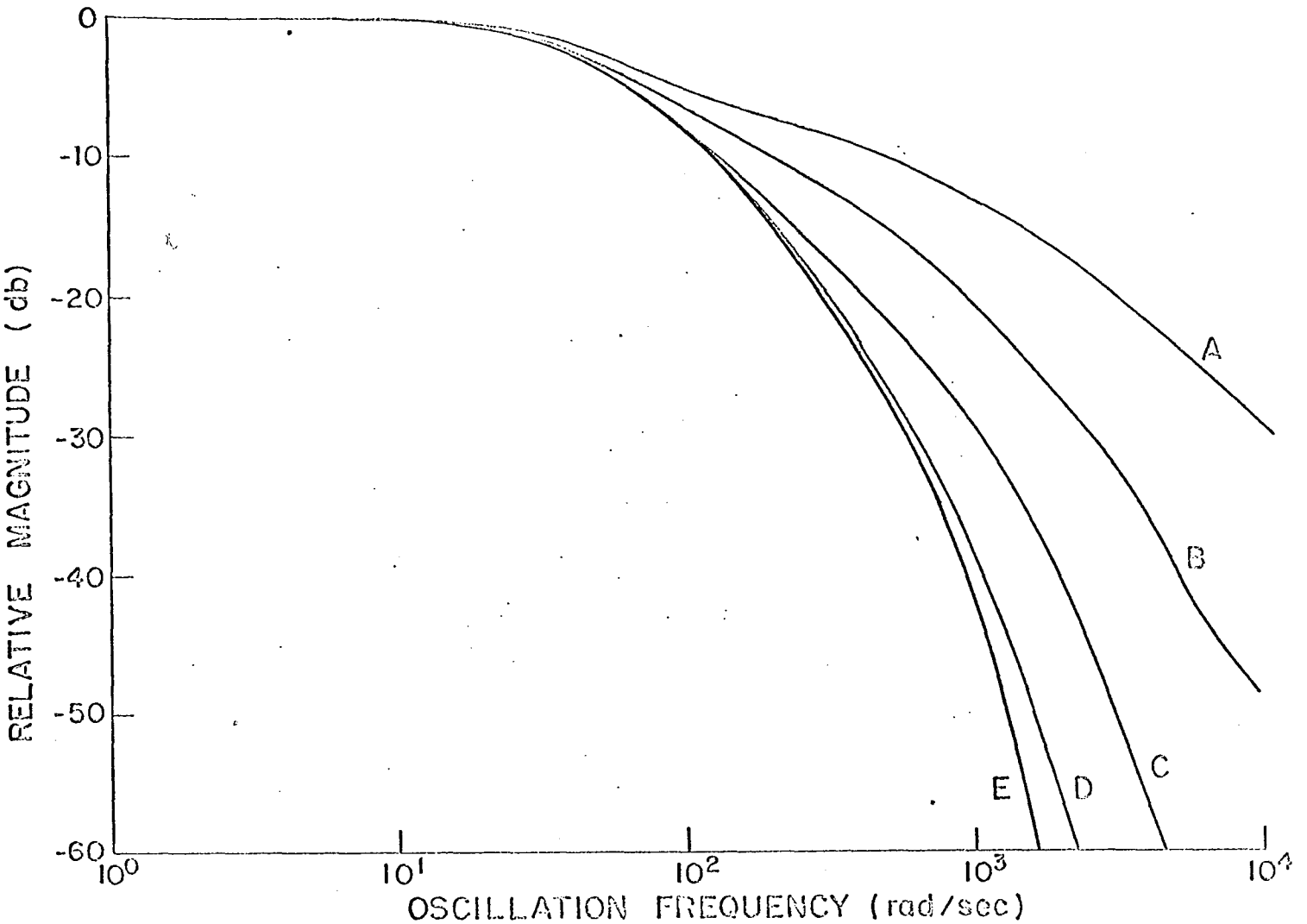

Figure V.14. Magnitude of frequency response, oscillator at position 1.

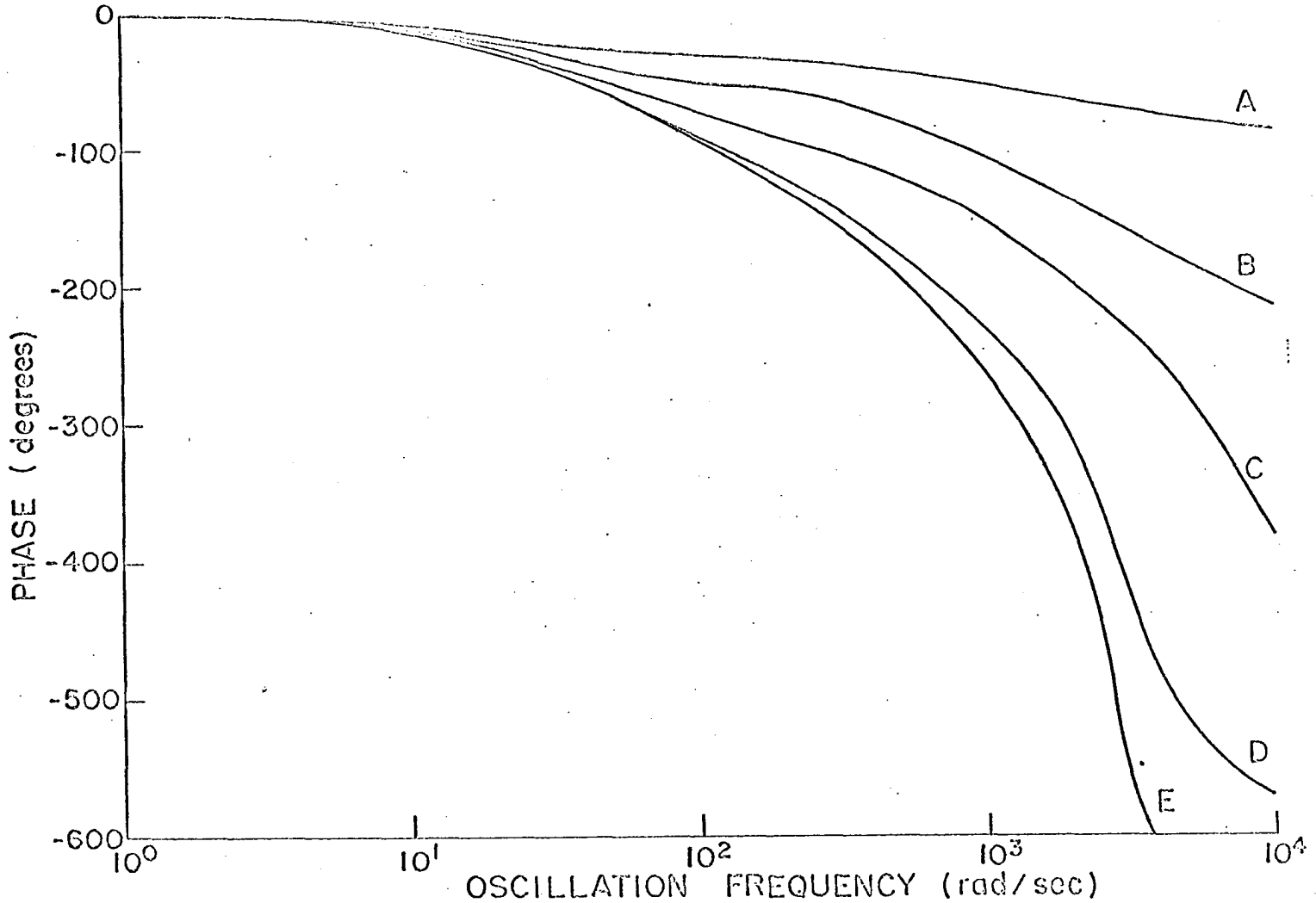

Figure V.15. Phase of frequency response, oscillator at position 1.

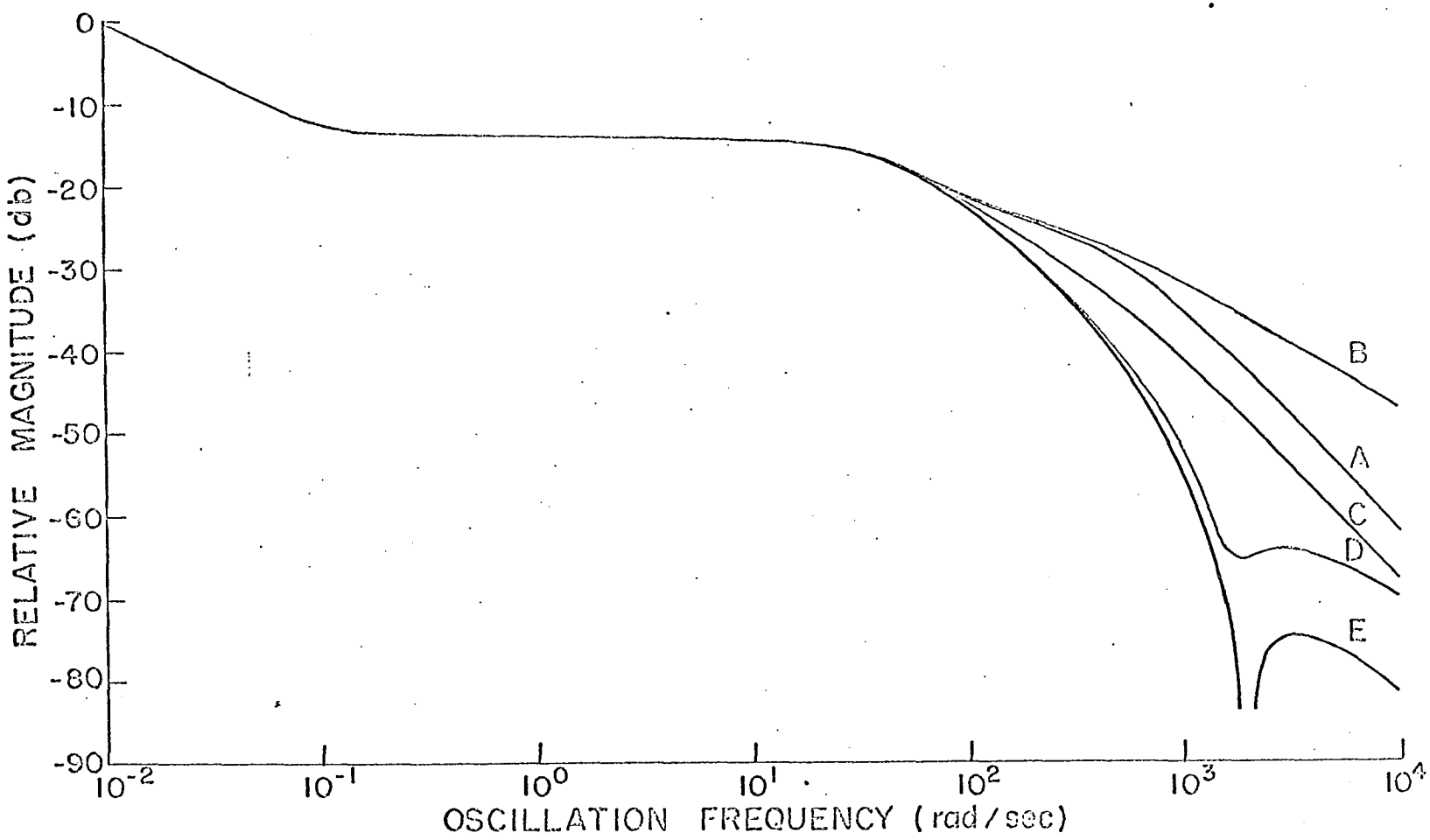

Figure V.16. Magnitude of frequency response, oscillator at position 2.

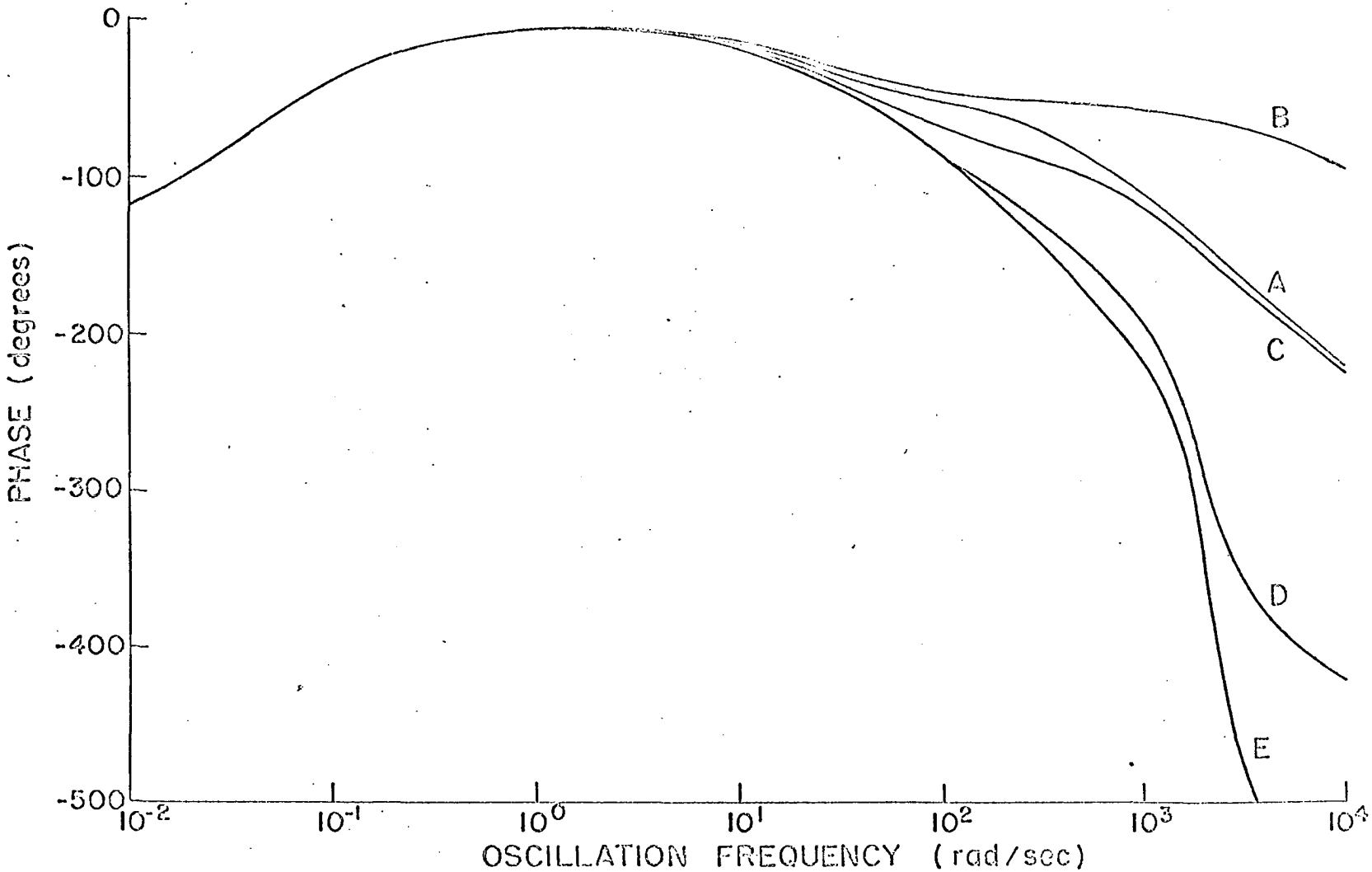

Figure V.17. Phase of frequency response, oscillator at position 2.

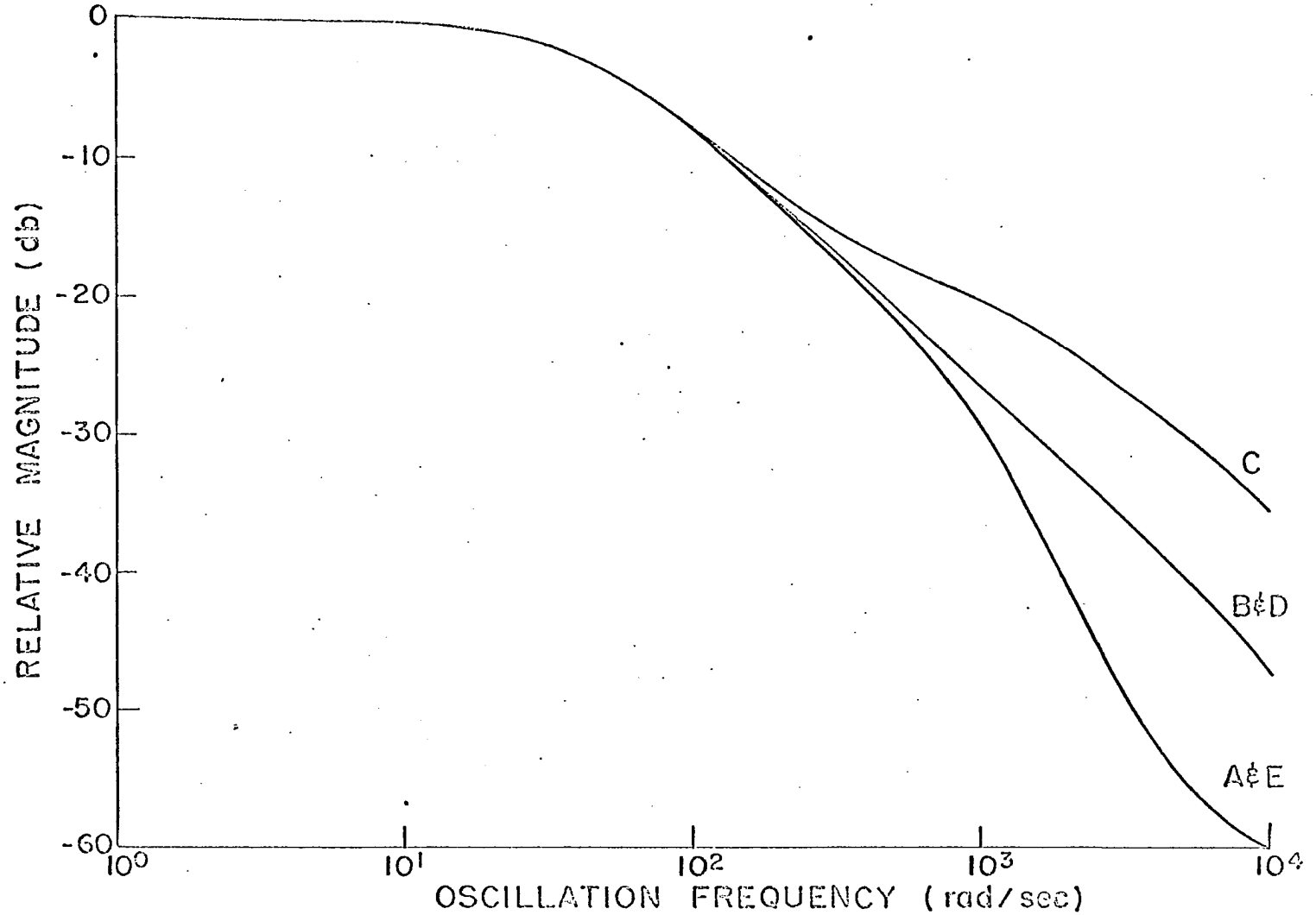

Figure V.18. Magnitude of frequency response, oscillator at position 3.

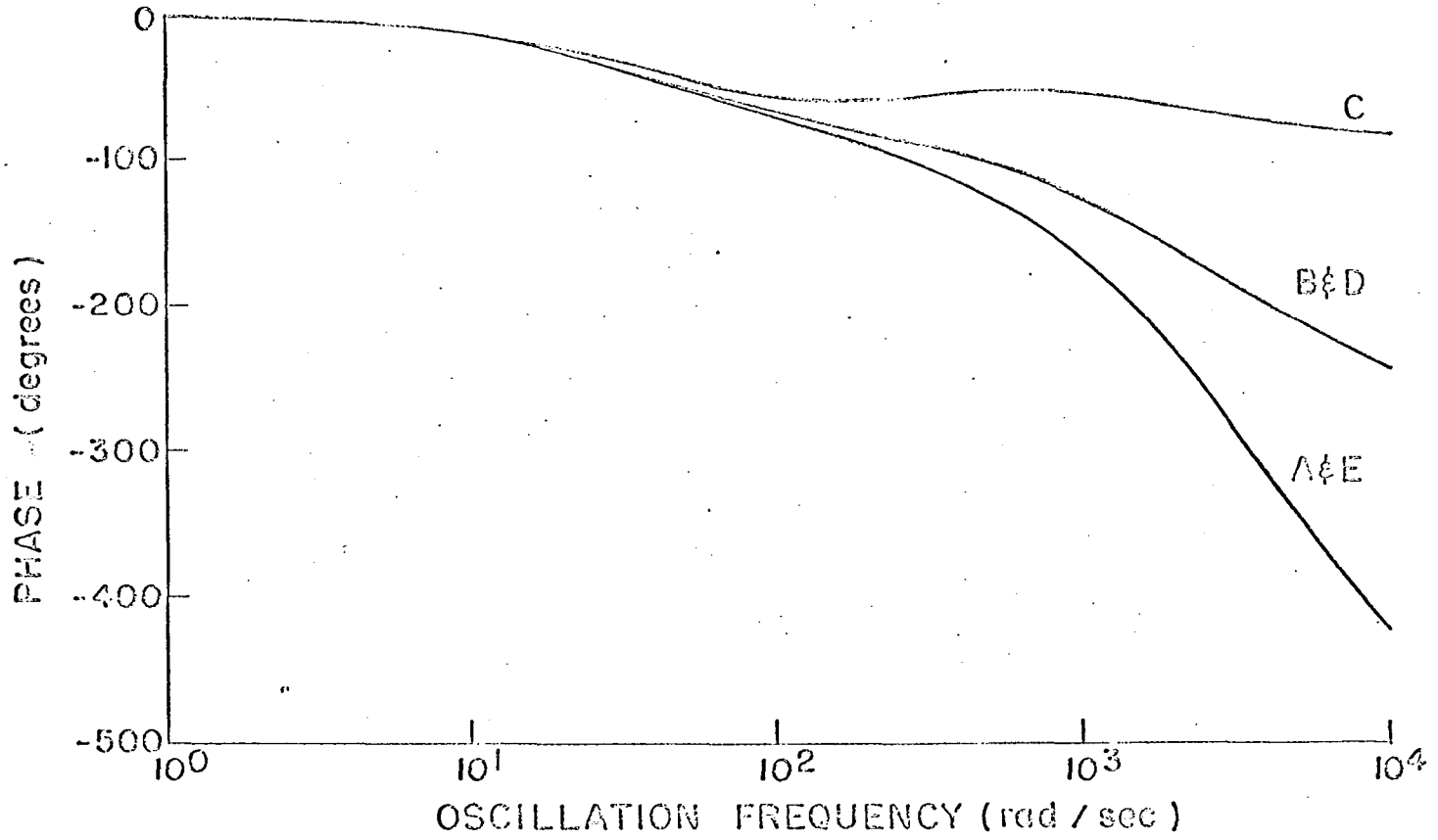

Figure V.19. Phase of frequency response, oscillator at position 3.

they are: (1) 12 cm from the south side of the south core tank, (2) in the center of a core tank, and (3) in the center of the graphite coupling region between the two cores. These positions are shown in Figure III.6 and the frequency responses calculated under these conditions are shown in Figures V.14 through V.19.

By a comparison of Figures V.14 and V.15 with V.16 through V.19 it is seen that spatial dependence becomes important at the lowest frequencies when the oscillator is located at 93 cm, that is, in an external reflector. Further examination shows that when the detector is at the point of oscillation the β/ℓ break frequency moves from 56 to 47 to 43 rad/sec for the oscillator at positions 1, 2, and 3, respectively; yet all three situations predict the same break frequency of 43 rad/sec when the detector is far from the oscillator. This fact has been recognized in experimental work for some time (31) and oscillator measurements of the β/ℓ break are normally made with the detector and oscillator widely separated.

The spatial dependence of the reactor response is primarily a high frequency phenomenon, that is, it occurs above the β/ℓ break of 30-60 rad/sec for light-water reactors; hence one is generally not interested in the delayed-neutron region unless feedback is to be studied. However, the contribution of delayed neutrons to the frequency response will be included for completeness for the

case where the oscillator is at position 2.

With the oscillator at position 2, Figures V.16 and V.17, the frequency response looks much like that obtained from the prototype model, however due to the larger transverse buckling and slightly larger fuel loading (5% larger) the prompt neutron lifetime is smaller, so β/ℓ is larger, than in the prototype model. As a consequence, the magnitude response for the I.S.U. UTR-10 reactor is everywhere slightly larger than for the prototype model and similarly the phase shifts are generally less than for the prototype.

When the oscillator is moved to the center of the reactor the most apparent change in the frequency response is that the sink is no longer present in the magnitude response. The Bode plots for the oscillator at 142 cm, position 3, are shown in Figures V.18 and V.19 and look much like the spatially dependent frequency response obtained experimentally for the NORA reactor by Hansson and Foulke (20). This similarity is due to the fact that when the oscillator is in the center of the coupling region it is surrounded by fissile material on two sides and the graphite transmits the thermal-group oscillation to the cores with little attenuation. Since the reflected waves from one core to the other are very weak the cores do not interact significantly with each other and the detector sees essentially the frequency response of a reflected slab reactor.

Although sufficiently high frequencies are not included in these figures to illustrate the fact, the phase angles eventually reach an asymptotic value which depends upon the oscillator and detector location.

VI. SUMMARY AND CONCLUSIONS

The conclusions stated below are the results obtained from analyzing a family of coupled nuclear reactors based upon a UTR-10 prototype model. Conclusions which were probably to be expected but which had not been explicitly stated are as follows.

1. In order to describe a coupled nuclear reactor using Green's Function modes it is essential that a mode(s) representing the coupling region be present. These modes were first mathematically described by Carter (9), who suggested they were necessary, and subsequently proved by McFadden[1] to be necessary in the time domain by comparison with an exact solution. This investigation used two, five and seven mode representations to confirm that coupling-region modes are also required in order to adequately describe reactor behavior in the frequency domain.
2. The delayed neutron effect is easily added to the calculation, however as has been previously observed (11, 28), the low-frequency response is extremely sensitive to reactor criticality. If the low-frequency behavior is to be accurately

[1]McFadden, James, Ames, Iowa. Results of computer calculations. Private communication. 1968.

described, the criticality determinant must be made as nearly zero as the number of significant figures capable of being carried will allow.

3. In the low-frequency region, below about 10 rad/sec, the reactor response is essentially independent of spatial effects.

The following conclusions are more directly a result of this study of coupled-core reactors.

4. Five space modes, with one mode originating in each region of the reactor, allows sufficient convergence to adequately describe the frequency response of the UTR-10 prototype reactor up to 1500 rad/sec.
5. The spatially dependent frequency response changes significantly for a fixed oscillator location as the detector is moved about. In general the farther the detector is located from the oscillator the greater the attenuation and phase shift unless a sink is encountered. The frequency response is also strongly dependent upon the oscillator location with space dependence becoming apparent at lowest frequencies when the oscillator is in position 1 and with the sink occurring only when it is in position 2. One result of these observations is that a consistent measurement of β/ℓ is obtained irrespective of oscillator location if the detector is located far from the oscillator.

6. Small flux tilts have a negligible effect on the frequency response.
7. A change in the coupling distance of 10-15 cm has a pronounced effect on the frequency response in the range of coupling distances from 20-60 cm.
8. When one core is driven by a reactivity oscillation the other responds as if driven by an oscillating source. The response of the driven side of the reactor may show a sink in the magnitude of the response when the detector is in the driven core or in its external reflector, for certain core separation distances.
9. An increase in the thermal-neutron-group speed has the effect of shifting the sink to a higher frequency but causes no other significant change in the response of the prototype reactor. A smaller fast-neutron-group speed causes the magnitude response in the vicinity of the sink to be smoothed considerably and causes a definite change in the phase behavior of the prototype reactor when the detector is at position D. From analytical results obtained here it seems that the presence of the fast group is essential to a proper description of the system and the fast- and thermal-neutron-group speeds must be properly chosen if good agreement between experimental and analytical results is to be

achieved.

10. A possible explanation for the cause of the sink may be due to the oscillation in the fast group being propagated essentially instantly across the reactor and slowing down in the driven core. A sink occurs when the frequency of oscillation is such that the velocity of propagation of the thermal-neutron wave causes it to arrive at the driven core 180° out of phase with the thermalized fast wave.
11. The sink is not a characteristic of coupled nuclear reactors but may occur in any reactor under the proper circumstances. However it seems most likely that these conditions, such as large time delay and strong local moderation of the fast group, would occur most readily in coupled reactors.
12. The final conclusion is that the zero-power frequency response of an atypical reactor should not necessarily be assumed to be similar to the classical point reactor transfer function with minor space-dependent modifications. The differences could be quite substantial at high frequencies and at distances far from the oscillator.

VII. SUGGESTIONS FOR FURTHER WORK

The following topics are suggested as areas for future work in which a contribution in the area investigated here could be made.

1). Measure the spatially dependent frequency response of coupled-core reactors at high frequencies, > 100 rad/sec, in order to provide a check for analytic results.

This could be done with a high-frequency oscillator, or, more likely would employ the use of noise techniques (3).

2). Develop a mathematical model which would describe the magnitude and phase behavior of the frequency response in the vicinity of a sink.

3). Investigate the effect of the distribution of Green's Function modes on the frequency response and see whether a criterion could be developed to guarantee that if an approximation had converged in the time domain it could be assured of producing a good solution in the frequency domain.

4). Extend work of this type from one space dimension to two (16, 29).

5). Obtain a pole-zero representation of the reactor frequency response as a function of space by casting the reduced kinetics equations into state-variable form and obtaining the poles and zeros as suggested by Schultz and Melsa (36). This formulation of the response is desirable because it is the one most useful in control-system design (7).

VIII. ACKNOWLEDGEMENTS

The author wishes to express his gratitude to his major professors Dr. Glenn Murphy, Head of the Nuclear Engineering Department, and Dr. Richard Danofsky for their support and interest during the preparation of this thesis, to acknowledge the support of the Nuclear Engineering Department for a research assistantship to study the spatially dependent frequency response of coupled-core reactors, and to acknowledge the many helpful discussions and suggestions made by Dr. Danofsky during the course of this work.

In conclusion, the author wishes to acknowledge his wife, Carol, who has been most patient.

IX. LITERATURE CITED

1. Akcasu, A. Z. Theoretical feedback analysis in boiling water reactors. U.S. Atomic Energy Commission Report ANL-6221 [Argonne National Laboratory, Lemont, Illinois]. 1960.

2. American Standard Company. Atomic Energy Division. Reactor Physics of UTR-10. Redwood City, California, Author. 1957.

3. Anderson, C. A. High frequency transfer function measurements for coupled fast power reactors. U.S. Atomic Energy Commission Report LA-DC-8299 [Los Alamos Scientific Laboratory, Los Alamos, New Mexico]. 1967.

4. Avery, R. Theory of coupled reactors. Second International Conference on the Peaceful Uses of Atomic Energy 12: 182. New York, N.Y., United Nations. 1958.

5. Baldwin, G. C. Kinetics of a reactor composed of two loosely coupled cores. Nuc. Sci. and Eng. 6: 320-327. 1959.

6. Beckjord, E. S. Dynamic analysis of natural circulation boiling water power reactors. U.S. Atomic Energy Commission Report ANL-5799 [Argonne National Laboratory, Lemont, Illinois]. 1958.

7. Brown, R. G. and Nilsson, J. W. Introduction to linear systems analysis. New York, N.Y., John Wiley and Sons, Inc. 1962.

8. Carter, J. C., Sparks, D. W., and Tessier, J. H. Period effect in reactor dynamics. Atomic Energy Commission Symposium Series 2: 53-90. 1964.

9. Carter, N. Solution of space-time kinetic equations for coupled-core nuclear reactors. Unpublished Ph.D. thesis. Ames, Iowa, Library, Iowa State University of Science and Technology. 1967.

10. Carter, N. and Danofsky, R. The application of the calculus of variations and the method of Green's function to the solution of coupled core kinetics equations. In Chezem, C. G. and Köhler, W. H., editors. Conf. Coupled Reactor Kinetics, College Station, Texas, Jan. 1967. Pp. 249-269. College Station, Texas, The Texas A and M Press. 1967.

11. Cohn, C. E., Johnson, R. J., and Macdonald, R. N. Calculating space-dependent reactor transfer functions using statics techniques. Nuc. Sci. and Eng. 26: 198-206. 1966.

12. Danofsky, R. A. and Uhrig, R. E. The kinetic behavior of the coupled regions of the UTR-10 reactor. Nuc. Sci. and Eng. 15: 131-133. 1963.

13. Dougherty, D. E. and Shen, C. N. The space-time neutron kinetic equations obtained by the semi-direct variational method. Nuc. Sci, and Eng. 13: 141-148. 1962.

14. Foderaro, A. and Garabedian, H. L. A new method for the solution of group diffusion equations. Nuc. Sci. and Eng. 8: 44-52. 1960.

15. Foderaro, A. and Garabedian, H. L. Two group reactor kinetics. Nuc. Sci. and Eng. 14: 22-29. 1962.

16. Foulke, L. R. and Gyftopoulos, I. P. Application of the natural mode approximation to space-time reactor problems. Nuc. Sci. and Eng. 30: 419-435. 1967.

17. Friedman, B. Principles and techniques of applied mathematics. New York, New York, John Wiley and Sons, Inc. 1956.

18. Glasstone, S. and Edlund, M. C. The elements of nuclear reactor theory. New York, New York, D. Van Nostrand Co., Inc. 1952.

19. Gyftopoulos, E. P. Some applications of mathematical methods to Nuclear Engineering at the Massachusetts Institute of Technology. Atomic Energy Commission Symposium Series 7: 1-27. 1966.

20. Hansson, P. T. and Foulke, L. R. Investigations in spatial reactor kinetics. Nuc. Sci. and Eng. 17: 525-533. 1963.

21. Harrer, J. M., Boyar, R. E., Krucoff, D. Transfer function of Argonne CP-2 Reactor. Nucleonics 10: 32-36. 1952.

22. Hendrickson, R. A. Cross-spectral density measurements in a coupled-core reactor. Unpublished Ph.D. thesis. Ames, Iowa, Library, Iowa State University of Science and Technology. 1966.

23. Hildebrand, F. B. Methods of applied mathematics. Englewood Cliffs, N.J., Prentice-Hall, Inc. 1952.

24. Hurwitz, H., Jr. Notes on the theory of danger coefficients. U.S. Atomic Energy Commission Report KAPL-98 [Knolls Atomic Power Lab., Schenectady, New York]. 1948.

25. Kaplan, S. Modal analysis. In Radkowsky, A., editor. Naval reactor physics handbook. Vol. 1. Pp. 966-977. Washington, D.C., U.S. Govt. Print. Off. 1964.

26. Kaplan, S. The property of finality and the analysis of problems in reactor space-time kinetics by various modal expansions. Nuc. Sci. and Eng. 9: 357-361. 1961.

27. Kaplan, S., Marlowe, O. J. and Bewick, J. Application of synthesis techniques to problems involving time dependence. Nuc. Sci. and Eng. 18: 163-176. 1964.

28. Keepin, G. R. Physics of nuclear kinetics. Reading, Massachusetts. Addison-Wesley Publishing Co., Inc. 1965.

29. Kobayashi, K. Flux synthesis using Green's Function in two-dimensional group diffusion equations. Nuc. Sci. and Eng. 31: 91-101. 1968.

30. Kylstra, C. D. and Uhrig, R. E. Spatially dependent transfer function for nuclear systems. Nuc. Sci. and Eng. 22: 191-205. 1965.

31. Loewe, W. E. Space-dependent effects in the response of a nuclear reactor to forced oscillations. Nuc. Sci. and Eng. 21: 536-549. 1965.

32. Mortensen, G. A. and Smith, H. P., Jr. Neutron-wave propagation using the P. approximation. Nuc. Sci. and Eng. 22: 321-327. 1965.

33. Pluta, P. R. Coupled core kinetic behavior. Atomic Energy Commission Symposium Series 7: 544-565. 1966.

34. Potter, R. The transfer function of a steadily diverging reactor. J. Nuc. Energy 6: 291-299. 1958.

35. Reactor Physics Constants, 1963. U.S. Atomic Energy Commission Report ANL-5800 [Argonne National Laboratory, Lemont, Illinois]. 1963.

36. Schultz, D. G. and Melsa, J. L. State functions and linear control systems. New York, New York, McGraw-Hill Book Co., Inc. 1967.

37. Selengut, D. S. Variational analysis of multi-dimensional systems. U.S. Atomic Energy Commission Report HW-59126. [General Electric Co. Hanford Atomic Products Operation, Richland, Washington]. 1958.

38. Singer, S. The period equilibrium effect in reactor dynamics. U.S. Atomic Energy Commission Report LA-2654 [Los Alamos Scientific Laboratory, Los Alamos, New Mexico]. 1962.

39. Sturm, W. J. and Daavettila, D. A. Argonaut Reactor Data book. U.S. Atomic Energy Commission Report ANL-6285 [Argonne National Laboratory, Lemont, Illinois]. 1961.

40. Ussachoff, L. N. Equations for the importance of neutrons, reactor kinetics and the theory of perturbation. United Nations International Conference on the Peaceful Uses of Atomic Energy, 1st, Geneva, 1956, Paper 656. 1956.

41. Weinberg, A. M. and Schweinler, H. C. Theory of oscillating absorber in a chain reactor. Physical Review 74: 851-863. 1948.

42. Weinberg, A. M. and Wigner, E. P. The physical theory of neutron chain reactors. Chicago, Ill., The University of Chicago Press. 1958.

X. APPENDIX A: DESCRIPTION OF THE UTR-10 REACTOR

The UTR-10 reactor is a water-moderated and graphite-reflected coupled-core reactor licensed for operation up to 10 - KW. It is a commercial version of the Argonaut Reactor which was designed at Argonne National Laboratory. Each core consists of a 5-in. by 20-in. by 24-in. slab containing six fuel elements and each fuel element is an assembly of 12 MTR-type fuel plates containing fully enriched uranium. These fuel plates are cooled by deionized light water. The two core tanks are separated by approximately 18 inches of nuclear grade graphite which comprises the coupling region and acts as a flux trap for thermal neutrons. A 5-ft. by 5-ft. by 4-ft. thermal column is provided adjacent to the south core tank and a smaller (41.5-in. by 30-in. by 30-in.) thermal column is adjacent to the north core and leads to the shield tank as illustrated in Figure A.1.

An access port to the midplane of the south core tank is obtained by means of a removable stringer near the center of the thermal column.

The reactor is fueled by approximately 3 kg. of fully enriched uranium, i.e., greater than 93% U-235 with approximately equal masses of fuel being loaded into each core tank. The inequality of loading plus the effect of the control-rod configuration results in a maximum flux tilt in the UTR-10 of about 1.35 based on the ratio of the average

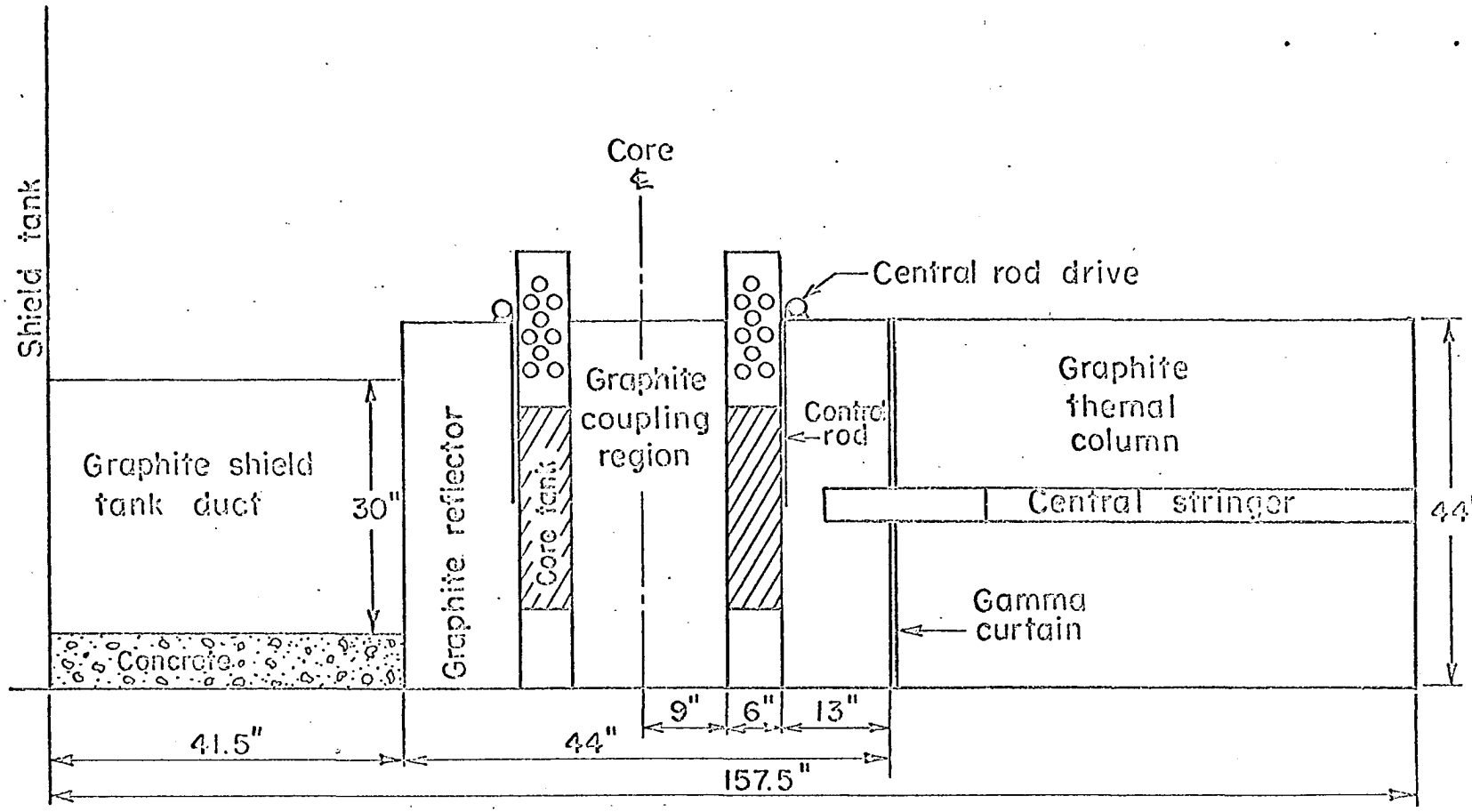

Figure A.1. Reactor section.

thermal fluxes across each core tank.

Control is accomplished by means of two safety rods, one shim-safety rod, and one regulating rod. During operation the safety rods are fully withdrawn and the shim-safety and regulating rod are positioned to achieve the desired operating conditions. When the reactor is scrammed the safety and shim-safety rods are rapidly driven in and a six-inch dump valve opens to drain the moderator from the core.

XI. APPENDIX B: DERIVATION OF THE EQUATIONS DESCRIBING THE TRANSFER FUNCTION OF A TWO-POINT REACTOR

A pair of cores is considered coupled if fissions in one core may be caused by neutrons which originated in the other core. If each of the cores is treated as a point reactor in which the system maintains its criticality by a mutual exchange of neutrons, then for two cores at criticality

$$k_1(t) = k_{11}(t) + k_{12}(t) = 1.0 \tag{B.1}$$

and

$$k_2(t) = k_{22}(t) + k_{21}(t) = 1.0 \tag{B.2}$$

where

$k_i(t)$ = the total multiplication constant of core i

$k_{ij}(t)$ = that part of the multiplication constant of core i due to neutrons which were born in core j.

The notation and formulation of the kinetic equations used in the frequency analysis of the two-point reactor will be that of Avery (4) and will employ only one group of delayed neutrons. The equations which describe the system are

$$\ell_{11} \frac{dS_{11}}{dt} = k_{11}(1-\beta)(S_{11}+S_{12}) - S_{11} + k_{11}\lambda C_1 \tag{B.3}$$

$$\ell_{12} \frac{dS_{12}}{dt} = k_{12}(1-\beta)(S_{12}+S_{22}) - S_{12} + k_{12}\lambda C_2 \tag{B.4}$$

$$\ell_{21} \frac{dS_{12}}{dt} = k_{21}(1-\beta)(S_{11}+S_{12}) - S_{21} + k_{21}\lambda C_1 \qquad (B.5)$$

$$\ell_{22} \frac{dS_{22}}{dt} = k_{22}(1-\beta)(S_{21}+S_{22}) - S_{22} + k_{22}\lambda C_2 \qquad (B.6)$$

$$\frac{dC_1}{dt} = \beta(S_{11}+S_{12}) - \lambda C_1 \qquad (B.7)$$

$$\frac{dC_2}{dt} = \beta(S_{21}+S_{22}) - \lambda C_2 \quad . \qquad (B.8)$$

The terms in Equations B.3 through B.8 are defined as

ℓ_{ij} = lifetime of neutrons in core i which originated in core j

S_{ij} = production rate of neutrons in core i which originated in core j

k_{ij} = the part of the multiplication constant in core i due to S_{ij} type neutrons

$\beta = \sum_{i=1}^{M} \lambda_i \beta_i$

λ = average delayed neutron decay constant

C = delayed neutron precursor concentration.

A. Oscillation of Core One

When the response of the two-point model to a sinusoidal oscillation of reactivity in core one is considered, assuming both cores to have the same nuclear properties, the various multiplication factors are described as follows

$$k_{11}(t) = k_{11}(0) + \delta k_{11}(t)$$

$$k_{12}(t) = k_{12}(0) + \delta k_{12}(t)$$
$$k_{21}(t) = k_{21}(0)$$
$$k_{22}(t) = k_{22}(0)$$

where $k_{1j}(t)$, $j = 1,2$ represents a small sinusoidal oscillation about the steady-state value $k_{1j}(0)$, $j = 1,2$. This oscillation of reactivity in core one causes all the neutron and precursor densities to be perturbed in the same manner, described by

$$\sum_{j=1}^{2} \sum_{i=1}^{2} S_{ij}(t) = \sum_{j=1}^{2} \sum_{i=1}^{2} \{S_{ij}(0) + \delta S_{ij}(t)\} \qquad (B.9)$$

$$\sum_{i=1}^{2} C_i(t) = \sum_{i=1}^{2} \{C_i(0) + \delta C_i(t)\} \; . \qquad (B.10)$$

By substituting these perturbed densities into Equations B.3 through B.8, collecting steady-state terms and setting them equal to zero, neglecting products of infinitesimals and simplifying, the equations of the system become

$$\ell_{11} \frac{d\delta S_{11}}{dt} = (k_{11}^{o}(1-\beta)-1)\delta S_{11} + k_{11}(1-\beta)\delta S_{12} + \delta k_{11} S_1^{o} + k_{11}^{o}\lambda \delta C_1 \qquad (B.11)$$

$$\ell_{12} \frac{d\delta S_{12}}{dt} = k_{12}^{o}(1-\beta)\delta S_{21} + k_{12}^{o}(1-\beta)\delta S_{22} + \delta k_{12} S_2^{o} - \delta S_{12} + k_{12}^{o}\lambda \delta C_2 \qquad (B.12)$$

$$\ell_{21} \frac{d\delta S_{21}}{dt} = k_{21}^{o}(1-\beta)\delta S_{11} + k_{21}^{o}(1-\beta)\delta S_{12} - \delta S_{21} + k_{21}^{o}\lambda \delta C_1 \qquad (B.13)$$

$$\ell_{22} \frac{d\delta S_{22}}{dt} = k^{o}_{22}(1-\beta)\delta S_{21} + k^{o}_{22}(1-\beta)\delta S_{22} - \delta S_{22} + k^{o}_{22}\lambda C_2 \tag{B.14}$$

$$\frac{d\delta C_1}{dt} = \beta\delta S_{11} + \beta\delta S_{12} - \lambda\delta C_1 \tag{B.15}$$

$$\frac{d\delta C_2}{dt} = \beta\delta S_{21} + \beta\delta S_{22} - \lambda\delta C_2 \tag{B.16}$$

where

$$k^{o}_{ij} = k_{ij}(0)$$

$$S_i = S_{ii}(0) + S_{ij}(0) \ .$$

Equations B.11 through B.16 may be rewritten in matrix form as follows

$$\Lambda\dot{A} = KA + \underline{\alpha}(t) \tag{B.17}$$

where

$$\Lambda = \begin{bmatrix} \ell_{11} & 0 & 0 & 0 & 0 & 0 \\ 0 & \ell_{12} & 0 & 0 & 0 & 0 \\ 0 & 0 & \ell_{21} & 0 & 0 & 0 \\ 0 & 0 & 0 & \ell_{22} & 0 & 0 \\ 0 & 0 & 0 & 0 & 1 & 0 \\ 0 & 0 & 0 & 0 & 0 & 1 \end{bmatrix} \tag{B.18}$$

$$A = \text{col}[\delta S_{11} \ \delta S_{12} \ \delta S_{21} \ \delta S_{22} \ \delta C_1 \ \delta C_2] \tag{B.19}$$

$$K = \begin{bmatrix} k^{o}_{11}(1-\beta)-1 & k^{o}_{11}(1-\beta) & 0 & 0 & k^{o}_{11}\lambda & 0 \\ 0 & -1 & k^{o}_{12}(1-\beta) & k^{o}_{12}(1-\beta) & 0 & k^{o}_{12}\lambda \\ k^{o}_{21}(1-\beta) & k^{o}_{21}(1-\beta) & -1 & 0 & k^{o}_{21}\lambda & 0 \\ 0 & 0 & k^{o}_{22}(1-\beta) & k^{o}_{2}(1-\beta)-1 & 0 & k^{o}_{22}\lambda \\ \beta & \beta & 0 & 0 & -\lambda & 0 \\ 0 & 0 & \beta & \beta & 0 & -\lambda \end{bmatrix} \tag{B.20}$$

and $\underline{\alpha}(t)$ represents the time dependent driving function

$$\underline{\alpha}(t) = \text{col}[\delta k_{11} S_1^o \ \delta k_{12} S_2^o \ 0 \ 0 \ 0 \ 0] \ . \tag{B.21}$$

This matrix driving function may be written in terms of a single driving function if there is no flux tilt, that is, if $S_1^o = S_2^o$. The effective multiplication factor of a reactive assembly may be written

$$k_{eff} = \eta \ \epsilon \ pf \ P_f P_s \tag{B.22}$$

where

P_f = fast nonleakage probability

P_s = slow nonleakage probability,

and the notation is that of Glasstone and Edlund (18). For a small change in the thermal utilization (absorption cross section) such that $f(t) = f(0) + \delta f(t)$, where $k_{eff} = 1.0$ when $\delta f(t) = 0$, then

$$\frac{\delta k}{k} \quad \frac{k_{eff}-1}{k_{eff}} \cong \frac{\eta \epsilon p (f_o+\delta f) P_f P_s - 1}{\eta \epsilon p \ f_o P_f P_s} = \frac{\delta f}{f_o} \tag{B.23}$$

and

$$\frac{\delta f}{f_o} = \frac{\delta k_{11}}{k_{11}^o} = \frac{\delta k_{12}}{k_{12}^o} \tag{B.24}$$

or

$$\delta k_{12} = \delta k_{11} k_{12}^o / k_{11}^o \ . \tag{B.25}$$

The matrix driving function may be rewritten

$$\underline{\alpha}(t) = \delta k_{11} S_1^o \begin{bmatrix} 1 \\ k_{12}^o/k_{11}^o \\ 0 \\ 0 \\ 0 \\ 0 \end{bmatrix} = \delta k_{11} S_1^o \underline{F} \ . \qquad (B.26)$$

The description of the system is now in the time domain. To obtain the frequency response assume

$$\delta k_{11}(t) = |\delta k_{11}| \ e^{j\omega t} \qquad (B.27)$$

that is, assume that the change in multiplication constant is of magnitude δk_{11} and is oscillating at a frequency ω. The change of the output, δS_{ij}, will be of the same form as the change in the input so

$$\delta S_{ij} = \delta \hat{S}_{ij} e^{j\omega t} \qquad (B.28)$$

where $\delta \hat{S}_{ij}$ is a complex number which describes the phase behavior and ω is the frequency at which the oscillator and neutron density oscillate. Substituting into Equation B.17 and dividing by $e^{j\omega t}$ yields

$$j\omega \Lambda \hat{A} = K\hat{A} + \underline{\alpha}(t)$$

or

$$(-K + j\omega\Lambda)\hat{A} = \underline{\alpha}(t) \qquad (B.29)$$

where $\hat{A}$ is the complex frequency-dependent solution vector. This equation may be solved for $\hat{A}$ by separating the vector into real and imaginary parts and solving a real set of simultaneous equations or by solving directly for the $\hat{A}$ vector using complex arithmetic.

If

$$A = \text{col}[Re + jIm]$$

then the magnitudes and phases for the partial sources δS_{11} are defined as

$$|\delta S_{11}(\omega)| = \sqrt{Re^2_{11}(\omega) + Im^2_{11}(\omega)}$$

and phase of

$$\delta S_{11}(\omega) = \tan^{-1} Im_{11}(\omega)/Re_{11}(\omega) \ .$$

The total source in core one for a given frequency is

$$\delta S_1 = \delta S_{11} + \delta S_{12} = Re_{11} + jIm_{11} + Re_{12} + jIm_{12}$$

$$= (Re_{11} + Re_{12}) + j(Im_{11} + Im_{12})$$

and its magnitude and phase with respect to the oscillator are

$$|\delta S_1| = \sqrt{(Re_{11} + Re_{12})^2 + (Im_{11} + Im_{12})^2}$$

phase

$$\delta S_1 = \tan^{-1}(Im_{11} + Im_{12})/(Re_{11} + Re_{12}) \ .$$

These identities and their analogs may be used to obtain the various partial or total population responses.

B. Oscillation of Coupling Between Cores

To oscillate the coupling between cores a sinusoidal driving function is impressed upon the multiplication factors representing the exchange of neutrons between two

cores. The multiplication factors then become

$$k_{11}(t) = k_{11}(0)$$
$$k_{12}(t) = k_{12}(0) + \delta k_{12}(t)$$
$$k_{21}(t) = k_{21}(0) + \delta k_{21}(t)$$
$$k_{22}(t) = k_{22}(0) \quad .$$

Again allowing perturbation of all of the densities S_{11}, S_{12}, S_{21}, S_{22}, C_1 and C_2, substituting back into the point kinetics Equations B.3 through B.8, and simplifying as before, the kinetics equations become

$$\ell_{11} \frac{d\delta S_{11}}{dt} = k_{11}^o(1-\beta)\delta S_{11} + k_{11}^o(1-\beta)\delta S_{12} - \delta S_{11} + k_{11}^o \lambda \delta C_1 \tag{B.30}$$

$$\ell_{12} \frac{d\delta S_{12}}{dt} = k_{12}^o(1-\beta)\delta S_{21} + k_{12}^o(1-\beta)\delta S_{22} - \delta C_{12} + \delta k_{12}(S_{21}^o + S_{22}^o) + k_{12}^o \lambda \delta C_2 \tag{B.31}$$

$$\ell_{21} \frac{d\delta S_{12}}{dt} = k_{21}^o(1-\beta)\delta S_{11} + k_{21}^o(1-\beta)\delta S_{12} + k_{21}^o \lambda C_1 - \delta S_{21} + \delta k_{21} S_1^o \tag{B.32}$$

$$\ell_{22} \frac{d\delta S_{22}}{dt} = k_{22}^o(1-\beta)\delta S_{21} + k_{22}^o(1-\beta)\delta S_{22} - \delta S_{22} + k_{22}^o \lambda \delta C_2 \tag{B.33}$$

$$\frac{d\delta C_1}{dt} = \beta \delta S_{11} + \beta \delta S_{12} - \lambda \delta C_1 \tag{B.34}$$

$$\frac{d\delta C_2}{dt} = \beta \delta S_{21} + \beta \delta S_{22} - \lambda \delta C_2 \quad . \tag{B.35}$$

When these equations are put into the form of B.29,

$$(-K + j\omega\Lambda)\hat{A} = \underline{\alpha}(t),$$

Λ, K, and $\hat{A}$ are found to be the same as when core one was oscillated, however, the driving function, $\underline{\alpha}(t)$, is different. $\underline{\alpha}(t)$ is now

$$\underline{\alpha}(t) = \text{col}[0\ 0\ \delta k_{12} S_2^o\ \ \delta k_{21} S_1^o\ \ 0\ 0]. \tag{B.30}$$

If there is no flux tilt and the reactivity change is made symmetrically in both coupling terms the driving function becomes

$$\underline{\alpha}(t) = {}^{\delta}k_{12} S_1^0 \begin{bmatrix} 0 \\ 0 \\ 1 \\ 1 \\ 0 \\ 0 \end{bmatrix} \tag{B.31}$$

and the partial and total population responses may be obtained as before.

XII. APPENDIX C: DEVELOPMENT OF EQUATIONS FOR THE GREEN'S FUNCTION MODES

The first part of this appendix is a review of the method used to obtain the Green's Function modes as proposed by Dougherty and Shen (13) and modified by Carter (9).

The multigroup diffusion equations may be written in operator form

$$L\Phi = V^{-1} \frac{\partial \Phi}{\partial t} \tag{C.1}$$

and the solution is to be expressed in the form

$$\varphi(x,t) \cong \sum_{i=1}^{N} \psi_i(x) a_i(t) \tag{C.2}$$

where the functions $\psi_i(x)$ and $a_i(t)$ are to be determined. After the space modes, $\psi_i(x)$, have been determined, the corresponding time dependent coefficients, $a_i(t)$, may be obtained by using the semidirect method of the calculus of variations (23).

Although other characteristics have been mentioned (16), some desirable properties of any set of space modes are that they be "readily" calculable in complex geometries, that they economize the expansion, and that they permit being tailored to perturbations about which one may have a priori information. One set of modes which satisfies these three criteria may be generated by first rewriting Equation C.1 as an integral equation (17).

$$\varphi(x,t) - \varphi_o(x) = \int_o^t \int_{x_o}^{x_n} dt'dx' \{G(x,t;x',t')\nu M(x',t') \times \varphi(x',t')\} \qquad (C.3)$$

where the multigroup operator, L, has been redefined in terms of a removal and a fission operator so that

$$L = L_r - \nu M .$$

The kernel of C.3 is given by the equation

$$(L_r - V^{-1}\frac{\partial}{\partial t}) G(x,t;x',t') = \delta(x-x')\delta(t-t') \qquad (C.4)$$

and $G(x,t;x',t')$ must satisfy the homogeneous boundary conditions satisfied by $\varphi(x,t)$. The integrand of C.3 is now approximated by a finite sum

$$G(x,t;x',t')\nu M(x',t')\varphi(x',t') \cong \sum_{i=1}^{N} C_i(t')G_o(x,x')\nu M_o(x')\varphi_o(x')A_i(x') \qquad (C.5)$$

where

zero subscripts indicate steady state values

$G_o(x,x')$ is the initial steady state Green's Function defined by

$L_{r_o} G_o(x,x') = \delta(x-x')$ plus the usual homogeneous boundary conditions

$$\Delta_i(x') = \begin{cases} \text{unity in the ith reactor region} \\ \text{zero elsewhere} \end{cases}$$

and

$C_i(t')$ is the time varying coefficient in the ith region.

Substituting the above approximation into the integrand of C.3 and integrating with respect to t'

$$\varphi(x,t) - \varphi_o(x) \cong \sum_{i=1}^{N} \left[\int_o^t C_i(t') \left\{\int_{x_o}^{x_n} dx' G_o(x,x') \nu M_o(x') \right.\right.$$

$$\left.\left. x \quad \varphi_o(x') \Delta_i(x') \right\} dt' \right] \qquad (C.6)$$

an equation of the form

$$\varphi(x,t) \cong \sum_{i=1}^{N} \psi_i(x) a_i(t)$$

is obtained if the space modes satisfy an equation of the form

$$\psi_i(x) = \int_{x_o}^{x_n} dx' G_o(x,x') \nu M_o(x') \varphi_o(x') \Delta_i(x'). \qquad (C.7)$$

Operating on both sides of C.7 with L_{r_o}, the space modes are found to satisfy the differential equation

$$L_{r_o} \psi_i(x) = \int_{x_o}^{x_n} dx' \delta(x-x') \nu M_o(x') \varphi_o(x') \Delta_i(x')$$

or

$$L_{r_o} \psi_i(x) = \nu M_o(x) \varphi_o(x) \Delta_i(x); \; i=1,2,\ldots,N. \qquad (C.8)$$

This equation, C.8, is solved to obtain the space modes, $\psi_i(x)$, which are used to approximate the flux. These modes may be added together as follows

$$L_{r_o} \sum_{i=1}^{N} \psi_i(x) = \nu M_o \varphi_o(x),$$

but since

$$L = L_{r_o} - \nu M$$

then

$$L_{r_o} \sum_{i=1}^{N} \psi_i(x) = L_{r_o}\varphi_o - L\varphi_o .$$

Therefore

$$\varphi_o(x) = \sum_{i=1}^{N} \psi_i(x) \tag{C.9}$$

and the modes must sum to the initial steady-state flux.

Equation C.6 may be written as

$$\varphi(x,t) - \varphi_o(x) \cong \sum_{i=1}^{N} \psi_i(x) \int_o^t C_i(t')dt'$$

or

$$\varphi(x,t) \cong \sum_{i=1}^{N} \psi_i(x) \{1 + \int_o^t C_i(t')dt'\}$$

which is in the form desired for the approximation

$$\varphi(x,t) \cong \sum_{i=1}^{N} \psi_i(x) a_i(t)$$

if

$$a_i(t) = 1 + \int_o^t C_i(t')dt' . \tag{C.10}$$

In a similar manner the adjoint space modes can be shown to satisfy the equation

$$L_{r_o}^T \psi_i^+(x) = \nu M_o^T \varphi_o^+(x) \Delta_i(x); \quad i = 1,2,\ldots,N \tag{C.11}$$

plus the usual homogeneous boundary conditions.

In order to obtain modes in the nonmultiplying regions,

it is necessary to redefine the steady-state loss operator, L_{r_o}. The kinetics equations can be written

$$L\bar{\Phi} = V^{-1} \frac{\partial \bar{\Phi}}{\partial t} \tag{C.1}$$

where L is a space- and time-dependent matrix operator and the elements of the diagonal matrix V^{-1} are the reciprocals of the neutron-group speeds. At steady state $\frac{\partial \bar{\Phi}}{\partial t} = \underline{0}$ so that Equation C.1 becomes

$$L\bar{\Phi} = \underline{0}.$$

The operator L may then be broken into two parts

$$L = L_{r_o} - \nu M \tag{C.12}$$

where L_{r_o} is a steady-state removal operator and M is a neutron production operator. Applying two-group diffusion theory to C.12 it becomes

$$\begin{bmatrix} D_F\nabla^2 - \Sigma_r & \nu\Sigma_f \\ \Sigma_r & D_s\nabla^2 - \Sigma_a \end{bmatrix} = \begin{bmatrix} D_F\nabla^2 - \Sigma_r & 0 \\ \Sigma_r & D_s\nabla^2 - \Sigma_a \end{bmatrix} - \nu \begin{bmatrix} 0 & -\Sigma_f \\ 0 & 0 \end{bmatrix} .$$

Hence the operator M will be nonzero only in regions which contain fuel, so that in the moderator regions the equation to be solved becomes

$$L_{r_o}\psi_i(x) = 0 \tag{C.13}$$

plus the usual homogeneous boundary conditions. This problem admits only the trivial solution.

It has been shown[1] (9) that in order to obtain the

[1] McFadden, James, Ames, Iowa. Results of computer analysis. Private communication. 1968.

correct time response for coupled-core reactors, a mode(s) must be present to represent the coupling region. When a mode of this type is not present and a disturbance is made in one core, the perturbation is not correctly propagated to the driven core and neither the time nor the frequency behavior of the reactor is predicted correctly.

In order to reformulate the problem so that a mode is generated for each region (9, 10), the L-operator can be rewritten as

$$L = \mathcal{L}_r - \mathcal{M} \tag{C.14}$$

where $\mathcal{L}_r$ is a removal operator and $\mathcal{M}$ can be thought of as a pseudoproduction operator. The matrix $\mathcal{M}$ must be constructed so that there will be a nonhomogeneous term, or source, in each region to be represented by a mode. This may be accomplished by dividing the L-operator as follows

$$\begin{bmatrix} D_F\nabla^2-\Sigma_r & \nu\Sigma_f \\ \Sigma_r & D_s\nabla^2-\Sigma_a \end{bmatrix} = \begin{bmatrix} D_F\nabla^2-\Sigma_r' & 0 \\ 0 & D_s\nabla^2-\Sigma_a' \end{bmatrix} - \begin{bmatrix} \Sigma_r'' & -\nu\Sigma_f \\ -\Sigma_r & \Sigma_a'' \end{bmatrix}$$

where

$$\Sigma_r = \Sigma_r' + \Sigma_r''$$

and

$$\Sigma_a = \Sigma_a' + \Sigma_a''$$

It has also been found (9) that the fraction of Σ_r residing in Σ_r' and Σ_r'' does not affect the final solution of the problem, provided that the split is not infinitessimal.

The new equation the modes must satisfy is

$$\mathcal{L}_{r_o} \psi_i(x) = m\varphi_o(x)\Delta_i(x) \qquad (C.15)$$

plus the usual homogeneous boundary conditions; an equation analogous to C.15 is obtained for the adjoint modes.

The operators of the two-group diffusion equation must now be defined so they will be compatible with this new formulation for the space modes. When it is assumed that fast absorption is negligible and that all fissions are due to thermal neutrons, the usual two-group time-dependent neutron diffusion equations become

$$\frac{1}{v_f}\frac{\partial \varphi_F}{\partial t} = \nabla\cdot D_F\nabla\varphi_F - \Sigma_r\varphi_F + \nu\Sigma_f(1-\beta)\varphi_s + \sum_{i=1}^{M}\lambda_i C_i \qquad (C.16)$$

$$\frac{1}{v_s}\frac{\partial \varphi_s}{\partial t} = \nabla\cdot D_s\nabla\varphi_s - \Sigma_a\varphi_s + \Sigma_r\varphi_F \qquad (C.17)$$

$$\sum_{i=1}^{M}\left\{\frac{dC_i}{dt} = \beta_i\nu\Sigma_f\varphi_s - \lambda_i C_i\right\} \qquad (C.18)$$

The precursor concentration can be eliminated as an explicit dependent variable by first finding the response of the ith precursor-group concentration to an impulse function in the slow flux, $\delta\varphi_s$, as follows

$$\frac{dC_i}{dt} = \beta_i\nu\Sigma_f\delta\varphi_s - \lambda_i C_i \ .$$

The Laplace-transform technique can be used to solve for $C_i(t)$ after assuming zero initial conditions.

$$SC_i(S) = \beta_i \nu\Sigma_f - \lambda_i C_i(S)$$

$$(S+\lambda_i)C_i(S) = \beta_i \nu\Sigma_f$$

$$C_i(S) = \beta\nu\Sigma_f/(S+\lambda_i)$$

or

$$C_i(t) = \beta_i \nu\Sigma_f e^{-\lambda_i t}$$

From this impulse response it is possible to synthesize the precursor response to any input using a convolution as follows

$$C_i(t) = \beta_i \nu\Sigma_f \int_{-\infty}^{t} \varphi_s(\tau) e^{-\lambda_i (t-\tau)} d\tau \ . \qquad (C.19)$$

Then an operator S_D can be defined where

$$\sum_{i=1}^{M} \lambda_i C_i(t) = S_D \varphi_s(t) \qquad (C.20)$$

so that

$$S_D = \nu\Sigma_f \sum_{i=1}^{M} \lambda_i \beta_i \int_{-\infty}^{t} e^{-\lambda_i (t-\tau)} d\tau \qquad (C.21)$$

and the two-group diffusion equation may be rewritten

$$\frac{1}{v_F} \frac{\partial \varphi_F}{\partial t} = \nabla \cdot D_F \nabla \varphi_F - \Sigma_r \varphi_F + \nu\Sigma_f (1-\beta)\varphi_F + S_D \varphi_s \qquad (C.22)$$

$$\frac{1}{v_s} \frac{\partial \varphi_s}{\partial t} = \nabla \cdot D_s \nabla \varphi_s - \Sigma_a \varphi_s + \Sigma_r \varphi_F \ . \qquad (C.23)$$

In order to account for transverse leakage the fluxes are assumed to satisfy the wave equation in the y- and z-directions. Hence for the z-direction

$$\frac{d^2\varphi}{dz^2} + B_z^2 \varphi = 0$$

or

$$\frac{d^2}{dz^2} = -B_z^2 \ .$$

Then the leakage rate is $D\frac{d^2\varphi}{dz^2} = -DB_z^2\varphi$. Since the total transverse buckling is $B_T^2 = B_y^2 + B_z^2$ and since the multigroup diffusion equations can be written

$$L\Phi = V^{-1}\frac{\partial\Phi}{\partial t} \tag{C.1}$$

the loss terms can be regrouped to obtain the form

$$\begin{bmatrix} D_F\frac{\partial^2}{\partial x^2} - (\Sigma_r + D_F B_T^2) & \nu\Sigma_f(1-\beta) + S_D \\ \Sigma_r & D_s\frac{\partial^2}{\partial x^2} - (\Sigma_a + D_s B_T^2) \end{bmatrix} \begin{bmatrix} \varphi_F \\ \varphi_s \end{bmatrix} \ .$$

$$= \begin{bmatrix} \frac{1}{v_f} & 0 \\ 0 & \frac{1}{v_s} \end{bmatrix} \frac{\partial}{\partial t} \begin{bmatrix} \varphi_F \\ \varphi_s \end{bmatrix} \tag{C.24}$$

It is then convenient to define an effective removal cross section, Σ_{re},

$$\Sigma_{re} = \Sigma_r + D_F B_T^2 \tag{C.25}$$

an effective absorption cross section, Σ_{ae},

$$\Sigma_{ae} = \Sigma_a + D_s B_T^2 \tag{C.26}$$

and a fast neutron production operator, G,

$$G = \nu\Sigma_f(1-\beta) + S_D \tag{C.27}$$

so that the matrix L in C.1 becomes

$$\begin{bmatrix} D_F\frac{\partial^2}{\partial x^2} - \Sigma_{re} & G \\ \Sigma_r & D_S\frac{\partial^2}{\partial x^2} - \Sigma_{ae} \end{bmatrix}$$

The form of the L-operator has been defined making it possible to solve the equations for the space modes. Since

$$L = \mathcal{L}_{r_o} - \mathcal{M} \tag{C.14}$$

or

$$\begin{bmatrix} D_F \frac{\partial^2}{\partial x^2} - \Sigma_{re} & G \\ \Sigma_r & D_s \frac{\partial^2}{\partial x^2} - \Sigma_{ae} \end{bmatrix} = \begin{bmatrix} D_F \frac{\partial^2}{\partial x^2} - \Sigma'_{re} & 0 \\ 0 & D_s \frac{\partial^2}{\partial x^2} - \Sigma'_{ae} \end{bmatrix}$$

$$- \begin{bmatrix} \Sigma''_{re} & -G \\ -\Sigma_r & \Sigma''_{ae} \end{bmatrix}$$

Equation C.15 for the direct modes

$$\mathcal{L}_{r_o} \psi_i(x) = \mathcal{M} \varphi_o \Delta_i(x) \tag{C.15}$$

becomes

$$\begin{bmatrix} D_F \frac{\partial^2}{\partial x^2} - \Sigma'_{re} & 0 \\ 0 & D_s \frac{\partial^2}{\partial x^2} - \Sigma'_{ae} \end{bmatrix} \begin{bmatrix} \psi_F \\ \psi_s \end{bmatrix} = \begin{bmatrix} \Sigma''_{re} & -G \\ -\Sigma_r & \Sigma''_{ae} \end{bmatrix} \begin{bmatrix} \varphi_F \\ \varphi_s \end{bmatrix} \Delta_i(x)$$

(C.28)

and the equation for the adjoint modes

$$\mathcal{L}^T_{r_o} \psi^+_i(x) = \mathcal{M}^T \varphi^+_o \Delta_i(x)$$

becomes

$$\begin{bmatrix} D_F \frac{\partial^2}{\partial x^2} - \Sigma'_{re} & 0 \\ 0 & D_s \frac{\partial^2}{\partial x^2} - \Sigma'_{ae} \end{bmatrix} \begin{bmatrix} \psi^+_F \\ \psi^+_s \end{bmatrix} = \begin{bmatrix} \Sigma''_{re} & -\Sigma_r \\ -G & \Sigma''_{ae} \end{bmatrix} \begin{bmatrix} \varphi^+_F \\ \varphi^+_s \end{bmatrix} \Delta_i(x)$$

(C.29)

Finally the two-group diffusion equations obtain the form

$$\mathcal{D}\frac{\partial^2}{\partial x^2}\bar{\Phi} + H\bar{\Phi} = V^{-1}\frac{\partial\bar{\Phi}}{\partial t} \qquad (C.30)$$

which is the form required for substitution into the functional, II.8, used to obtain the time coefficients. Here

$$\mathcal{D} = \begin{bmatrix} D_F & 0 \\ 0 & D_s \end{bmatrix}, \qquad \bar{\Phi} = \begin{bmatrix} \varphi_F \\ \varphi_s \end{bmatrix}$$

$$H = \begin{bmatrix} -\Sigma_{re} & G \\ \Sigma_r & -\Sigma_{ae} \end{bmatrix}, \qquad V^{-1} = \begin{bmatrix} \frac{1}{v_F} & 0 \\ 0 & \frac{1}{v_s} \end{bmatrix}.$$

XIII. APPENDIX D: SIGNIFICANCE OF $K_o A_o$ BEING ZERO

A natural consequence of the linearization of Equation II.19 is the observation that the matrix product $K_o A_o$ equals $\underline{0}$. This fact is worthy of special attention because it provides additional insight into the problem and also because it provides a check of computational accuracy.

For simplicity of exposition, consider a two-energy-group two-mode representation of the reactor. For this case the K_o matrix is expressed on the following page.

At the steady-state condition all the elements of A_o are unity and for this heuristic example the product $K_o A_o$ yields a 4 x 1 row vector, the first element of which is

$$\left\langle - \frac{\partial \psi^+_{F1}}{\partial x} D_F \frac{\partial \psi_{F1}}{\partial x} + \psi^+_{F1} \Sigma_{re} \psi_{F1} - \frac{\partial \psi^+_{F1}}{\partial x} D_f \frac{\partial \psi_{F2}}{\partial x} \right.$$

$$\left. + \psi^+_{F1} \Sigma_{re} \psi_{F2} + \psi^+_{F1} \nu\Sigma_f \psi_{s1} + \psi^+_{F1} \nu\Sigma_f \psi_{s2} \right\rangle = 0$$

or

$$\left\langle - \frac{\partial \psi^+_{F1}}{\partial x} D_F \frac{\partial \varphi_F}{\partial x} + \psi^+_{F1} \Sigma_{re} \varphi_F + \psi^+_{F1} \nu\Sigma_f \varphi_s \right\rangle = 0$$

The other N-1 equations for the fast group are identical except for the subscript of the fast-adjoint mode. This equality requires that when the approximate solution to the fast-diffusion equation is weighted with the jth fast-adjoint mode the result is zero. This implies that there is no net rate of change of importance of "type j" in the reactor. When all modes are considered this corresponds

$$
\begin{bmatrix}
- \frac{\partial \psi_{F1}^{+}}{\partial x} D_F \frac{\partial \psi_{F1}}{\partial x} + \psi_{F1}^{+} \Sigma_{re} \psi_{F1} & - \frac{\partial \psi_{F1}}{\partial x} D_F \frac{\partial \psi_{F2}}{\partial x} + \psi_{F1}^{+} \Sigma_{re} \psi_{F2} \\
- \frac{\partial \psi_{F2}}{\partial x} D_F \frac{\partial \psi_{F1}}{\partial x} + \psi_{F2}^{+} \Sigma_{re} \psi_{F1} & - \frac{\partial \psi_{F2}}{\partial x} D_F \frac{\partial \psi_{F2}}{\partial x} + \psi_{F2}^{+} \Sigma_{re} \psi_{F2} \\
\psi_{s1}^{+} \Sigma_r \psi_{F1} & \psi_{s1}^{+} \Sigma_r \psi_{F2} \\
\psi_{s2}^{+} \Sigma_r \psi_{F1} & \psi_{s2}^{+} \Sigma_r \psi_{F2}
\end{bmatrix}
$$

Matrix D.1. $K_o A_o$ matrix for the two-mode case.

$$\begin{bmatrix} \psi^+_{F1}\nu\Sigma_f\psi_{s1} & \psi^+_{F1}\nu\Sigma_f\psi_{s2} \\ \psi^+_{F2}\nu\Sigma_f\psi_{s1} & \psi^+_{F2}\nu\Sigma_f\psi_{s2} \\ -\frac{\partial\psi^+_{s1}}{\partial x}D_s\frac{\partial\psi_{s1}}{\partial x}+\psi^+_{s1}\Sigma_{ae}\psi_{s1} & -\frac{\partial\psi^+_{s1}}{\partial x}D_s\frac{\partial\psi_{s2}}{\partial x}+\psi^+_{s1}\Sigma_{ae}\psi_{s2} \\ -\frac{\partial\psi_{s2}}{\partial x}D_s\frac{\partial\psi_{s1}}{\partial x}+\psi^+_{s2}\Sigma_{ae}\psi_{s1} & -\frac{\partial\psi^+_{s2}}{\partial x}D_s\frac{\partial\psi_{s2}}{\partial x}+\psi^+_{s2}\Sigma_{ae}\psi_{s2} \end{bmatrix}$$

Matrix D.1 (Continued)

to a classical definition of criticality (4) which states that the net rate of change of importance in a critical reactor is zero. This argument applies to each neutron energy group in the approximation.

The product $K_o A_o$ can be used as a check of the computational accuracy by actually evaluating the matrix product to see how near it is to the zero vector. This introduces no significant problem since the elements of K_o must be calculated anyway to obtain the frequency response. It is necessary to make the product, $K_o A_o$, as small as possible because if it is not sufficiently small the convergence of the solution is destroyed. For the model studied, if each of the elements of $K_o A_o$ was not several orders of magnitude smaller than the largest elements of K_o the effect was observable in the solution and an error could be suspected.